

Generation of photoswitchable peptide ligands by phage display

THÈSE N° 6483 (2015)

PRÉSENTÉE LE 23 JANVIER 2015

À LA FACULTÉ DES SCIENCES DE BASE
LABORATOIRE DE PROTÉINES ET PEPTIDES THÉRAPEUTIQUES
PROGRAMME DOCTORAL EN CHIMIE ET GÉNIE CHIMIQUE

ÉCOLE POLYTECHNIQUE FÉDÉRALE DE LAUSANNE

POUR L'OBTENTION DU GRADE DE DOCTEUR ÈS SCIENCES

PAR

Silvia BELLOTTO

acceptée sur proposition du jury:

Dr S. Gerber, présidente du jury
Prof. C. Heinis, Dr H. A. Wegner, directeurs de thèse
Prof. B. Fierz, rapporteur
Prof. D. Gillingham, rapporteur
Prof. P. Gorostiza, rapporteur



ÉCOLE POLYTECHNIQUE
FÉDÉRALE DE LAUSANNE

Suisse
2015

Acknowledgements

First of all I would like to thank Prof. Heinis and Prof Wegner for being my advisors and giving me the possibility to work in their labs. You always supported me and helped me during these years. I really enjoyed having the opportunity to work on challenging and stimulating projects. I think that this teamwork is an example of the immense power of collaboration in science.

I would like to thank Prof. Fierz, Prof. Gillingham and Prof. Gorostiza for being part of the committee and giving me the chance to present you my work. Thank you to Dr. Sandrine Gerber for chairing the committee.

A huge thank to all the people of the three labs I have worked in. Starting in chronological order the lab in Basel. Thank you Simon, Raphael, Florence, Johnathan, Luca. It was a pleasure to start my adventure in your company and work with you during the first year of my PhD. Thank you for helping me and always supporting me. I had a great time.

Thank you very much LPPT. I have spent here two and a half years and it was wonderful. I learnt a lot from all of you. I will always remember the happy atmosphere and the smiles. Some of the greatest friendships I have now started here. Thank you very much Lisa for introducing me to the lab, to always believe in me and help me no matter what. Thank you Ale for being always there and to be a great friend. Thank you to the rest of the 'italian community of the LPPT' Bea, Davide, Emma, Miriam. Thank you for your support and for your friendship also outside the lab. Thank you Vanessa for the French-Italian tandem sessions and for giving me your precious advices. Thank you Philippe, I couldn't have asked for a better bench mate. Thank you Ranga for being always supportive and ready to help. Thank you Charlottina, you thought me a lot with your determination, thank you Inma to have always a solution for many problems and for proofreading my thesis. Thanks Camille, it was fun to share the lab with you. My deepest thanks also to Julietta, Shiyu, Sangram, Jonas, Raphael, Khan.

Thank you to my third lab in Giessen. Thank you Luca (yes, again after Basel) for welcoming me in Germany, it was a great pleasure to collaborate with you and thank you for always being there to help me. I have learned a lot. Thank you Sebastian for hosting me in your lab for a while and for being always supportive and a friend. Thank you also to Zhen Pin, Sebastian 2, Marcel and all the students who joined the lab in the last six months. Thank you also to the great people I met in Giessen, it was really a great pleasure and I hope to see you again.

Thank you also to all my other friends in Lausanne, Basel, Giessen, Padova and Portogruaro. You are wonderful people and I am honored to be your friend. Thank you for always being there.

Last but not list, a huge thank you to my family. My mum, my dad, my brother Luca and my gran mothers Ida and Velia, to zia Santa e Mirella. I am really lucky to have you, you always believed in me, often more than I did, you always kept me up in my down moments and you did everything for me. You love me more than everything and I do too.

Lausanne 9 October 2014

Abstract

Photoswitchable ligands are used to control and study complex biological systems such as folding of proteins and peptides, enzymatic reactions or neuronal signaling. They are typically developed by conjugating photochromic compounds to known ligands so that exposure to light results in the change of the binding affinity of the ligand. Many light-responsive ligands are based on azobenzene, a molecule that undergoes a pronounced change in geometry upon photoisomerization from *trans* to *cis* in picoseconds. Currently, photoswitchable ligands are available only to a limited number of targets and their development by rational design is complex. Furthermore, they show low affinity and a relatively small change in binding affinity between the *cis* and *trans* conformation. In my PhD work, I aimed at overcoming these shortcomings by establishing an *in vitro* evolution method to generate light-controlled peptide ligands to targets of choice. Combining the expertise on phage display technology of the Heinis' lab and the knowledge about azobenzene photoswitches of the Wegner's lab, I screened large combinatorial libraries of cyclic peptides containing an azobenzene-based linker for the generation of light controlled ligands.

In a first project I synthesized and studied the photochemical properties of oligo-*ortho*-azobenzenes in order to get familiar with organic synthesis and azobenzene characterization. Even though several procedures are reported for the synthesis of azobenzene compounds, none of them was suitable for the preparation of *ortho*-nitrogen-substituted azobenzenes. Using a method that was previously developed in the Wegner group and that is based on modified Mills reaction conditions, I prepared several mono-, bis-, tris- and tetra- *ortho*-nitrogen-substituted azobenzenes. For the synthesis of bis-*ortho*-azobenzenes, a one-pot procedure was used. The analysis of their UV-VIS spectra revealed that their absorbance depends on the substituents and that only the *ortho*-nitrogen substituted mono-azobenzenes underwent *trans* → *cis* isomerization upon UV irradiation.

In a second project I aimed at developing a phage selection method for the isolation of photoswitchable peptide ligands. The goal was to cyclize random peptides displayed on phage with a photoswitchable azobenzene compound and to isolate in affinity selections those peptides that bind to an immobilized protein target in either *cis* or *trans* conformation. As a model protein target, I used streptavidin. Phage-encoded peptide libraries with the formats CX₇C and XCX₅CX were cyclized with the linker 3,3'-bis(sulfonato)-4,4'-bis(bromoacetamido)azobenzene, irradiated *in situ* with UV light and screened for the binding to streptavidin. Peptides isolated in two rounds of selection shared high sequence similarities. A range of peptides were synthesized and tested for binding streptavidin before and after irradiation at 365 nm. Several peptides bound with high affinity when cyclized with the azobenzene linker and their affinity

could be modulated by UV light. The best peptide showed a 3-fold higher affinity in the *cis* compared to the *trans* conformation.

In a third project, I applied the established phage selection method to a second target, the serine protease urokinase-type plasminogen activator (uPA) which is implicated in tumor growth and metastasis formation. A primary goal of this study was to develop photoswitchable peptide ligands that show a larger difference in binding affinity between *cis* and *trans* conformation. I had previously observed that the change in affinity depends much on the binding site of the peptide. I was therefore interested to find azobenzene peptides binding to many different epitopes of the uPA target. Towards this end, I applied high-throughput sequencing technology to analyze phage-selected peptides. This approach led to the identification of more than ten different consensus sequences. Peptides from six of these consensus sequences could be synthesized and characterized. Peptides with the consensus motif VCXIIIPYCR and WQERYCR showed the largest, yet relatively modest change in affinity. The result of this study confirmed that peptide ligands containing azobenzene groups can be developed to virtually any target with the new phage display-based approach. At the same time, the result showed that it is challenging to generate peptide ligands with large differences in affinity between the *cis* and *trans* conformation. The work suggests that new photoswitchable groups that impose larger conformational changes upon light switching should be developed and applied for the phage selection of light-responsive peptide ligands.

Keywords

photoswitchable peptides, cyclic peptides, phage display, azobenzene, streptavidin, photocontrol, urokinase-type plasminogen activator.

Sommario

Ligandi fotocontrollabili vengono utilizzati per monitorare e studiare sistemi biologici complessi come il folding (ripiegamento) di proteine e peptidi, le reazioni enzimatiche e il signaling (sistema di segnalazione) neuronale. Di solito i ligandi sono creati mediante la coniugazione chimica di composti fotocromatici con ligandi peptidici noti in modo tale che l'esposizione alla luce risulti in un cambiamento dell'affinità di legame del ligando stesso. Molti ligandi foto sensibili sono basati sull'azobenzene, una molecola chimica che, quando sottoposta a foto-isomerizzazione, subisce in pochi millisecondi un notevole cambiamento della propria geometria strutturale da *trans* a *cis*. Attualmente sono disponibili peptidi ciclici foto controllabili solo per un numero ristretto di target e il loro sviluppo razionale è assai complesso. Inoltre questi peptidi presentano una bassa affinità di legame, la quale risulta essere relativamente poco diversa tra le conformazioni *cis* e *trans*. Lo scopo del mio progetto di dottorato è stato superare queste limitazioni sviluppando un sistema di *in vitro* finalizzato alla scoperta di ligandi foto-controllabili per ben definiti target. Combinando le competenze del laboratorio del Prof. Heinis in merito alla tecnologia del phage display e le conoscenze del laboratorio del Prof. Wagner a proposito della fotoisomerizzazione degli azobenzeni, ho potuto esaminare ampie librerie fagiche di peptidi ciclicizzati con un composto di natura azobenzenica in grado di generale ligandi foto controllabili.

Nel primo progetto ho sintetizzato e studiato le proprietà fotochimiche di azobenzeni orto-sostituiti per diventare familiare con la loro sintesi organica e caratterizzazione chimica. Sebbene siano note in letteratura diverse procedure per la sintesi degli azobenzeni, nessuna fra queste risultava adatta per la sintesi di azobenzeni mono-bis-tris-tetra-orto-sostituiti con gruppi azotati. Applicando una procedura precedentemente sviluppata nel laboratorio del Prof. Wagner e basata sulla modifica delle condizioni della reazione di Mills, ho preparato diversi azobenzeni mono-bis-tris-tetra-orto-sostituiti con gruppi azotati. Per la loro sintesi si è applicata una singola reazione. L'analisi dei rispettivi spettri UV-Vis ha rivelato come la loro assorbanza dipenda dai sostituenti introdotti e che solo gli azobenzeni mono-orto sostituiti isomerizzano quando sottoposti a irradiazione con raggi UV.

Lo scopo del secondo progetto è stato sviluppare un metodo di phage display per la selezione di ligandi peptidici foto-controllabili. L'idea consisteva nel ciclizzare librerie peptidiche espresse dai fagi utilizzando un azobenzene foto-controllabile e nell'isolare i peptidi che legano la proteina target nella conformazione *cis* o *trans*. Come proteina modello si è scelta la streptavidina. Librerie fagiche che codificano per i format peptidici CX₇C e XCX₅CX sono state ciclizzate con il composto

BSBBA, irradiate *in situ* con luce UV e diversamente selezionate a seconda dell'affinità di legame per la streptavidina. Sequenze consenso ben definite sono state individuate dopo solo due round di selezione. Diversi peptidi selezionati sono stati sintetizzati e testati per definire la loro affinità di legame prima e dopo irradiazione a 365 nm. L'isomero *cis* ha rivelato una affinità di legame 3 volte superiore a quella dell'isomero *trans*.

Nel terzo ed ultimo progetto ho applicato questo metodo di phage display precedentemente sviluppato ad un secondo target, la serin proteasi urochinasi (attivatore del plasminogeno), proteina implicata nei processi di crescita tumorale e metastasi. Il principale obiettivo di questo studio era sviluppare ligandi fotocontrollabili che mostrassero una maggiore variazione di affinità tra le conformazioni *cis* e *trans*. Come osservato in precedenza, il cambio di affinità dipende molto dal sito di legame del peptide. Di conseguenza era mio interesse cercare peptidi modificati con l'azobenzene in grado di legare epitopi differenti dell'urochinasi. Con questo scopo ho usufruito la tecnologia del sequenziamento di DNA ad alta prestazione per analizzare i peptidi precedentemente selezionati. Questo approccio ha permesso di indentificare piu' di 10 sequenze consenso diverse. È stato possibile sintetizzare e caratterizzare solo peptidi appartenenti a 6 di queste famiglie di sequenze consenso. Peptidi con il consenso VCXIIPYCR and WQERYCR hanno mostrato la maggiore variazione di affinità, sebbene sia comunque relativamente modesta, e hanno rivelato una migliore attività inibitoria nella conformazione *trans*. Il risultato complessivo di questo secondo studio suggerisce come ligandi contenenti azobenzene possano essere identificati con il nuovo approccio da noi sviluppato. Allo stesso tempo lo studio dimostra che nuove molecole foto controllabili, in grado di introdurre più ampie variazioni conformazionali quando irradiate, debbano essere create e utilizzate per la selezione di ligandi peptidici foto-controllabili.

Parole chiave

Peptidi fotocontrollabili, peptidi ciclici, sistema di display su fagi, azobenzene, streptavidina, fotocontrollo, urochinasi (attivatore del plasminogeno).

Abbreviations

aa	Amino acid
ACN	Acetonitrile
Ala or A	Alanine
AMC	7-amino-4-methylcoumarin
AMPB	4-(aminomethyl)phenylazobenzoic acid
AMPP	[3-(3-aminomethyl)-phenylazo]]phenylacetic acid
AP2	Activator protein 2
APB	(4-amino)phenylazobenzoic acid
Arg or R	Arginine
Asn or N	Asparagine
Asp or D	Aspartic acid
Bak	Bcl-2 homologous antagonist/killer
Bcl-2	B-cell lymphoma 2
Bcl-XL	B-cell leukemia XL
BPDB	4,4'-bis(4-(2-chloroacetamido)phenyl)diazenylbiphenyl
BPDBS	4,4'-bis(4-(2-chloroacetamido)phenyl)diazenylbiphenyl-2,2'-disulfonate
BSA	Bovine serum albumin
BSBBA	3,3'-bis(sulfonato)-4,4'-bis(bromoacetamido)
BSBCA	3,3'-bis(sulfonato)-4,4'-bis(chloroacetamido)azobenzene
CAP	Catabolite activator protein
cm	Centimeter
Cys or C	Cysteine
Da	Dalton
DCM	Dichloromethane
DDPBA	3'-diazene-1,2-diylbis{6-[2-sulfonato-4-(chloroacetyl-amino)phenylethynyl]benzene sulfonic acid
DIPEA	N,N-diisopropylethylamine
DMF	Dimethylformamide
DMSO	Dimethylsulfoxide
DNA	Deoxyribonucleic acid
DPPC	1,2-dipalmitoyl-sn-glycero-3-phosphocholine

dsDNA	Double-stranded DNA
<i>E</i> → <i>Z</i>	<i>Entgegen</i> (<i>trans</i>) → <i>Zusammen</i> (<i>cis</i>)
<i>E. coli</i>	Escherichia coli
EDT	1,2-ethanedithiol
EDTA	Ethylenediaminetetraacetic acid
ELISA	Enzyme linked immunosorbent assay
Fmoc	Fluorenylmethyloxycarbonyl
Fp	Fluorescence polarization
Gln or Q	Glutamine
Glu or E	Glutamic acid
Gly or G	Glycine
h	Hour
H-bond	Hydrogen bond
His or H	Histidine
HOBt	1-hydroxy-benzotriazole
HPLC	High-performance liquid chromatography
IC ₅₀	Half-maximal inhibitory concentration
iGluR	Ionotropic glutamate receptor
Ile or I	Isoleucine
ITAM	Immunoreceptor tyrosine-based activation motif
K _b	Binding constant
Kbp	Kilo base pair
K _d	Dissociation constant
kDa	Kilodalton
K _i	Inhibitory constant
LC	Liquid chromatography
Leu or L	Leucine
Lys or K	Lysine
Met or M	Methionine
mg	Milligram
min	Minute
mL	Milliliter
mm	Millimeter
mM	Millimolar
Mp	Melting point
MS	Mass spectrometry
ng	Nanogram
NGS	Next generation sequencing

NHS	N-hydroxysuccinimide
nm	Nanometer
nM	Nanomolar
NMR	Nuclear magnetic resonance
nNOS	Nitric oxide synthase
NO	Nitric oxide
ON	Overnight
PADPCC	p-azophenyldiphenylcarbonylchloride
PAI1/2	Plasminogen activator inhibitor type 1/2
PAP	phenylazophenylalanine
PCR	Polymerase chain reaction
PDB	Protein data bank
PEG	Polyethylene glycol
Phe or F	Phenylalanine
PIPPIs	Photoswitchable inhibitor of protein-protein interactions
Pro or P	Proline
RNA	Ribonucleic acid
RNase H/S	Ribonuclease H/S
rpm	Rotation per minute
RT	Room temperature
RT-PCR	Reverse-transcription polymerase chain reaction
Sc	Single chain
SDS-PAGE	Sodium dodecyl sulfate-polyacrylamide gel electrophoresis
Ser or S	Serine
SH2	Src homology 2
SPPS	Solid phase peptide synthesis
SPR	Surface plasmon resonance
S-S	Disulfide bridge
Syk	Spleen tyrosine kinase
TATA	1,3,5-triacryloyl-1,3,5-triazinane
TBAB	N,N',N''-(benzene-1,3,5-triyl)tris(2-bromoacetamide)
TBMB	1,3,5-tris(bromomethyl)benzene
tc	Two-chain
TCEP	Tris(2-carboxyethyl)phosphine
TFA	Trifluoroacetic acid
Thr or T	Threonine
Tm	Melting temperature
tRNA	Transfer RNA

Trp or W	Tryptophan
Tyr or Y	Tyrosine
UK	Urokinase
uPA	Urokinase-type plasminogen activator
UV	Ultraviolet
UV-VIS	Ultraviolet-visible
v/v	Percentage by volume
Val or V	Valine
w/v	Percentage by weight
λ	Lambda
$^{\circ}\text{C}$	Degree Celsius
μg	Microgram
μL	Microliter
μm	Micrometer
μM	Micromolar
\AA	Angstrom

Contents

Acknowledgements	i
Abstract	iii
Keywords	iv
Sommario	v
Parole chiave	vi
Abbreviations	vii
Contents	11
Chapter 1 Introduction	13
1.1 Objectives of the thesis	13
1.2 Photomodulation of biomolecules using azobenzene	13
1.2.1 Azobenzene, a brief overview	13
1.2.2 Photocontrol of nucleic acids, lipids and carbohydrates	14
1.2.3 Photoswitchable protein ligands.....	16
1.2.4 Photoswitchable aminoacids	17
1.2.5 Photocontrol of peptides	18
1.3 Directed evolution of photoswitchable peptides.....	25
1.3.1 Selection of cyclic peptides by phage display	26
1.3.2 Directed evolution of light-controlled peptides.....	26
1.4 Streptavidin	28
1.4.1 Structure and interaction with biotin	28
1.4.2 Selection of peptidic streptavidin binders by phage display.....	30
1.5 Urokinase-type plasminogen activator (uPA).....	31
1.5.1 uPA structure and function	31
1.5.2 Selection of peptidic uPA inhibitors by phage display	32
Chapter 2 Synthesis and photochemical properties of oligo-ortho-azobenzenes	35

2.1	Abstract.....	35
2.2	Introduction	35
2.3	Results and discussion	36
2.4	Conclusions	46
2.5	Experimental section	46
Chapter 3	Phage selection of photoswitchable peptide ligands	55
3.1	Abstract.....	55
3.2	Introduction	55
3.3	Results and discussion	56
3.4	Conclusions	61
3.5	Materials and methods	62
Chapter 4	Phage selection of photoswitchable peptides inhibitors of uPA	68
4.1	Abstract.....	68
4.2	Introduction	68
4.3	Results and discussion	70
4.4	Materials and methods	76
Chapter 5	Conclusions	79
5.1	Synthesis and characterization of <i>ortho</i> -substituted azobenzenes	79
5.2	Phage selection of photoswitchable peptides	79
Appendix	82
1.	Supplementary information chapter 2	82
2.	Supplementary information chapter 3	97
3.	Supplementary information chapter 4	98
References		99
Curriculum Vitae		103

Chapter 1 Introduction

1.1 Objectives of the thesis

The possibility to manipulate biomolecules in a spatio-temporal manner is of great interest because it potentially allows to study and control biological processes such as protein-protein interaction, enzyme catalysis and DNA replication. Thanks to their light-inducible isomerization properties, azobenzene-based compounds have been inserted into peptide ligands to control their structure and therefore generate photoswitchable ligands. However, the light-controlled binders reported in literature are generated mainly by rational design and are therefore available only for a restricted number of targets. Furthermore, they often have a low binding affinity and show a rather small change in affinity between the *cis* and *trans* conformation.

The goal of my thesis was to overcome these limitations by developing an *in vitro* evolution strategy which allows the selection of photoswitchable peptide ligands from large combinatorial phage-encoded libraries. Towards this aim I have i) gained experience with azobenzene chemistry by synthesizing and studying several *ortho*-substituted azobenzenes, ii) established the procedures for the chemical modification of phage-displayed peptide libraries with a photoresponsive linker, iii) performed phage display selections against two model targets streptavidin and urokinase-type plasminogen activator (uPA), and iv) isolated light-responsive peptide ligands.

1.2 Photomodulation of biomolecules using azobenzene

1.2.1 Azobenzene, a brief overview

Azobenzene is a diazine in which the hydrogens of the double bond $\text{NH}=\text{NH}$ are substituted by phenyl rings. Its photoisomerization between *cis* and *trans* was first described by Hartley in 1936.¹ The *trans* isomer, characterized by a planar structure, isomerizes to the *cis* conformation upon UV irradiation. Its backisomerization can be mediated by thermal relaxation or by exposure to visible light. The azobenzene absorption spectrum is characterized by two bands: the first one is at around 320 nm and corresponds to the $\pi-\pi^*$ transition (*trans-cis* isomerization) while the second one at around 430 nm corresponds to the $n-\pi^*$ transition (*cis* to *trans* backisomerization) (Figure 1.1).^{2,3}

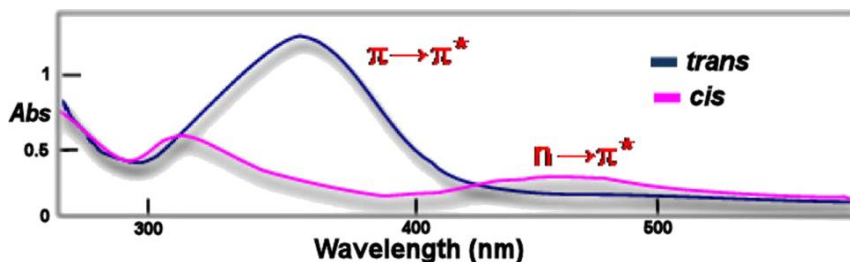


Figure 1.1. Absorption spectrum of an azobenzene compound. Figure taken from Merino et al. 2012.⁴

Two main pathways of $E \rightarrow Z$ isomerization have been reported: rotation and inversion. In the rotation mechanism, the double bond $N=N$ is broken so that the single $N-N$ bond allows the rotation. The inversion mechanism takes place in plane since the $C-N=N-C$ angle is conserved while the $N=N-C$ forms an angle of 180° (Figure 1.2).⁵

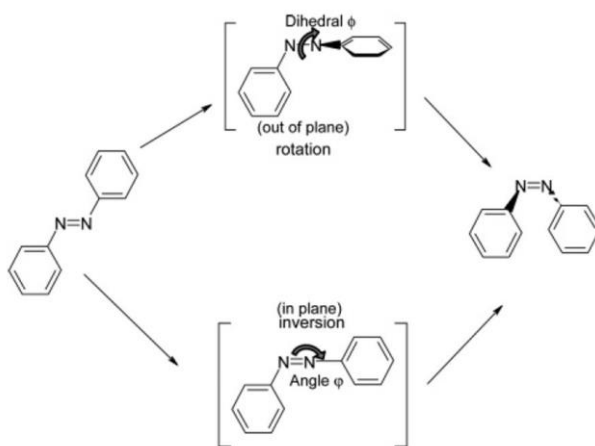


Figure 1.2. Schematic depiction of the mechanism of azobenzene backisomerization (rotation and inversion). Figure taken from Crecca et al. 2006. Permission approved by American Chemical Society (Copyright 2006).⁵

Azocompounds were initially mainly used as dyes and pigments. However, due to their isomerization properties, they have also been applied for the photocontrol of cage-like structures, surfaces and polymers.^{6,7} Recently, the use of azobenzene compounds to regulate structure and function of biomolecules has raised particular interest as it would allow the control of biological processes in a spatial and temporal manner.³

1.2.2 Photocontrol of nucleic acids, lipids and carbohydrates

Several examples of nucleic acids manipulation using azobenzene derivatives have been reported in literature. For example, Nakatani and co-workers proposed a method to induce DNA hybridization of two single strands that would not happen spontaneously. They used an azobenzene molecule linked to two naphthyridine carbamate units that recognize guanidines. The formation of the dsDNA (double-stranded DNA) was allowed only after isomerization to the *cis* conformation and the process could be followed measuring the T_m (melting temperature) (Figure 1.3a).⁸ Komiyama and colleagues were able to modulate the activity of RNase H, an enzyme that is capable of degrading

the RNA only when it is bound to its complementary DNA sequence (antisense DNA). They designed a DNA molecule complementary to the antisense DNA (sense DNA) that included one or multiple azobenzene units. When kept in the darkness, the sense DNA could hybridize with the antisense DNA, keeping it from binding to the RNA (and thereby preventing its degradation). When the azobenzene unit was irradiated, the DNA denatured and the antisense DNA could hybridize with the RNA, allowing its degradation (Figure 1.3b).⁹ The effect of azobenzene isomerization on DNA conformation was further investigated by the Burghardt's group. They generated an azobenzene tethered DNA and showed that both isomers induced perturbation of the helical structure. Nevertheless, the *trans* isomer generated a more stable system thanks to stacking interactions of the azo unit with the base pairs.¹⁰

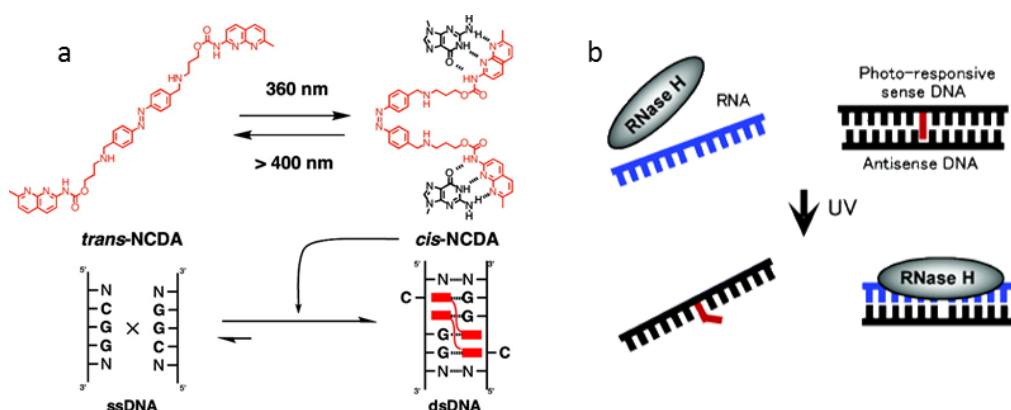


Figure 1.3. a) Azobenzene modified naphthyridine carbamate units interact with guanidines and induce DNA hybridization upon UV irradiation. Figure taken from Dohno et al. 2007. Permission approved by American Chemical Society (Copyright 2007).⁸ **b)** Azobenzene tethered DNA is denatured after *trans/cis* isomerization and is recognized by the enzyme RNase H. Figure taken from Matsugana et al. 2004. Permission approved by American Chemical Society (Copyright 2004).⁹

Photoresponsive phospholipids can be used to alter the structure of cell membranes and to control their biological properties. For instance, membrane permeability is extensively studied for its importance in drug delivery. Engberts and co-workers studied the effect of isomerization on lipid monolayers composed by both azobenzene modified and unmodified phospholipids 1,2-dipalmitoyl-sn-glycero-3-phosphocholine (DPPC). They showed that the *trans* to *cis* isomerization favored interaction with water and therefore induced a higher degree of disorder.¹¹ The same group synthesized and studied single and double-tailed azobenzene-substituted phosphate amphiphiles. Their isomerization to the *cis* form caused an alteration of the packing and this effect was stronger the closer the azobenzene unit was located to the head group.^{12,13} A method to control membrane morphology by light was also recently proposed based on a synthetic azo-amphiphilic. The changes of the vesicles properties were monitored by phase-contrast microscopy. They found that the photoswitch was inducing budding phenomena which could be explained with changes in membrane surface area.¹⁴

The interaction between proteins and carbohydrates is involved in many processes such as target recognitions and it is known to be the result of a complex net of interactions. Jayaraman tried to modulate the binding of carbohydrates to proteins linking an azobenzene core to several sugar units and studying their binding to lectin. They showed that carbohydrates units bound to the protein in a cooperative manner. The affinity was higher when the azobenzene core was switched to *cis* and the backisomerization rate was significantly slow.^{15,16}

1.2.3 Photoswitchable protein ligands

Protein function is often regulated by the binding of a ligand that can act as inhibitor, activator or allosteric modulator. This process can be controlled in a spatial and temporal fashion by conjugating the ligand to an azobenzene unit or, alternatively, by introducing the azobenzene moiety into the protein of interest.³

One of the first examples was reported by Erlanger et al.¹⁷ In this study, the known chymotrypsin inactivator phenylcarbonylchloride was modified with an azobenzene unit to obtain *p*-azophenyldiphenylcarbonylchloride (PADPCC). They showed that the enzyme inactivation was higher after isomerization of the *trans* isomer to the *cis* and that it was totally reversible after complete backisomerization.¹⁷ Few years later the same group described two light-controlled activators of the acetylcholine receptor, a protein which regulates the flux of ions in electrogenic membranes. They first synthesized 3,3'-bis[α -(trimethylammonium)methyl]azobenzene dibromide (Bis-Q). The *trans* form depolarized the membrane with a K_d of around 10^{-7} M while the *cis* counterpart had almost no activity. A similar result was obtained with 3-(α -bromomethyl)-3'-[α -(trimethylammonium)methyl]azobenzene bromide (QBr) which was covalently attached to the receptor by reacting it with the reduced thiol groups of the protein.¹⁸

Trauner and colleagues were able to regulate the inotropic glutamate receptor (iGluR) with photoswitchable moieties. This protein forms channel pores in neuronal cells and it is activated by the binding of glutamate. After structural studies, the agonist was linked to the channel through an azobenzene unit. Upon irradiation at 380 nm and isomerization of the photoswitchable core the ligand bound the receptor causing the opening of the channel and the flow of positive ions (Na^+ , K^+ , Ca^{2+}) (Figure 1.4).¹⁹

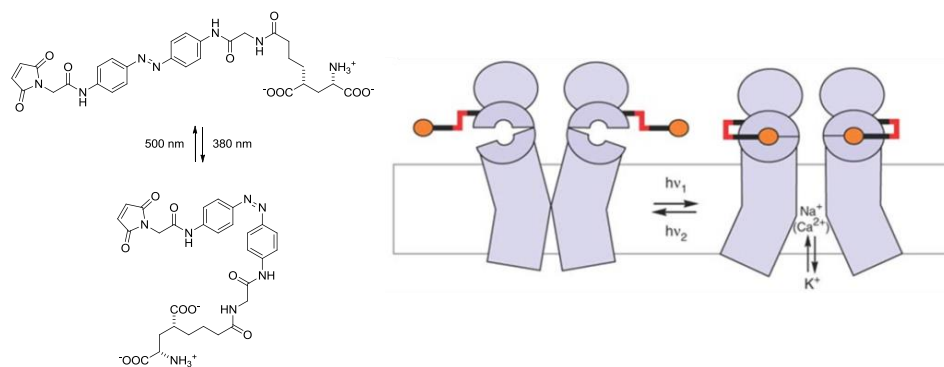


Figure 1.4. Photocontrol of glutamate receptor by a covalently tethered azobenzene agonist. Figure adapted from Volgraf et al. 2006. Permission approved by Nature Publishing Group (Copyright 2006).¹⁹

More recently, the same research group showed how the iGluR can be regulated using red-shifted azobenzene molecules simplifying the use of the photoswitch in biological systems (more information about red-shifted azobenzene linkers in paragraph 1.2.5).²⁰

Gramicidin is a peptide which is known to form channels for monovalent cations in membranes. Woolley and co-workers covalently attached azobenzene moieties at each end of the peptide ion channel without altering its structure. After irradiation at 337 nm a change in current was observed although the channel was not fully blocked.²¹ Azobenzene could also be used to photocontrol antibiotic activity. Recently, the group of Feringa synthesized several photoswitchable antibiotics introducing an azobenzene core in quinolones. The compound that showed the largest difference between the *trans* and *cis* isomer had a MIC of respectively 16 $\mu\text{g}/\text{mL}$ and 2 $\mu\text{g}/\text{mL}$ and the inhibition of bacterial growth could be reverted when incubated in the dark (Figure 1.5).^{22,23}

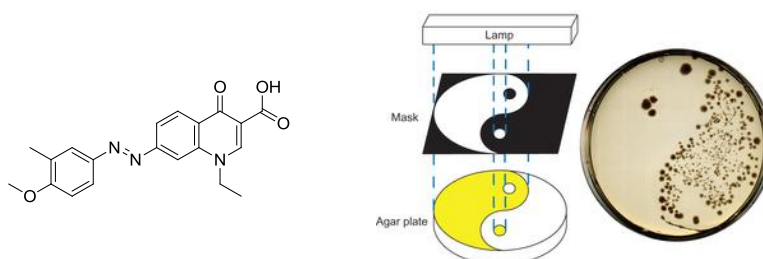


Figure 1.5. The quinolone-based compound (left) showed to inhibit bacterial growth only after irradiation at 365 nm. Figure adapted from Velema et al 2013. Permission approved by Nature Publishing Group (Copyright 2013).²²

1.2.4 Photoswitchable amino acids

In 2005 Schultz reported the incorporation of azobenzene based amino acids into *Escherichia coli* for the photoregulation of the catabolite activator protein (CAP). This protein is a transcription activator that controls several operons in bacteria. The unnatural amino acid was successfully introduced into the protein using an amber codon. The change in affinity of CAP for a promoter containing a CAP binding site was measured and it was shown that after UV irradiation, the azobenzene

modified protein had a 4-fold lower K_b .²⁴ In order to achieve photo-control of enzymes, Woolley tested the effect caused by the introduction of the unnatural amino acid phenylazophenylalanine (PAP) in RNase S. This enzyme can be cleaved in two parts (called peptide S and protein S) by subtilisin causing the loss of its activity. It is known that the activity can be restored establishing a non-covalent interaction between peptide S and protein S. Woolley synthesized several analogs of peptide S introducing PAP at different positions, incubated them with protein S and measured the effect of PAP isomerization on enzyme activity. A maximum of 5-fold difference in the kinetic constant was reached upon irradiation.^{25,26} Mutants of the horseradish peroxidase were generated inserting L-*p*-phenylazophenylalanine (azoAla) at different positions using an *Escherichia coli in vitro* translation system. The study revealed that the activity could be either increased or decreased depending on the azobenzene position and isomerization state. In the case of the mutant Phe179azoAla the enzyme was completely inactive in the *cis* form and the activity was recovered after backisomerization.²⁷ The group of Freitag modified the FLAG tag peptide DYKDDDDK by substituting two or three Asp residues with a photoswitchable amino acid. Two of the tested peptides showed a clear change in affinity for the anti-FLAG-tag antibody M1 of 130 and 300 times respectively after irradiation.²⁸

1.2.5 Photocontrol of peptides

As peptides play a key role in countless biological processes, many attempts have been made in order to control their conformation and binding affinity in a light-controlled fashion. In the last years great effort has been put into the establishment of light regulated systems by the introduction of azobenzene moieties and many examples are reported in literature.

1.2.5.1 Azobenzene-based molecules for the photocontrol of peptides

Many studies have been made to optimize the properties of azobenzene-based linkers used for the photo-regulation of peptides. Several parameters should indeed be considered for the design of new linkers. As the *trans* isomer usually cannot be isomerized to 100% *cis*, it is preferable to produce peptides which affect the target activity only after UV irradiation. The yield of isomerization should be as high as possible to maximize the effect induced by the photoswitch while the half-life reduced or increased depending on the application. For *in vivo* use, higher excitation wavelengths (600-1200 nm) should be considered. It is indeed known that UV-light induces DNA mutations and that at wavelengths lower than 600 nm the tissue penetration is prevented by absorption of endogenous chromophores (i.e. hemoglobin). On the other hand, water absorbs at higher wavelengths ($\lambda > 1200$ nm).²³

(4-amino)phenylazobenzoic acid (APB, Figure 1.6, compound **11**) and (4-aminomethyl)phenylazobenzoic acid (AMPB, Figure 1.6 compound **12**) are the linkers that were first used for peptide cyclization.²⁹ They can be directly incorporated into the peptide backbone. AMPB presents an additional CH_2 spacer to increase both flexibility and length. Upon isomerization the end

to end distance decreases from 12 to 9 Å. The red shift is also reduced due to the disruption of the π -system by the CH₂ group.^{29,30} 3,4- or 3,3-AMPB were also used to induce the desired β -turn geometry of the peptide attached after UV irradiation.³¹

Woolley and co-workers designed several linkers for amino acids side chain modification to introduce the photoswitch into peptides and proteins.³²⁻³⁴ They synthesized symmetric molecules to obtain only one product after peptide modification and reduced at the minimum the number of single bonds between the azo-core and the amino acids to maximize the conformational change upon UV irradiation.³⁵ The first studies were performed using a diiodoacetamide azobenzene (**14**) which allows the cross reaction with two cysteine side chains. The S-S distances were reported to be between 6 and 14.6 Å for the *cis*, 17.1-18.7 Å for the *trans* isomer and a 75% content of *cis* at the pss (photostationary state).³⁶ In order to improve the solubility in aqueous solutions, the water soluble linker 3,3'-bis(sulfonato)-4,4'-bis(chloroacetamido)azobenzene BSBCA (**15**) was synthesized.³² It showed an end-to-end distance of 11-15 Å for the *cis* and 19-23 Å for the *trans*.

To induce a larger conformational change, longer and more rigid linkers were synthesized. Moroder and colleagues used compound **16** which showed an end-to-end distance of 12 Å for the *trans* and 7 Å for the *cis* to modulate collagen unfolding. Another example is represented by 3,3'-diazene-1,2-diylbis{6-[2-sulfonato-4-(chloroacetyl-amino)phenylethynyl]benzene sulfonic acid (DDPBA, Figure 1.6, compound **17**). Its length varies from 30-33 Å (*trans*) to 13-24 Å (*cis*) but unfortunately it showed a low switching efficiency (24% at 20°C).³³ To overcome this limitation Samanta and colleagues synthesized 4,4'-bis(4-(2-chloroacetamido)phenyl)diazanyl biphenyl (BPDB, Figure 1.6, compound **18a**) and 4,4'-bis(4-(2-chloroacetamido)phenyl)diazanyl biphenyl-2,2'-disulfonate (BPDBS, Figure 1.6, compound **18b**), two bis-azobenzene scaffolds. The S-S distance can go from 5 to up to 23 Å and the *cis* isomer can be obtained in 80% yield upon UV-irradiation.³⁴

It is known that the introduction of substituents which stabilize the excited state of azobenzene leads to a red shift of the absorption spectrum (i.e. push pull systems). Sadovski et al. published recently several *ortho*-amino substituted cross-linkers which exhibited high λ_{max} . It was observed that the higher is the red shift, the shorter is the half-life. Compound **19** showed the most prominent red shift (λ_{max} 530 nm) even though its half-life was of only 0.7 sec.³⁷ The group of Andrew Woolley reported that the introduction of bulky electron-rich substituents in *ortho*-position allows the isomerization in high yield (~98%) with irradiation at 630-660 nm (compound **10a,b**). The switching efficiency was confirmed *in vivo* after injection in zebrafish embryos and the chlorinated linker showed resistance to glutathione-mediated reduction. Furthermore, unlike other red shifted azobenzene these molecules exhibited a slow backisomerization rate at 37°C, which ranged from 2 to 45 h depending on the scaffold used.³⁸

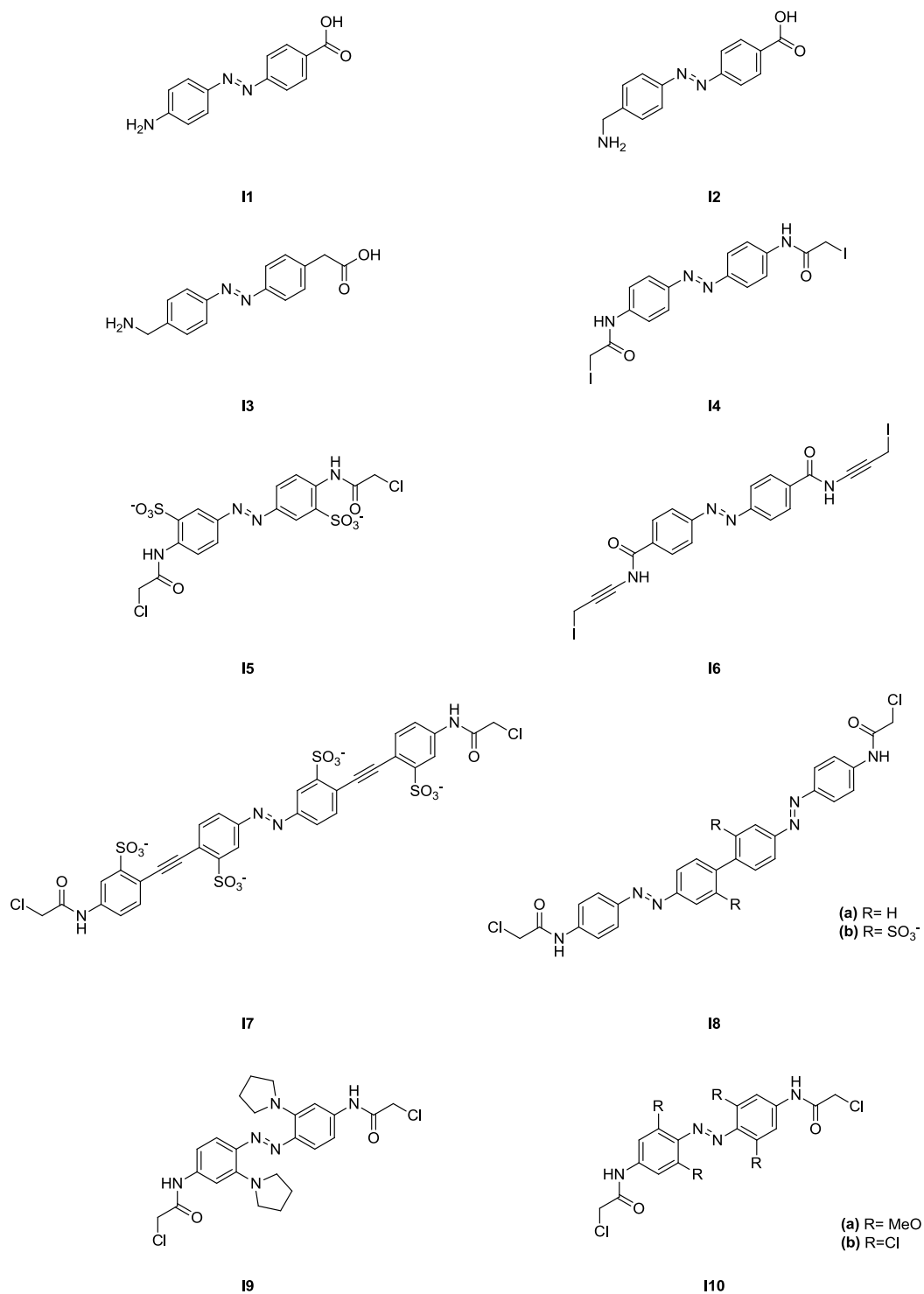


Figure 1.6. Structure of the most used azobenzene-based scaffold for photocontrol of cyclic peptides.

1.2.5.2 Peptides controlled with azobenzene-based molecules

β -hairpin is a well-known secondary protein structure often involved in protein and peptide interactions. Renner and co-workers studied the folding of a β -hairpin peptide based on tryptophan zipper motif (Figure 1.7). They substituted the amino acids naturally forming the β -turn with [3-(3-aminomethyl)-phenylazo]]phenylacetic acid (AMPP) (compound **13**, Figure 1.6). After isomerization to *cis* the azobenzene core was supposed to mimic the β -turn motif.

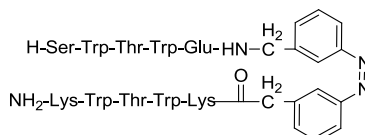


Figure 1.7. β -hairpin decapeptide containing the photoswitchable unit AMPP. Figure redrawn from Dong et al. 2006.³⁹

They demonstrated that after *trans* to *cis* isomerization the tested decapeptide folds into the desired β -hairpin structure.³⁹ Another example of β -hairpin photoswitchable peptide was developed by Beyermann et al. based on the β -finger structure present in the PDZ domain of nNOS (nitric oxide synthase). This motif is fundamental for the interaction of nNOS with α -1-syntrophin. The binding leads to the production of NO that plays a key role in muscle contraction. They generated a cyclic peptide that simulates the nNOS β -finger and incorporated an azobenzene based amino acid. Surface plasmon resonance (SPR) studies showed that the *cis* isomer was able to bind syntrophin with a K_d of 10.6 μ M, while the corresponding *trans* form was almost not binding at all the target protein (Table 1.1 entry 1).⁴⁰ In a following study the same group verified the effect of this cyclic peptide in living skeletal muscle fibers showing that the *cis* isomer inhibits almost completely the fiber contraction.⁴¹ A similar approach was applied to generate photoswitchable somatostatin analogues. Somatostatin is a cyclic peptide involved in several biological processes such as neurotransmission, cell proliferation and regulation of the insulin/glucagon equilibrium. Its activity is determined essentially by four amino acids (Phe-Trp-Lys-Thr) which fold in a β -turn conformation. Ulysse et al. synthesized a cyclic octapeptide containing the sequence Phe-Trp-Lys-Thr and the β -turn conformation was induced by UV irradiation of the incorporated azobenzene unit. The *cis* isomer was found to inhibit the somatostatin receptor with a K_i twice as much potent as the corresponding dark adapted form (Table 1.1, entry 2).⁴²

Azobenzene was also used to modulate other secondary structures such as α -helix. Moroder and collaborators developed a photoresponsive structure based on an octapeptide found in the active site of thioredoxin reductase that presents a 3_{10} -helix conformation. This short peptide was cyclized with 4-(aminomethyl)phenylazobenzoic acid (AMPB) (compound **12**, Figure 1.6) to form a monocyclic peptide. An even more rigid bicyclic structure could be generated by oxidation of the two cysteine residues present in the sequence. NMR studies revealed that the *trans* isomer in the monocyclic format induced a pretzel-like structure, more rigid than the corresponding relaxed *cis* form.

The *trans*-bicyclic peptide also showed a more structured conformation than the *cis* isomer which seemed not to show any structural preference.²⁹ Woolley is one of the main expert in α -helix photomodulation.³⁵ He synthesized different linkers such as diiodoacetamide azobenzene **14** (Figure 1.6) or 3,3'-bis(sulfonato)-4,4'-bis(chloroacetamido)azobenzene (BSBCA) **15** (Figure 1.6) which can react with two cysteine residues introduced at different spacing in the peptide sequence. He showed that, due to the different end to end distance, the helix formation is favored with $i, i+4$ and $i, i+7$ spacing when the linker **14** is in the *cis* conformation and $i, i+11$ if the scaffold is in the *trans* (Figure 1.8)^{3,32,33}

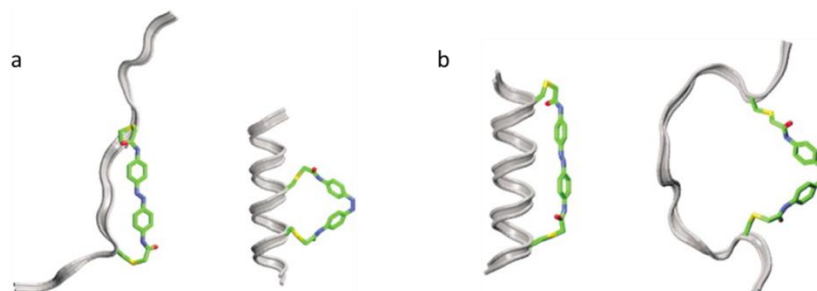


Figure 1.8. Molecular models of peptide cyclized with compound **14** having a) $i, i + 4$ and b) $i, i + 11$ spacings between cysteine residues. Figure taken from Flint et al. 2002. Permission approved by Elsevier (Copyright 2002).⁴³

Recently, the same group published a study in which the photoswitching of a 4,4'-bis(chloroacetamido)azobenzene modified peptide was controlled and monitored *in vivo*. Zebrafish embryos were injected with the compound coupled to fluorescein in order to monitor the isomerization in real time. The proximity of the photoswitchable unit to the fluorophore was supposed to induce a change in the emission upon irradiation. In their system the fluorescence signal decreased during the isomerization to the *cis* form and it increased during the backisomerization proving that the photoswitching took place. *In vivo*, the percentage of *cis/trans* at the photostationary state was confirmed to be the same than *in vitro* while the half-life was 25% lower.⁴⁴

Bcl-XL is an antiapoptotic protein which was shown to have a role in cancer progression together with other members of the Bcl-2 family such as Bak and Bid. Structural studies revealed that Bak binds to Bcl-XL through an amphipathic helix. Alleman et al. designed several peptides based on Bak fragment responsible for Bcl-XL recognition.⁴⁵ The peptides were synthesized with different cysteine spacing and cyclized with BSBCA **15** (Figure 1.6) to modulate the helix content and therefore the affinity for Bcl-XL upon isomerization of the linker. The binding of the different formats and isomers to the target protein Bcl-XL could be controlled by UV irradiation and were measured by fluorescence polarization.⁴⁵ The K_d values are reported in table 1.1, entry 3. Several groups generated photoswitchable RGD (Arg-Gly-Asp) peptides to control cell adhesion that is important in biological processes such as immunological response, tissue healing and metastasis. Moroder and collaborators for example synthesized a heptapeptide cyclized with AMPB containing the well-known integrin binding motif RGD. The binding affinity of the two isomers for $\alpha V \beta 3$ integrin was measured by SPR (surface plasmon resonance). They were able to demonstrate that the *cis* form had a 40% lower

binding affinity than the dark adapted isomer (Table 1.1, entry 4).⁴⁶ Another example was reported by Kessler and coworkers. Several cyclo RGD peptides containing the 4-[(4-aminophenyl)azo]benzocarbonyl linker were synthesized. It was shown that the *trans* form induced higher cell adhesion than the corresponding UV irradiated isomer (Table 1.1, entry 5).⁴⁷

In another approach, Liskamp and colleagues used azobenzene moieties in order to control mast cell degranulation. This cellular process is activated by the binding of two SH2 domains of the spleen tyrosine kinase Syk to ITAM (Immunoreceptor tyrosine-based activation motif). They synthesized several ITAM analogs introducing photoswitchable units of different lengths to modulate their binding to the SH2 domains upon UV irradiation. After isomerization of the shortest azobenzene linker to the *cis* conformation, the affinity decreased of 4-fold. They also demonstrated that in the case of molecules smaller than the wild type ITAM, the *cis* and the *trans* isomers bind the SH2 domains in a monovalent or divalent manner respectively (Figure 1.9).⁴⁸

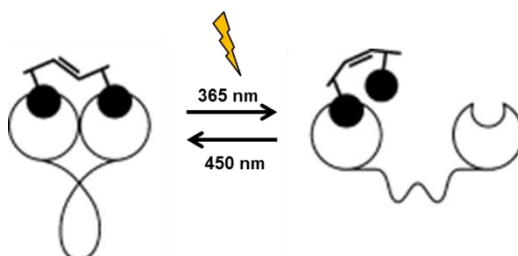


Figure 1.9. Schematic representation of Syk tSH2 switching between a divalent and a monovalent binding as a result of isomerization of short linkers. Figure modified from Kiul et al. 2009. Permission approved by Wiley (Copyright 2009).⁴⁸

Recently, the groups of Giralt and Gorostiza showed that clathrin-mediated endocytosis, which has a role in many cell processes such as cell signaling regulation and surface protein expression, can be modulated by UV light. They generated photoswitchable inhibitors of protein-protein interactions (PIPPIs) which bind AP2, a well-known protein involved in endocytic trafficking. They designed the binders based on the C-term of β -arrestin which interacts with AP2 thanks to an α -helix secondary structure. Based on this sequence, they synthesized peptides with different spacing between two cysteine residues and cyclized them with BSBCA 15 to regulate the helix content upon UV light irradiation. They obtained peptides that presented higher inhibitory activity either in the *trans* or in the *cis* conformation depending on the format ($i,i+11$ and $i,i+7$). The K_i values are reported in table 1.1, entry 6.⁴⁹

Chapter 1. Introduction

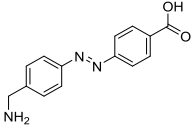
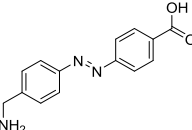
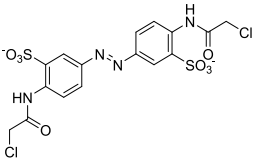
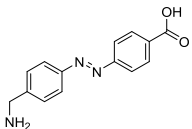
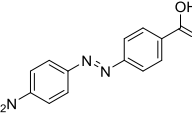
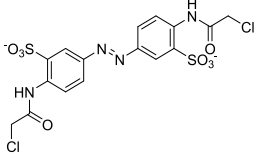
Entry	Scaffold	Cyclic Peptide	Target	Binding/Inhibition
1		14 aa LTTF β -finger binding motif	α -1-syntrophin	K_d <i>cis</i> = 10.6 μ M K_d <i>trans</i> = no binding
2		8 aa FTKT β -turn binding motif	Somatotropin release-inhibiting factor (SRIF) receptor	K_i <i>cis</i> = 1 μ M K_i <i>trans</i> = 2.6 μ M
3		Bak72-87(<i>i</i> +7) BaK 72-87(<i>i</i> +11) Bid91-111(<i>i</i> +4)	Bcl-xL	K_d [nM] Bak72-87(<i>i</i> +7) BaK 72-87(<i>i</i> +11) Bid91-111(<i>i</i> +4) linear 134 \pm 16 328 \pm 19 117 \pm 48 <i>trans</i> 825 \pm 157 21 \pm 1 1275 \pm 139 <i>cis</i> 42 \pm 9 48 \pm 10 55 \pm 4
4		7 aa RGD binding motif	$\alpha\beta$ 3 Integrin	Values not shown <i>trans</i> 50% stronger binding than <i>cis</i>
5		5 aa RGD binding motif	PMMA surfaces	<i>cis</i> = same as uncoated surface <i>trans</i> = 17% enhancement
6		<i>i</i> +11 aa (<i>trans</i> bound) <i>i</i> +7 aa (<i>cis</i> bound)	AP2 (β -adaptn)	TL-1 <i>trans</i> bound K_i TL-2 <i>cis</i> bound K_i <i>trans</i> 8 \pm 1 240 \pm 150 <i>cis</i> 31 \pm 3 19 \pm 0.3

Table 1.1. Summary of K_i/K_d of the photoswitchable cyclic peptides inhibitors/binders before and after irradiation.

1.3 Directed evolution of photoswitchable peptides

In vitro evolution of proteins and peptides is a powerful method for discovery and development of biomolecules such as therapeutics, biosensors and catalysts.⁵⁰ Rational drug design requires deep knowledge of the structure of the target protein and of their interaction partners. The binders have to be accurately designed since only few of them can be produced and tested.⁵¹ On the other hand combinatorial strategies allow the simultaneous screening of billions of compounds through iterative cycles of selection and amplification.⁵²

Phage display technology is a revolutionary *in vitro* technique which allows the screening of large combinatorial polypeptide libraries for the selection of binders to virtually any target.⁵³ Classically, the libraries are generated so that every phage particle displays on its surface one or several copies of different polypeptides fused to the coat protein. The library is subjected to iterative cycles of affinity selection against the target of interest and amplification of the isolated binders. The linkage between genotype and phenotype consents the fast identification of the ligands by PCR amplification and DNA sequencing (Figure 1.10).

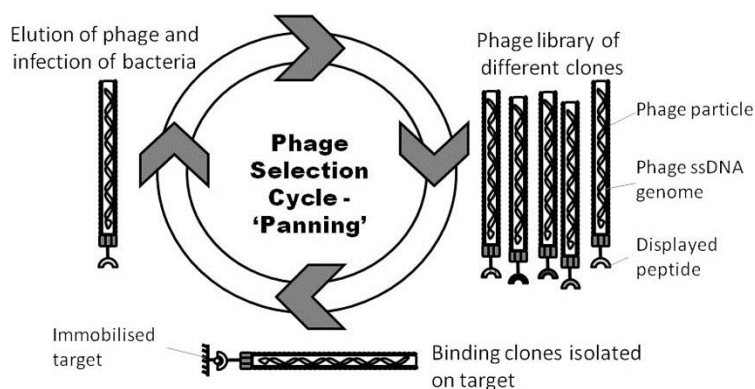


Figure 1.10. Phage display selection process. The phage library containing billions of different clones is panned against the immobilized target. The bound clones are eluted, amplified and subjected to the following cycle. Image modified from Ullman et al. 2011. Permission approved by Oxford University Press (Copyright 2011).⁵⁴

The most common strains of phage employed for display technologies are f1, M13 and fd. They infect gram negative bacteria from which they are secreted without causing their lysis. The genome of about 6.4 kbp is coded by single stranded DNA and encapsulated in a tubular structure constituted by five coat proteins: pIII, pVI, pVII, pVIII, pIX. Classically, pVIII and pIII are mainly used to display proteins. pVIII is the major coat protein and it is found in several thousands of copies per virion. However, to preserve its functionality, only short peptides (6-8 residues) can be fused to it. pIII is a minor coat protein and 3 to 5 copies are expressed at the tip of the phage particle. It is usually preferred since it allows the introduction of large inserts at its N-term and it is compatible with monovalent display.⁵⁵

1.3.1 Selection of cyclic peptides by phage display

Peptides offer an attractive format for the development of therapeutics. Peptide ligands evolved by phage display can bind with high affinity and selectivity to protein targets. Furthermore, peptides are accessible to chemical synthesis and due to their small size, they can diffuse into tissues. It is generally preferred to develop cyclic rather than linear peptides for the following reasons. The cyclic format allows the formation of constrained structures with reduced entropy, higher binding affinity, selectivity and stability to proteolytic cleavage. The most common way of generating cyclic peptides on phage is to oxidize a pair of cysteines present in the sequence forming a disulfide bridge. Classically, the phage-encoded peptide libraries present the format CX_nC , where the peptide contains n random amino acids (X) flanked by two cysteine residues (C). The format $X_1CX_mCX_n$ has also been widely used. In order to increase the number of interaction sites between the peptide and the target, several random positions can be inserted at both ends. For example libraries with the format $XCX_{4,6,8}CX$ were generated and screened for the binding to different monoclonal antibodies.⁵⁶

Peptides cyclized with one disulfide bridge could be isolated against a wide range of protein targets. However, most of these monocyclic peptides displayed rather weak binding affinities (micromolar range). Christian Heinis in collaboration with Sir Greg Winter had developed a method to screen libraries of bicyclic peptides by phage display.^{53,57,58} Linear peptides containing three cysteine residues spaced by random amino acids are cyclized using the linker tris-(bromomethyl)benzene (TBMB) (Figure 1.11). Compared to the monocyclic, the more rigid bicyclic format is expected to induce a higher binding affinity. Furthermore, in this peptide format, two peptide rings can interact with protein targets and the resulting affinity is higher.

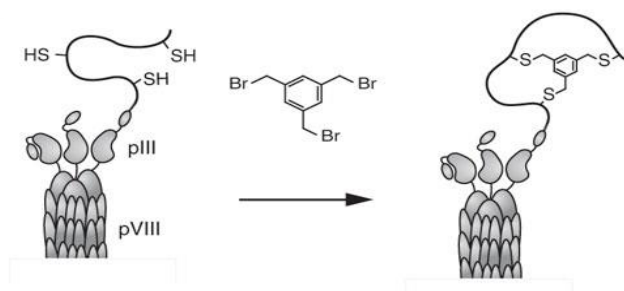


Figure 1.11. Cyclization of peptide containing three cysteine residues with tris-(bromomethyl)benzene. Image modified from Heinis et al. 2009. Permission approved by Nature Publishing Group (Copyright 2009).⁵³

1.3.2 Directed evolution of light-controlled peptides

As described above, many of the photocontrolled protein and peptides described in literature were obtained by molecular design. Only recently, two strategies were developed for the *in vitro* evolution of photoswitchable peptide ligands and they will be described in the following two paragraphs.^{59,60}

Liu et al. proposed in 2012 a method for the selection of peptides containing non-natural photoswitchable amino acids using ribosome display.⁶⁰ A tRNA carrying the amber anticodon was linked to an azobenzene-containing modified lysine residue and was mixed with mRNA encoding a peptide library to allow protein translation using the PURE SYSTEM technology. The library was incubated with the model target streptavidin for half an hour and the non-binders were removed. In order to select for *trans* binders, the solution was irradiated with UV light to induce the isomerization and therefore the release of the peptides binding in the *cis* form (Figure 1.12). The isolated clones were collected and sequenced after RT-PCR. 81 clones were identified.

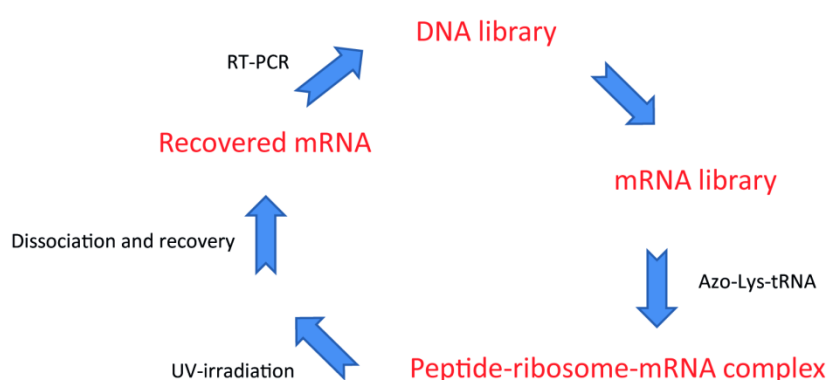


Figure 1.12. Ribosome display strategy for the selection of photoresponsive peptide aptamers reported by Liu et al 2012.

Only the sequences LA37 VLIMVAVXASS and LA40 HSCXVTIDVFF (where X indicates the modified lysine residue) were found several times. Additionally, five clones had incorporated two non-natural amino acids suggesting that they could show the largest conformational change. Peptides LA81 (sequence GVTXRRFIXYV), LA37 and LA40 were synthesized with the FLAG sequence DYKDDDDKA and tested for binding to streptavidin with an anti-FLAG antibody in an ELISA assay. The fluorescence intensity in the ELISA assay dropped 50% after UV irradiation. Overall, the efficiency of the method was not well evaluated as the binding affinity of the isolated peptides was not reported. The change in binding observed in the ELISA assay is only moderate.

Recently, the group of Derda reported the first example of phage selection of light-responsive peptides. Their goal was to isolate ligands binding the protein target in *trans* conformation and released after UV irradiation. A phage encoded library displaying heptamers flanked by cysteine residues (format CX₇CA, diversity of 2×10^8) was first reduced using immobilized TCEP and afterwards cyclized with the azobenzene reagent BSBKA. Affinity selection was performed against the model target streptavidin. In a control experiment, the phage panning was carried out with unmodified phage peptide. A scheme of the general selection strategy is reported in figure 1.13.

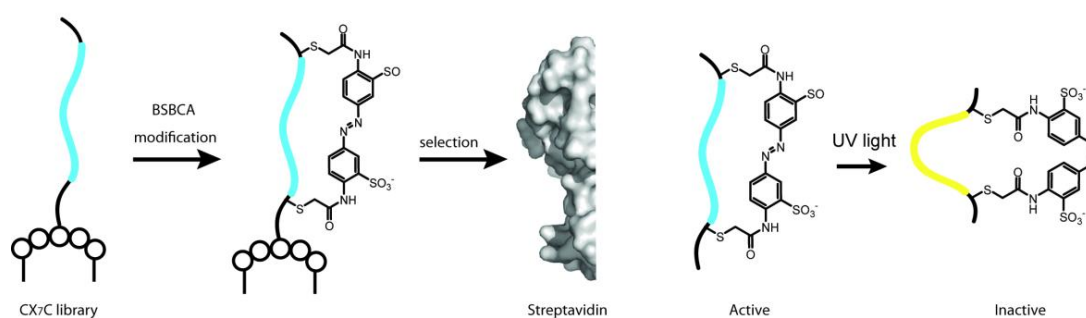


Figure 1.13. Phage display selection strategy applied by Derda et al. for the isolation of light-responsive cyclic peptides.⁵⁹

After three iterative rounds of selection 80 clones were sequenced and only 48 contained the insert. No consensus sequence was identified. The binding to streptavidin was measured by phage ELISA for the BSBCA-modified peptides, and in parallel for the disulfide cyclized peptides. Only three clones (P36, P42, P57) showed a significant affinity after BSBCA cyclization. To verify whether the binding of these ligands could be photo-modulated, they were subjected to an ESI-MS binding assay before and after UV irradiation. A peptide selected in the unmodified population presenting the streptavidin binding motif HPQ was also tested (P81). As additional control a peptide (P5) classified as “non-binder” was tested too. The table summarizing the K_d values is shown below (Table 1.2).

S-S peptides			BSBCA peptides		
peptide	sequence	K_d (μM)	K_d^{dark} (μM)	K_d^{light} (μM)	ΔK_d
P5	ACMSNKYSLCG	> 2000	> 2000	> 2000	N/A
P36	ACGFERERTCG	> 2000	452±63	> 2000	> 4.5
P42	ACLSQRDGNCG	> 2000	368±103	814±55	2.2
P57	ACSVKLHTHCG	> 2000	506±89	1223±201	2.4
P81	ACTSHQPRVCG	158±76	229±21	239±41	1.0

Table 1.2. Table summarizing the K_d values determined by ESI-MS binding assay.⁵⁹

All the measured K_{ds} were in the high micromolar range and the best ligands exhibited a 4.5-fold difference of affinity between the *trans* and the *cis* conformation. Overall, the binding affinities of the peptides were rather low. Previously, several groups had isolated disulfide cyclized peptides against streptavidin and the affinities of those peptides were nearly 1000-fold better.

1.4 Streptavidin

1.4.1 Structure and interaction with biotin

Streptavidin is a tetrameric protein of 159 amino acids (molecular weight ~64kDa) which was first isolated in 1963 during a screening of new antibacterial molecules produced by *Streptomyces avidinii* that are active against gram negative bacteria.⁶¹ Due to its highly specific and strong

binding affinity for the vitamin biotin ($K_d \sim 10^{-15}$ M), this protein has been extensively used in molecular biology and chemistry.⁶² The most common applications include protein purification,⁶³ diagnostic and immunological assays, microscopy, protein and nucleic acids detection.⁶⁴ Its tetrameric structure can be considered as a dimer of dimers. Each streptavidin subunit is constituted by an eight-stranded antiparallel β barrel (Figure 1.14).⁶⁵ Two monomers are associated tightly through van der Waals interactions and every pair of barrel is further organized in dimers weakly stabilized by hydrogen bonds and van der Waals interactions.^{66,67}



Figure 1.14. Crystal structure of tetrameric streptavidin. PDB file 1NBX.⁶⁵

The binding of biotin to streptavidin has been characterized and studied by X-ray crystallography. The biotin binding pocket is localized in the dimer-dimer interface so that every tetramer can bind up to four biotin molecules. The ureido oxygen of biotin forms H-bonds with the residues Asn-23, Ser-27 and Tyr-43, the ureido amino groups with Ser-45 and Asp-128, the sulfur with Thr-90 and the carboxyl group with Asn-49 and Ser-88. The thiophene ring and the alkyn chain establish van der Waals interactions with the hydrophobic part of the pocket composed by Trp-79, -92, -108, -120, Leu-25, Val-47, Leu-110 and by Trp-120 of the adjacent subunit (Figure 1.15).

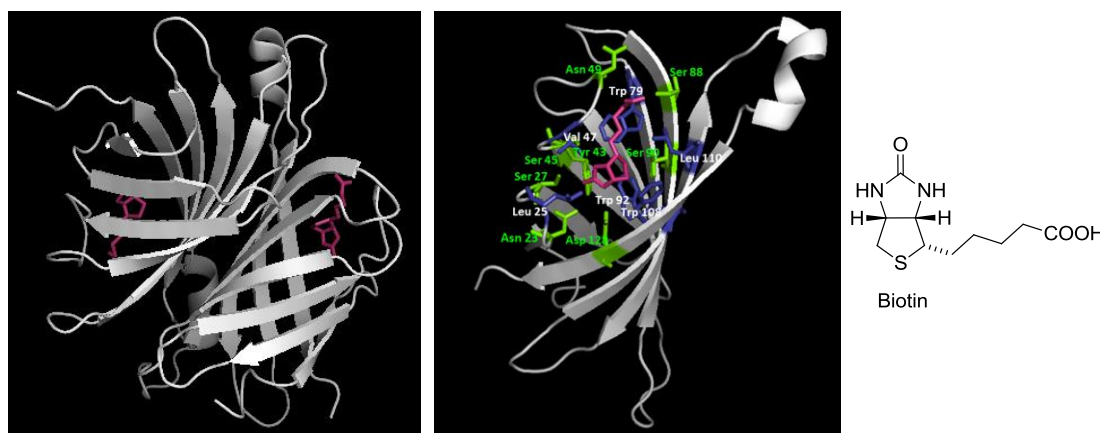


Figure 1.15. i) X-ray structure of biotin in magenta bound to a subunits dimer in gray (left). ii) Biotin (magenta) bound to a streptavidin monomer (right). The residues forming H bonds are represented in green, the amino acids involved in hydrophobic interactions are shown in dark blue. PDB file 3RY2.⁶⁵

1.4.2 Selection of peptidic streptavidin binders by phage display

Classically, drug synthesis and development is based on the structure of the natural protein binders. In the case of streptavidin, several studies have been performed using an opposite approach: the analysis and the characterization of its natural non-peptide ligand have been used as starting point for the development of peptide binders. The comparison of the mechanism with which two different molecules binds to the same pocket can indeed reveal important information applicable to rational drug design.⁶⁸

Giebel et al. performed phage display selection against streptavidin using three cyclic peptide libraries with the format CX₄C, CX₅C and CX₆C.⁶⁹ It was shown that the disulfide bridge constrained peptides had a much higher binding affinity than the linear ones that are characterized by a high degree of flexibility and therefore elevated entropy.^{68,69} Many of the peptides identified as streptavidin binders showed the HPQ motif which is known to bind the biotin binding pocket.^{69,70}

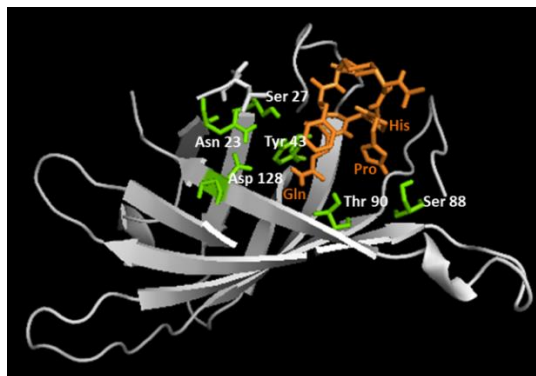


Figure 1.16. Crystal structure of peptide cyclo-Ac-CHPQFC-NH₂ (orange) complexed with a streptavidin monomer. The protein residues involved in the formation of H bonds are represented in green. PDB file 1SLD.⁷⁰

Figure 1.16 shows the key streptavidin residues (Asn-23, Ser-27, Tyr-43, Ser-88, Thr-90, Asp-128) which establish hydrogen bonds with the peptide cyclo-Ac-CHPQFC-NH₂. Crystallographic studies demonstrated that the Gln side chain of the HPQ sequence is partly superimposable to biotin. Furthermore, the amino acids flanking the HPQ binding motif can increase the number of interactions playing a role in the binding.^{70,71} A second consensus (EPDW) was isolated using a phage display library of linear decapeptides.⁷¹ This motif shared similarities with a previously published streptavidin binder GDWVFI.^{72,73} A well-known tag used for protein purification called Strep-tag® (sequence AWRHPQFGG, K_d: 10⁻⁵ M) was also selected from a genetically encoded peptide library.^{74,75} Its sequence was further optimized thanks to crystallographic studies and rational design. Strep-tag II® (sequence: NWSHPQFEK) which binds Strep-Tactin® (a genetically modified streptavidin with higher binding capacity) with a K_d of 1 μM was obtained.⁶³

1.5 Urokinase-type plasminogen activator (uPA)

1.5.1 uPA structure and function

Human uPA is a serine protease produced and secreted as a pro-enzyme, also called (sc) uPA (single chain uPA), a protein of 411 amino acids with low proteolytic activity (MW ~ 54 kDa). It is converted to its active form (tc) uPA (two-chain u-PA) through the proteolytic cleavage of the peptide bond between Lys-158 and Ile-159. The two corresponding chain A (residues 1-158) and chain B (residues 159-411) are linked by a disulfide bridge (Cys-148 and Cys-279). Its active site is composed by the catalytic triad His-57, Asp-102, Ser-195 located in the chain B (Figure 1.17). The A chain of the tc form is further cleaved between the residues Lys-135 and Lys-136 originating a new truncated form called LMW-uPA (low molecular weight uPA).⁷⁶

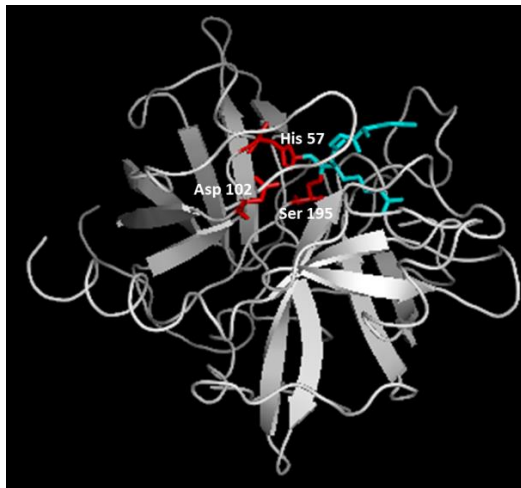


Figure 1.17. X-ray structure of uPA catalytic triad His-57, Asp-102, Ser-195 (red) complexed with the inhibitor Glu-Gly-Arg chloromethyl ketone (cyan). PBD 1LMW.⁷⁶

uPA is involved in the plasminogen activation system. It binds to urokinase-type plasminogen activator receptor in its zymogen form. Once uPA is activated, it cleaves plasminogen converting it to plasmin which mutually cleaves pro-uPA. Plasmin further participates to the degradation of the extra cellular matrix, fibrinolysis and activation of the matrix metalloproteinases cascade. This system is negatively regulated by two uPA inhibitors, the serpins PAI1 and PAI2 and by α 2-antiplasmin responsible for the inhibition of plasmin.⁷⁷ Due to its essential function in tissue remodeling, it plays a crucial role in cell migration, proliferation and invasion. uPA was indeed found to be overexpressed in many pathologies such as inflammation and cancer becoming an interesting drug target.^{78,79}

1.5.2 Selection of peptidic uPA inhibitors by phage display

Numerous protein or peptide based inhibitors of uPA have been identified by phage display technology. The group of Dario Neri isolated an uPA inhibitor from an antibody phage display. Unfortunately it did not show any effect *in vivo*, probably due to the low penetration rate into tumors tissues.⁸⁰ Andreassen et al. selected from a phage-encoded peptide library upain-1, a disulfide bridge cyclic peptide of twelve amino acids which inhibits u-PA with a K_i of around 7 nM.⁸¹ UK18, a highly potent and selective bicyclic peptide inhibitor cyclized with 1,3,5-tris(bromomethyl)benzene (TBMB) was discovered in our laboratory ($K_i = 53$ nM). The crystal structure of the UK18-uPA complex (Figure 1.18) revealed high similarities to protein-protein interaction: the peptide is constrained and it has a large contact interface stabilized by 14 H-bonds.⁵⁷ The substitution of L-Ser with D-Gly improved its proteolytic stability 4-fold and its inhibitory activity 1.8-fold.⁸²

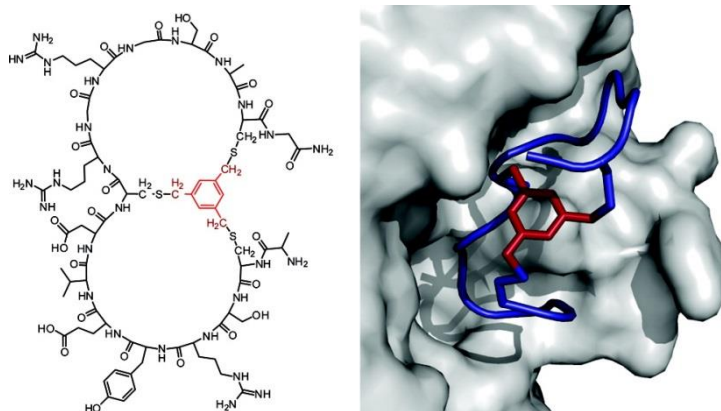


Figure 1.18. Bicyclic peptide inhibitor UK18 and crystal structure of its complex with uPA. Figure taken from Angelini et al.2012. Permission approved by American Chemical Society (Copyright 2012).⁵⁷

Recently, several lab members performed phage selection against uPA using different linkers such as 1,3,5-triacryloyl-1,3,5-triazinane (TATA), and *N,N,N'*-(benzene-1,3,5-triyl)tris(2-bromoacetamide) (TBAB) (Figure 1.19).

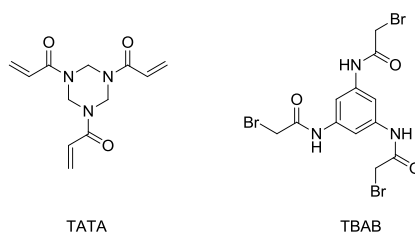


Figure 1.19. Structure of TATA and TBAB.

It was found that the use of different chemical linkers leads to the isolation of diverse consensus sequences and that their interaction with peptides stabilizes the conformation and promote the isolation of high affinity binders (Figure 1.20).⁵⁸

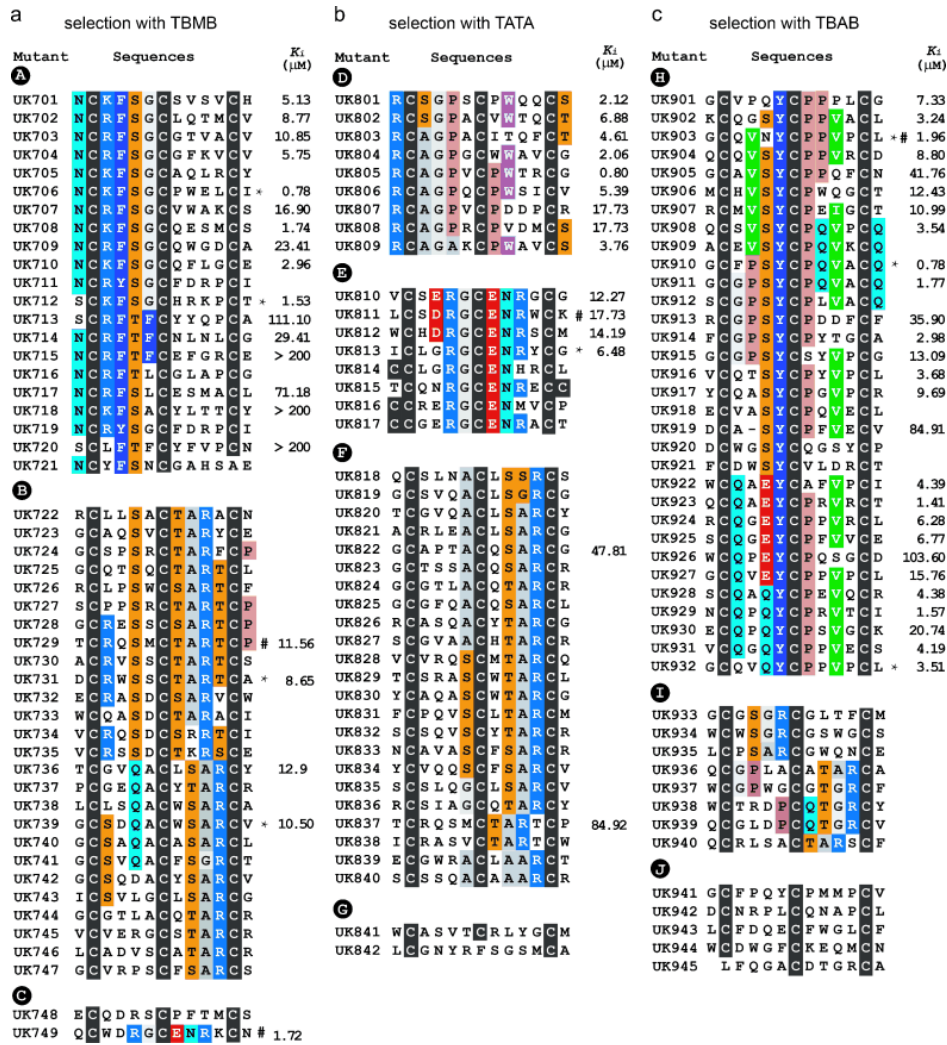


Figure 1.20. Peptides isolated by phage selections against uPA from the XCX₄CX₄CX library after modification with the linkers TBMB (a), TATA (b), and TBAB (c). The consensus sequences are highlighted in colours. The figure is taken from Chen et al. 2014. Permission approved by Wiley (Copyright 2014).⁵⁸

In another work, panning of a peptide library with the format XCX₄CX₄CX against uPA yielded many peptides with four cysteines (Figure 1.21). A study of the isolated peptides revealed that pairs of cysteines formed disulfide bridges. The peptides had thus bicyclic structures based on two disulfide bridges.⁸³

Chapter 1. Introduction

A Cyclization by oxidation				B Cyclization with TBMB			
Mutant: Amino acid sequences	#	K_i (μM)		Mutant: Amino acid sequences	#	K_i (μM)	
UK501 1 2 3 4 5 6 7 8 9 10 11 12 13 C C R E R G C E N M V C P	8	4.3		UK537 1 2 3 4 5 6 7 8 9 10 11 12 13 N C R F S G C G T V A C V	2	10.9	
UK502 C C R E R G C E G Q V C P				UK538 N C R F S G C L Q T M C V	2	8.8	
UK503 C C S E R G C E N V F C G				UK539 N C R F S G C V W A K C S			
UK504 C C L G R G C E N H R C L	4	7.7		UK540 N C K F S G C S V S V C H		5.1	
UK505 C C Q G R G C E N T W C V				UK541 N C K F S G C P W E L C I		0.8	
UK506 C C L D R S C D G L M C I				UK542 N C K F S G C Q F L G C E			
UK507 C C R E P P C Y N P L C I		73.8		UK543 S C K F S G C H R R K P C T			
UK508 C C G Q A P C Y L P A C G		299.7		UK544 N C K F S A C Y L T T C Y			
UK509 G C C V S G C G Y M S C G				UK545 N C R F T L C G L A P C G			
UK510 W C S C R G C E N G G C R		82.7		UK546 S C L F T F C Y F V P C N			
UK511 S C G C R G C E N R F C A		118.8		UK547 N C R Y S G C F D R P C I			
UK512 Q C P M D C C S R G L C W		67.1		UK548 G C Q T S Q C T A R T C L		8.6	
UK513 Y C P Q D C C S R H V C M				UK549 D C R W S S C T A R T C A			
UK514 G C P D D C C S R G L C L		50.3		UK550 G C R E S S C S A R T C P			
UK515 S C V R G G C C G S A C G				UK551 V C R Q S D C S R R T C I			
UK516 V C P Q D G C A V C P C R				UK552 E C R A S D C S A R V C W			
UK517 N C L Y S G C L Q V G C C		> 1000		UK553 R C L P S W C S A R T C F			
UK518 N C L F A G C L G S M C C				UK554 R C L L S A C T A R A C N			
UK519 N C L F S A C Q G L T C C				UK555 G C A Q S V C T A R Y C E			
UK520 N C T A R S C A S P D C C				UK556 I C S V L G C L S A R C G		10.5	
UK521 Y C N T A R C G Q A Y C L		> 1000		UK557 G C S D Q A C W S A R C V			
UK522 G C G T G R C G Q V W C T				UK558 G C S V Q A C F S G R C T			
UK523 V C V T A R C Q L Q W C L				UK559 T C G V Q A C L S A R C Y	2	12.9	
UK524 V G R L S Y C S A R T C P				UK560 P G E Q A C Y T A R C R			
UK525 Y C S M D P C G T G R C R		444.7		UK561 L C L S Q A C W S A R C A			
UK526 D C L V T Y C P Q V R C Q				UK562 V C V E R G C S T A R C R			
UK527 L C A L R G C E N R S C S				UK563 L C A D V S C A T A R C R			
UK528 N C K Y S L S A S S D C Q				UK564 E C Q D R S C P F T M C S			
UK529 M C N A Y F A G D L C	2			UK565 N C Y F S N C G A H S A E			
UK530 V C S I Y F A L G C							
UK531 R C I S S A R M G T L C S							
UK532 V C A V G G R L Q E N C L							
UK533 N C K Y T L C S G V L W		> 1000					
UK534 L F Q G A C D T G R C A	2						
UK535 R C D R C R							
UK536 G C S V Y F T C Q							

Figure 1.21. Phage selection of bicyclic peptides against u-PA. The peptides were isolated from the XCX₄CX₄CX library cyclized either by oxidation (A) or by modification with TBMB (B). Consensus sequences are highlighted in colours. The figure is taken from Chen et al. 2013. Permission obtained from American Chemical Society (Copyright 2013).⁸³

Chapter 2 Synthesis and photochemical properties of oligo-*ortho*-azobenzenes

This chapter is based on the following publication. Bellotto S., Reuter R., Heinis C., and Wegner H.A. Synthesis and photochemical properties of oligo-*ortho*-azobenzenes. J. Org. Chem. 2011, 76: 9826-9834. Reprinted with permission from the American Chemical Society. Copyright 2011.

2.1 Abstract

Azobenzenes have attracted great interest in recent years due to their ability to change conformation upon irradiation. This property has been featured in several applications not only in organic chemistry but also in biology. Even though mono-azobenzenes have been extensively studied and documented in literature, only few methods are available for the synthesis of oligo-*ortho*-azobenzenes. Also, their photochemical properties have not been reported so far. This study shows an efficient strategy for the preparation of oligo-*ortho*-azobenzenes and the investigation of their photochemical properties. It is demonstrated that the absorption spectra are highly influenced by the substituents. Interestingly, none of the *ortho*-bis-, tris- or tetra-azobenzene showed any *E* → *Z* isomerization. Only the *ortho*-nitrogen substituted mono-azobenzenes photochromic behavior upon UV irradiation was observed.

2.2 Introduction

Since their discovery in the nineteenth century, azocompounds have been extensively used as dyes and pigments.¹ Therefore, several synthetic strategies have been developed to prepare azobenzene derivatives. Among all, the most relevant and common methods found in literature are the oxidation of anilines, reduction of nitro-substituted aromatic compounds, the Mills reaction⁸⁴ (condensation of an aniline with a nitroso compound) and the diazo-coupling via diazonium salts.⁸⁵ Re-

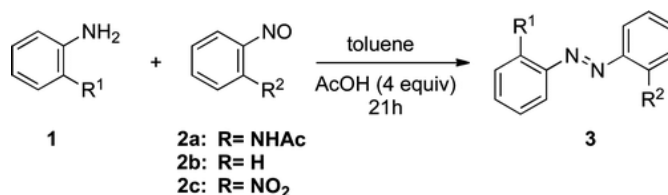
cently, a new synthetic strategy was proposed, in which a Pd-catalyzed coupling reaction was employed.⁸⁶ Additional to their use as colorants, a well-known property of azobenzenes is the photoisomerization from the *E* to the *Z* isomer and back.⁸⁷ The two isomers can be switched with ultraviolet light. The more intense absorption at 320 nm corresponds to the $\pi\text{-}\pi^*$ (S_2 state) transition and irradiation at this wavelength leads to $E \rightarrow Z$ isomerization, while the *Z* isomer absorbs at longer wavelength, around 430 nm which is due to the $n\text{-}\pi^*$ (S_1 state) transition inducing $Z \rightarrow E$ isomerization. Since the *E* isomer is more stable by approximately 50 kJ/mol, the *Z* isomer can also easily relax back via $Z \rightarrow E$ isomerization upon heating.⁸⁸ Upon UV irradiation the distance between the *para* carbon atoms decreases from about 9.0 Å in the *E* isomer to 5.5 Å in the *Z* form.⁸⁹ Thanks to this property, azo compounds have been employed for different uses and applications such as in light controlled polymers,⁹⁰ liquid crystals,⁹¹ surfaces,⁹² catalysts⁹³ and more recently resulted to be really promising in controlling the structural and functional changes in biomolecules. Azobenzene derivatives, indeed, have been used for the photoswitching of proteins, like ion channels and receptors and for the photo-control of peptides,³⁴ nucleic acids, lipids and carbohydrates.³

Compounds containing isolated azobenzenes have been already thoroughly investigated;^{5,94,95} the interplay of multiple azobenzenes, however, has only been scarcely addressed. Bléger *et al.* investigated the photochromic and thermochromic behavior of four different *para*-bis(azo) connected by biphenyls.⁹⁶ Furthermore, the photochemical properties of a *meta*- and a *para*-bis(azo) derivative have been studied and compared. It has been shown that while the (*E,E*)-*m*-bisazobenzene has a similar behavior to the (*E*)-azobenzene, the (*E,E*)-*p*-azobenzene presents a red shift in the absorption spectrum and a lower photoreactivity upon UV-irradiation.⁹⁷ The corresponding *ortho*-bis azobenzenes, though, have not been investigated so far. One explanation might be the difficulties in the preparation of these structural themes with the known methods, making their synthesis quite challenging. Only a few examples have been reported in the literature. At the end of the nineteenth century Mendola published a diazotization by sodium nitrite.⁹⁸ The synthesis of *ortho*-bis-azobenzenes, performed by Mills reaction in acetic acid and sodium acetate was reported by Ruggli *et al.*⁹⁹⁻¹⁰¹ More recently, in addition to the preparations previously published by our group,⁸⁷ the treatment of azoxybenzenes with sodium sulphide,¹⁰² or a diazotization with sodium nitrite¹⁰³ have also been described for their synthesis. Herein, we present an efficient strategy for the preparation of oligo-*ortho*-azobenzenes and show the influence of conjugated azobenzene units and substituents in *ortho* position on the photochemical properties.

2.3 Results and discussion

Even though several procedures are known for the synthesis of azobenzenes, none of them proved to be suitable for the preparation of *ortho*-nitrogen substituted azobenzenes. The oxidative coupling with manganese dioxide, potassium superoxide, the reductive coupling with zinc and sodi-

um hydroxide, a Pd-catalyzed strategy and the Mills reaction were evaluated; none of them gave the expected product. For this reason a method previously developed in our group was used,⁸⁷ in which the Mills reaction was modified using toluene as solvent and AcOH in stoichiometric amounts. Several *ortho*-nitrogen-substituted azobenzenes have been synthesized using these optimized conditions (Table 2.1).

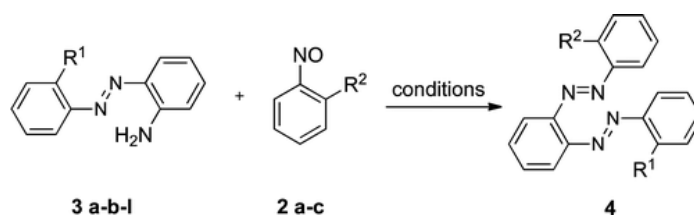


Entry	R ¹	R ²	T/°C	Product (Yield)
1	NH ₂	NHAc	60	3a (70%)
2	NH ₂	H	60	3b (33%)
3	NH ₂	NO ₂	RT	3c (4%)
4	H	NO ₂	60	3d (24%)
5	NO ₂	H	60	3e (n.r.)
6	NO ₂	NO ₂	60	3f (n.r.)
7	NHAc	NHAc	60	3g (4%)
8	NHAc	NO ₂	60	3h (48%)
9	NHAc	H	60	3i (11%)
10	H	NHAc	60	3i (72%)

Table 2.1. Synthesis of 2,2'-dinitrogen-substituted azobenzenes **3**.

The efficiency of the reactions was shown to be dependent on the substituents. The reaction of entry 3 (Table 2.1) proceeded at RT due to the electron withdrawing effect of the nitro group making the nitroso coupling partner **2** more reactive. However, 2-nitroaniline did not react either with nitrosobenzene (**2b**) (Table 2.1, entry 5) or 2-nitronitrosobenzene (**2c**) (Table 2.1, entry 6). Because of the presence of the nitro group in *ortho* position, the nucleophilicity of the amino group is greatly reduced towards an attack at the nitroso compound.

In order to obtain *ortho*-bis-azobenzenes, 2-amino substituted azobenzenes **3a**, **3b** and **3i** were subjected to the optimized Mills condition (AcOH, toluene). Interestingly, the classical condition (AcOH as solvent) gave in most cases superior results.



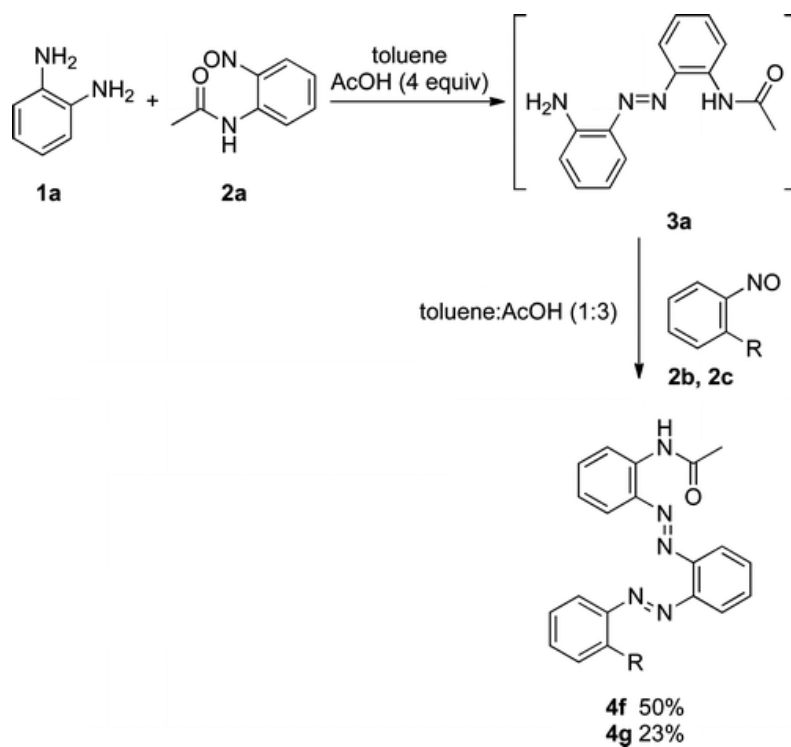
Entry	R ¹	R ²	T/°C	t	Condition ^a	Product (Yield)
1	NH ₂	NHAc	60	2,5 d	B	4a (16%)
2	NH ₂	H	60	21h	B	4b (16%)
3	NH ₂	NO ₂	RT	15 min	A	4c (81%)
4	H	NO ₂	60	21h	A	4d (17%)
5	NHAc	NHAc	60	21h	A	4e (44%)
6	NHAc	NO ₂	60	21h	A	4f (66%)
7	NHAc	H	60	21h	A	4g (2%)
					C	4g (44%)

^aA: AcOH; B: toluene, AcOH (4 equiv), C: **2** (4 equiv), toluene, AcOH (4 equiv).

Table 2.2. Synthesis of 2,2''-dinitrogen-bis-substituted azobenzenes **4**.

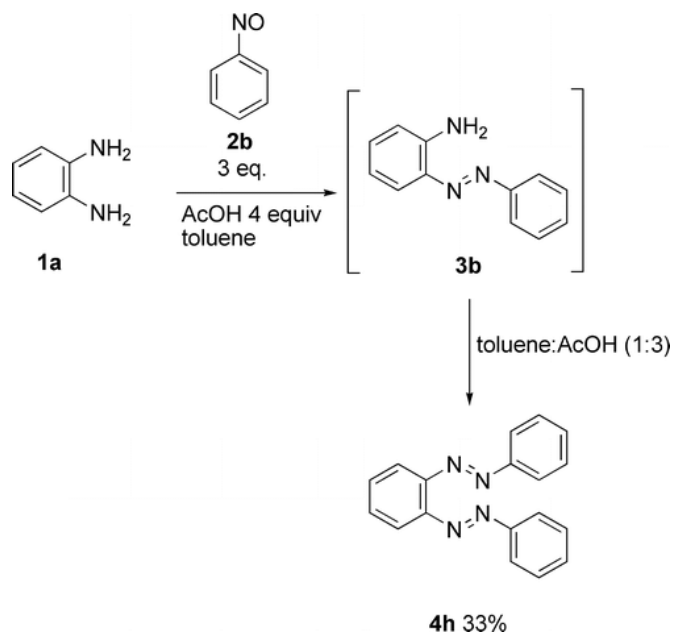
The reactivity of the nitroso compounds **2a**, **2b** and **2c** was similar to the one observed for the 2-substituted-anilines influenced by the electron withdrawing or donating effect of the substituents. Indeed, thanks to the presence of the nitro group, the reaction of the diamine with 2-nitronitrosobenzene (**2c**) (Table 2.2, entry 3), was completed after a few minutes at RT under classical Mills conditions, while the other products were only obtained after longer reaction times at 60°C. For example, when 2-nitrosoacetanilide (**2a**) was used, the reaction was completed after 2.5 days and the product was obtained in low yield (Table 2.2, entry 1). The reaction of entry 7 (Table 2.2) gave 2-phenylbenzotriazole as the main product. Only when four equiv of nitrosobenzene (**2b**) were used, the desired compound was obtained as the major product (Table 2.2, entry 7, condition C).

The different reactivity of *o*-phenylenediamine (**1a**) and 2-amino substituted azobenzenes opens the possibility to obtain 2,2''-dinitrogen-substituted-bisazobenzenes in a one-pot procedure. The method was shown to be efficient for the preparation of the non-symmetric 2,2''-di-substituted bis-*ortho*-azobenzenes. Indeed, compounds **4f** and **4g** were obtained in good to moderate yields starting from *o*-phenylenediamine (**1a**) (Scheme 2.1).



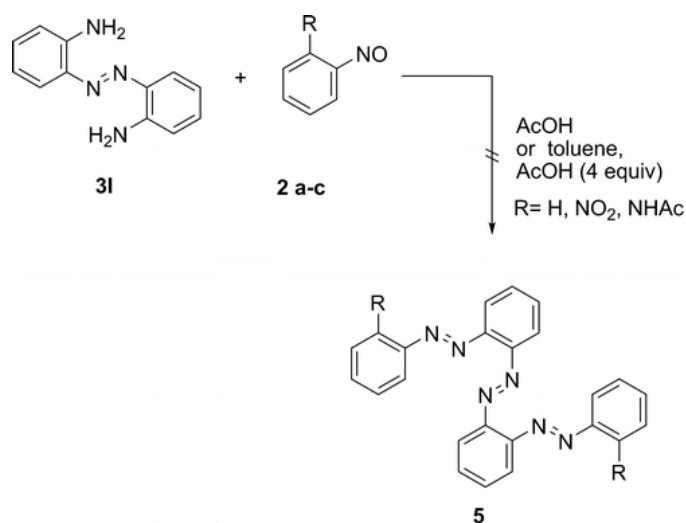
Scheme 2.1. One-pot preparation of non-symmetric 2,2''-di-substitued bis-*ortho*-azobenzenes.

The same procedure was followed in the preparation of the symmetric 2,2''-di-substitued bis-*ortho*-azobenzenes (Scheme 2.2). When nitrosobenzene (**2b**) and *o*-phenylenediamine (**1a**) were subjected to the modified Mills conditions, the product **4h** was isolated after 3 days in 33% yield. However, the reaction with the 2-nitronitrosobenzene did not give the desired product.



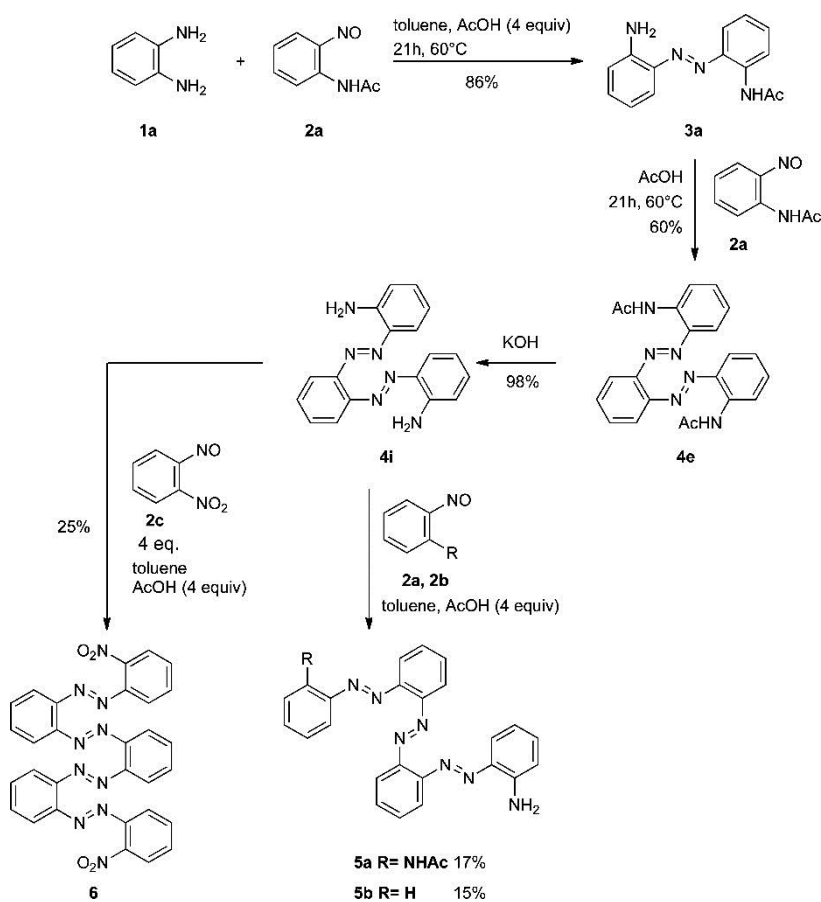
Scheme 2.2. One-pot preparation of the symmetric 2,2''-di-substitued bis-*ortho*-azobenzene **4h**.

Unfortunately, the same protocol was not applicable for the synthesis of symmetric 2,2''-di-substituted tris-*ortho*-azobenzenes **5** (Scheme 2.3).



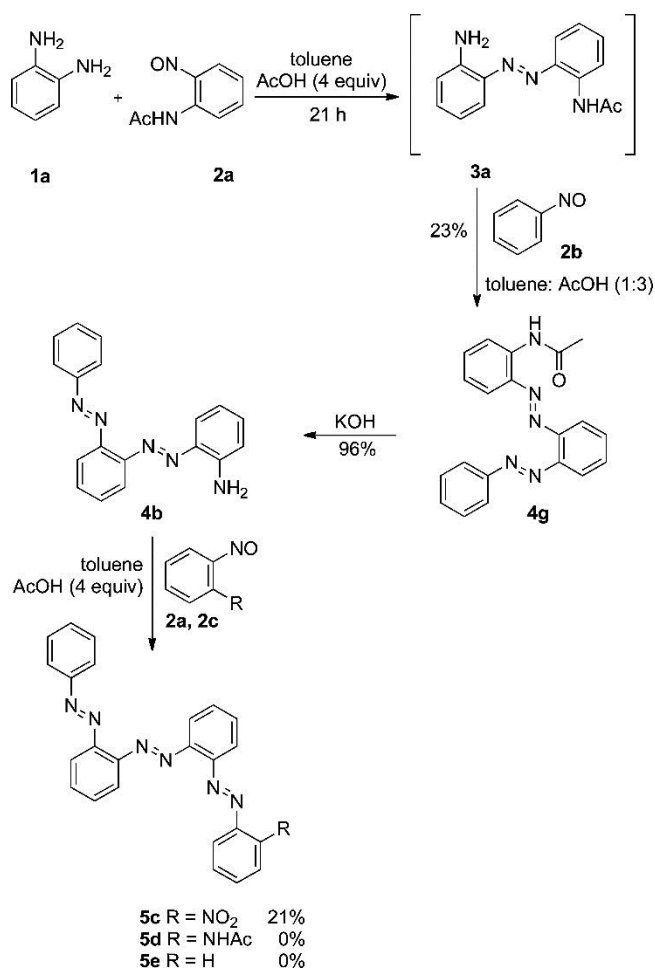
Scheme 2.3. Attempted one-pot preparation of symmetric 2,2''-di-substituted tris-*ortho*-azobenzenes **5**.

Therefore, a stepwise approach was chosen to access 2,2''-di-substituted tris-*ortho*-azobenzenes with different substituents (Scheme 2.4). The modified Mills reaction was found to be the best procedure. It was observed that the higher the number of the azobonds the longer is the reaction time. Indeed, the reaction required 8 days to provide the product in acceptable yield. The synthesis of the 2,2''-di-substituted tetra-*ortho*-azobenzenes was performed only for the dinitro-*ortho*-substituted **6**. As expected from the reactivity previously observed, the reaction was finished after only 4 days. The product was obtained in a moderate yield (25%) compared to the tris-*ortho*-azobenzenes **5a** and **5b**.



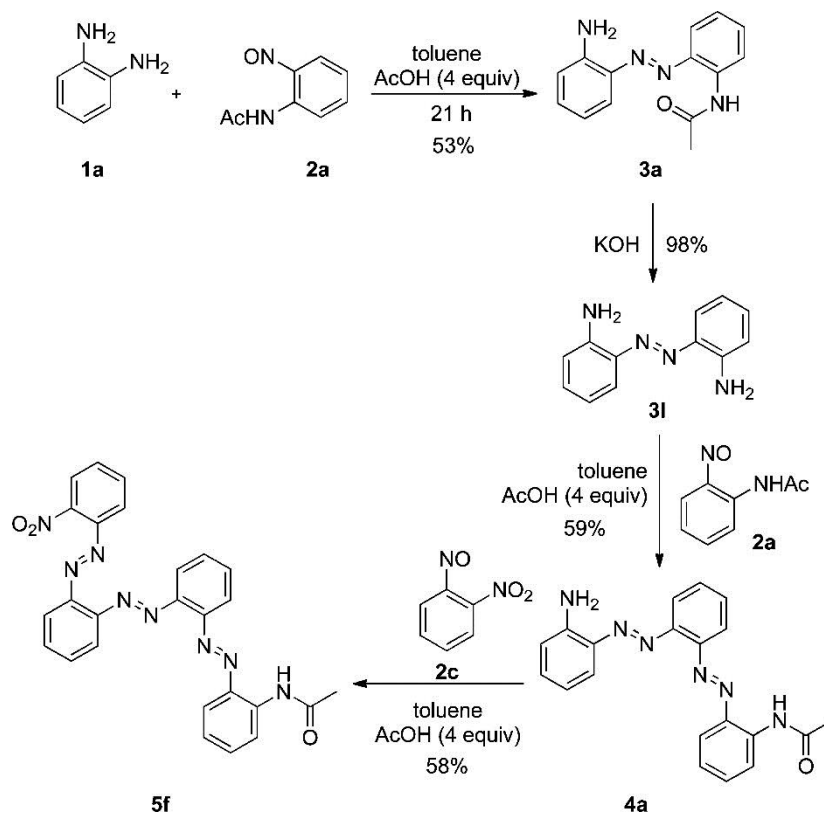
Scheme 2.4. Synthesis of non-symmetric 2,2'''-di-substituted tris-*ortho*-azobenzenes.

Other non-symmetric 2,2'''-di-substituted tris-*ortho*-azobenzenes were synthesized according to the strategy shown in Scheme 2.5 relying on the one-pot procedure to prepare the key intermediate **3a**. The deprotection of compound **4g** gave the amino-substituted bisazobenzene **4b**, followed by Mills reaction. The coupling with 2-nitrosoacetanilide (**2a**) and nitrosobenzene (**2b**) did not provide any of the desired products. When 2-nitronitrosobenzene (**2c**) was used, the reaction occurred and the corresponding tris-*ortho*-azobenzene **5c** was obtained after 6 days in 21% yield. Again, this reactivity can be rationalized by the reduced electron density of the nitroso functionality due to the electron-withdrawing effect of the nitro group.



Scheme 2.5. Synthesis of non-symmetric 2,2''-di-substituted tris-*ortho*-azobenzenes.

Accordingly, a similar strategy gave 2-nitro-2''-acetamido-tris-*ortho*-azobenzene **5f** as presented in Scheme 2.6. The *ortho*-substituted diamine **3i** was obtained by deprotection of 2-acetamido-2'-aminoazobenzene (**3a**). The following two Mills reactions gave first compound **4a** in 59% and the final product **5f** in 58% yield, respectively.



Scheme 2.6. Synthesis of 2-nitro-2''-acetamido-tris-*ortho*-azobenzenes (**5f**).

With all the different oligo-*ortho*-azobenzenes in hand, the photochemical properties were studied. The absorption spectra were acquired and the photoisomerization behavior was assessed. In particular, the influence of the conjugated systems and of the substituents was investigated. First, the absorption spectra of the *ortho*-nitrogen substituted mono-azo-benzenes were measured in chloroform. All of them showed the typical π - π^* transition at around 320 nm. However, depending on the substituents, specific characteristics can be distinguished. In all the amino substituted azobenzenes, where a free NH_2 group is present, the spectra present a broad peak at around 450 nm. The presence of the nitro group causes a slight bathochromic shift of the spectrum. This shift is also observed when the second substituent is an acetamido group or a free amino group. In the case where the nitro group is the only substituent, the spectrum is highly similar to the one of the azobenzene (Figure 2.1a). If all the acetamido substituted azobenzenes are compared, the presence of shoulders at around 400 nm is observed (Appendix, supporting information).

All the *ortho*-nitrogen substituted mono-azobenzenes were irradiated at 365 nm (hand-held lamp, 8 W) and the switching ability analysed by UV-spectroscopy (Figure 2.1b-d; Appendix, supporting information for details). Compound **3i** followed the classical well known behavior of azobenzene (Figure 2.1d). Indeed, the absorbance increased at 450 nm and decreased at 320 nm until it reached the photostationary state after a few seconds of irradiation. It completely relaxed back after 2 h at RT. Compounds **3a**, **3b** (Figure 2.1b), **3c**, **3d** (Figure 2.1c), **3g**, **3h** and **3l** after exposure to UV light,

showed a decrease in absorbance for both the *Z* and the *E* isomer (Appendix, supporting information for details). The photoisomerization was reversible even after several cycles of irradiation for all the mono-azobenzenes. Furthermore, all compounds except **3d** (Figure 2.1c), showed a higher absorbance than the initial state after incubation at RT, especially if kept in the dark (**3c**, **3g**, **3h**, **3i**, Appendix, supporting information) and could be completely converted back after exposure to visible light indicating a mixture of *E* and *Z* isomer in the photo-stationary state at these conditions. It was also shown that the presence of electron withdrawing groups caused only small changes in the absorbance (compound **3d**, Figure 2.1c, for compounds **3c** and **3h** Appendix, supporting information). Bandara *et al.* have also demonstrated the influence of substituents on the photoswitching behavior of azobenzene compounds. They describe, that in their system, based on azo-(aminomethyl)pyridine compounds, the presence of electron-donating groups reduces the photoisomerization properties. Similarly to what we observed, they reported a decreased absorbance for both *E* and *Z* isomer upon UV irradiation.¹⁰⁴ This behavior is unusual, since the *Z* isomer of azobenzene normally shows an increased intensity for the $n-\pi^*$ transition. Consequently a photochemical $E \rightarrow Z$ isomerization is observed after irradiation with visible light, whereas for most azobenzenes a $Z \rightarrow E$ isomerization takes place if irradiated at 450 nm.

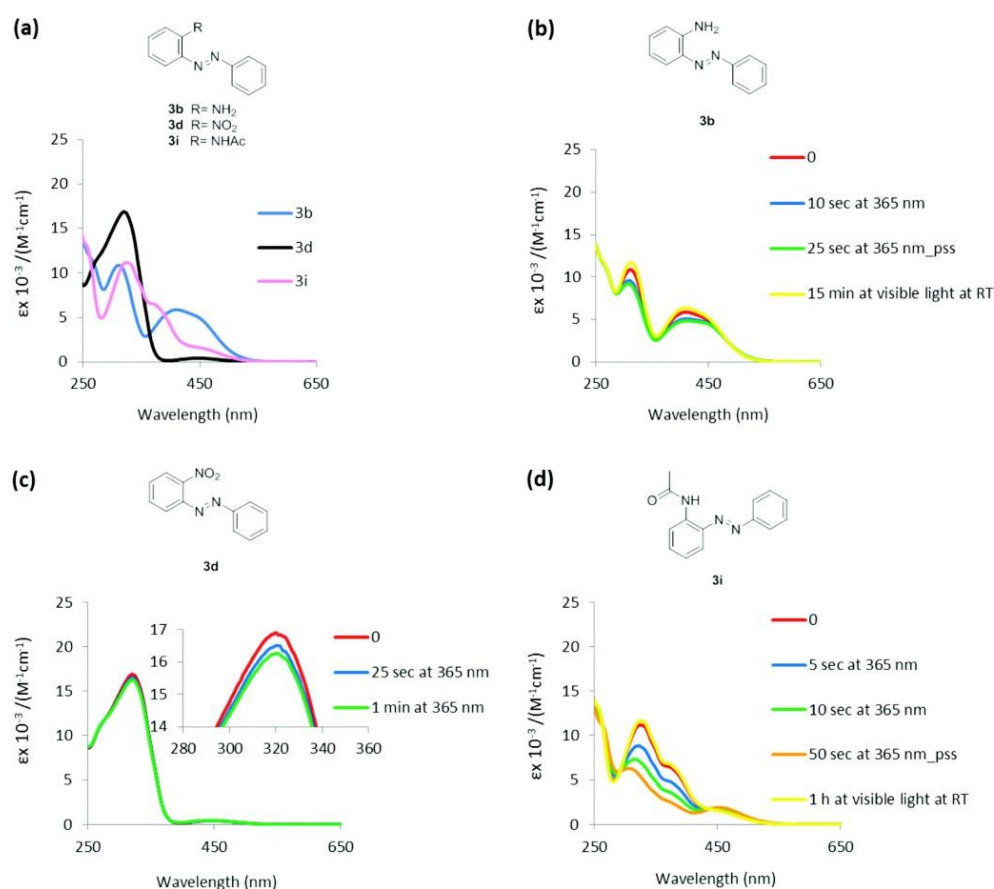


Figure 2.1. Absorption spectra (Figure 2.1a) and photoisomerization of a representative *ortho*-amino, nitro and acetamido substituted mono-azobenzenes (**3b**, **3d**, **3i** respectively, Figure 2.1b-d) in chloroform.

The absorption spectra of the bis-*ortho*-azobenzenes showed a similar behavior as for the monoazobenzenes (Figure 2.2). Indeed, as previously described, the nitro group caused a small shift in the spectra, while the presence of the amino group was easily detectable due to the broad and high absorbance at around 450 nm. Once again, the acetamido-substituted compounds showed the typical pattern with three maxima at 340 nm, 400 nm and 470 nm. Furthermore, close to the π - π^* transition at around 350 nm an additional shoulder can be noticed which is present in all bis-*ortho*-azobenzenes. In the case of the di-amino substituted derivative **4i** and 2-nitro-2''acetamido-bisazobenzene (**4f**) (Appendix, supporting information) only a broadening of the absorption can be seen.

In contrast to the switching behavior observed for mono-azobenzenes, none of bis-*ortho*-azobenzenes switched upon UV-irradiation. Cisnetti and co-workers have demonstrated that (*E,E*)-*m*-bisazobenzene behave similarly to azobenzene and that (*E,E*)-*p*-bisazobenzene also isomerizes although a decreased photoreactivity has been observed⁹⁷. The authors explain this fact by the larger electronic coupling in the *p*-bisazobenzene compared to the *m*-bisazobenzene, which they confirmed by quantum chemical calculations. If this increased electronic communication is the reason for the reduced isomerization, *o*-bisazobenzenes should exhibit an even lower isomerization tendency. Indeed, in our case, all the tested compounds showed complete inertness toward photoisomerization. One possible alternative explanation would be that the back-isomerization is faster than the minimum time required for the measurement (5 s). Flash photolysis studies have not been done so far to rule out this option.

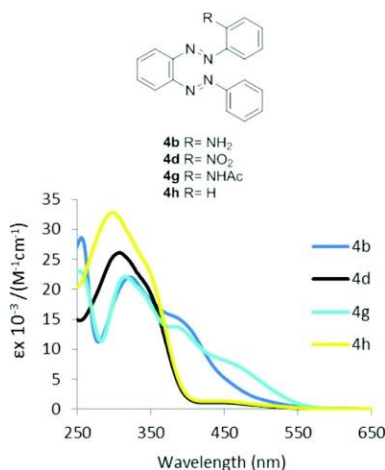


Figure 2.2. Absorption spectra of a representative *ortho*-amino, nitro, acetamido and hydrogen substituted bis-azobenzenes (**4b**, **4d**, **4g** and **4h** respectively) in chloroform.

An analog behavior was also observed for the tris and tetra-azobenzenes (Figure 2.3). The amino group causes also in these cases an increased absorbance at around 450 nm. The additional absorption caused by the acetamido group is less evident. The spectrum of *tetra*-azobenzene **6** is

comparable to the one of **4d** and **5c** due to the presence of the nitro groups. None of these compounds shows isomerization upon-UV irradiation as it was previously observed for the bis-*ortho*-azobenzenes.

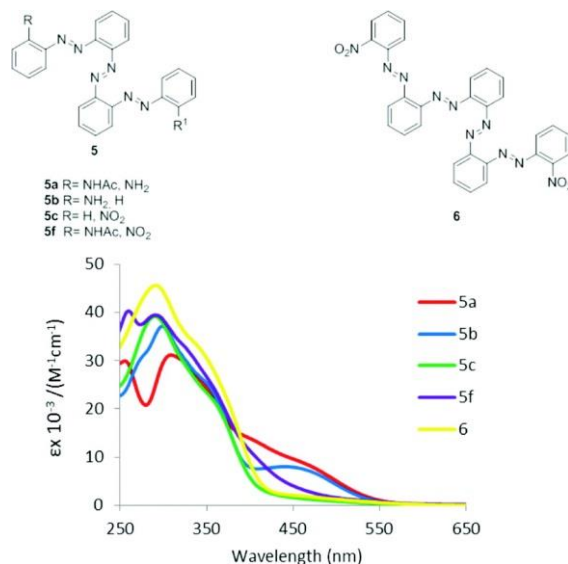


Figure 2.3. Absorption spectra of the di-substituted tris and tetra-*ortho*-azobenzenes in chloroform.

2.4 Conclusions

A stepwise convenient strategy for the preparation of oligo-*ortho*-azobenzenes and a one-pot procedure for the synthesis of bis-*ortho*-azobenzenes have been presented. The photochemical properties of these compounds have been thoroughly investigated. It has been shown that the absorption spectra exhibit common features depending on the substituent. Additionally, only the *ortho*-nitrogen substituted mono-azobenzenes isomerized upon UV irradiation. Furthermore, the presence of electron-withdrawing groups induced a decreased photochromism. Current efforts in the group address the reason for the inhibition of the photochromism by substitution with another azobenzene moiety in *ortho* position.

2.5 Experimental section

2-Nitrosoacetanilide (2a). A solution of *o*-phenylenediamine (**1a**) (10.0 g, 92.5 mmol, 1.00 equiv) in 150 ml EtOAc was cooled down below 5 °C. Then, an ice-cold solution of acetic anhydride (9.12 ml, 97.1 mmol, 1.05 equiv) in 80 ml EtOAc was added and stirred for 20 min. The precipitate that was obtained was filtered with a glass filter under vacuum to give 5.13 g (37%) of 2-aminoacetanilide. ¹H NMR (400 MHz, CDCl₃) δ 9.10 (s, 1H), 7.15 (dd, *J* = 7.8, 1.2 Hz, 1H), 6.92 – 6.85 (m, 1H), 6.70 (dd, *J* = 8.0, 1.3 Hz, 1H), 6.53 (td, *J* = 7.6, 1.4 Hz, 1H), 4.84 (s, 2H), 2.03 (s, 3H). The analytical data correspond to literature.¹⁰⁵ The acetylated diamine (5.00 g, 33.3 mmol, 1.00 equiv) was

suspended in 50 ml CH₂Cl₂. Oxone[®] (30.7 g, 49.9 mmol, 1.50 equiv), dissolved in 200 ml water, was added and stirred fiercely for 1h at RT. The organic phase was separated and the aqueous phase extracted with 100 ml CH₂Cl₂. The combined organic phases were washed with 1 M HCl (100 ml), sat. aq NaHCO₃ (100 ml) and water (100 ml). It was then dried over MgSO₄, concentrated and purified by flash column chromatography (SiO₂, hexane/EtOAc, 2:1) and the product was obtained as green solid (2.41 g, 44% yield). Mp = 107–108 °C. (lit. Mp 106-107 °C).¹⁰⁶ ¹H NMR (400 MHz, CDCl₃) δ 10.79 (s, 1H), 8.85 (dd, *J* = 8.6, 1.0 Hz, 1H), 7.71 (ddd, *J* = 8.5, 7.2, 1.4 Hz, 1H), 7.32 (s, 1H), 7.22 – 7.08 (m, 1H), 2.35 (s, 3H). The analytical data correspond to literature.⁸⁷

2-Nitronitrosobenzene (2c). Oxone[®] (20.0 g, 32.6 mmol, 1.50 equiv) was treated with 24 ml of concentrated H₂SO₄. The suspension was then poured onto 130 g of crushed ice, and the mixture was stirred at RT until all of the ice has melted. Then, 2-nitroaniline (3.00 g, 21.7 mmol, 1.00 equiv) was added and stirred at RT for 20 h. The mixture was extracted twice with 150 ml of CH₂Cl₂, dried over MgSO₄, the solvent removed and the titled compound was obtained as a brown solid (3.12 g, 94%). Mp: 119–122 °C (lit. 135–137 °C).¹⁰⁷ ¹H-NMR (400 MHz CDCl₃) δ 8.17 (d, *J* = 8.0 Hz, 1H), 7.96 (t, *J* = 8.0 Hz, 1H), 7.77 (t, *J* = 8.0 Hz, 1H), 6.63 (d, *J* = 8.0 Hz, 1H). The compound **2c** is in equilibrium with its dimer and the analytical data correspond to literature.¹⁰⁸

General procedure for the Mills reaction using AcOH (condition A). A solution of amine (1.00 equiv) in acetic acid (7 ml/mmol) was degassed with a nitrogen stream for 15 min. Then, the nitroso compound **2** (1.00 equiv) was added. The mixture was stirred at 60 °C for 21 h and the solvent was removed under reduced pressure. The residue was purified by flash column chromatography.

General procedure for the Mills reaction using AcOH/toluene (condition B). A solution of amine (1.00 equiv) in toluene (7 ml/mmol) was degassed with a nitrogen stream for 15 min. Then, the nitroso compound (1.00 equiv) and acetic acid (4.00 equiv) were added. The mixture was stirred at 60 °C for 21 h and the solvent was removed under reduced pressure. The residue was purified by flash column chromatography.

General procedure for the Mills reaction using AcOH/toluene (condition C). A solution of amine (1.00 equiv) in toluene (7 ml/mmol) was degassed with a nitrogen stream for 15 min. Then, the nitroso compound (4.00 equiv) and acetic acid (4.00 equiv) were added. The mixture was stirred at 60 °C for 21 h and the solvent was removed under reduced pressure. The residue was purified by flash column chromatography.

2-Acetamido-2'-amino-ortho-azobenzene (3a). The title compound **3a** was prepared according to general procedure (condition B) from *o*-phenylenediamine (**1a**) (0.821 g, 7.58 mmol, 1.00 equiv) and 2-nitrosoacetanilide (**2a**) (1.25 g, 7.71 mmol, 1.00 equiv). The residue was purified by

flash column chromatography (SiO₂, hexane/EtOAc, 1:1) and the title compound was obtained as red solid in 70% yield (1.35 g). Mp 148–150 °C (lit. 143 °C);¹⁰⁹ ¹H NMR (400 MHz, CDCl₃) δ 9.95 (s, 1H), 8.63 (d, *J* = 8.3 Hz, 1H), 7.70 (dd, *J* = 8.1, 1.6 Hz, 1H), 7.62 (dd, *J* = 8.1, 1.3 Hz, 1H), 7.45 – 7.37 (m, 1H), 7.29 – 7.22 (m, 1H), 7.18 – 7.10 (m, 1H), 6.87 – 6.71 (m, 2H), 5.40 (s, 2H), 2.27 (s, 3H); ¹³C NMR (101 MHz, CDCl₃) δ 168.6, 145.0, 137.5, 135.5, 133.2, 131.8, 124.4, 123.5, 122.2, 120.5, 120.2, 118.0, 117.4, 25.5.

2-Amino-*ortho*-azobenzene (3b). The title compound **3b** was prepared according to general procedure (condition B) from *o*-phenylenediamine (**1a**) (0.820 g, 7.58 mmol, 1.00 equiv) and nitrosobenzene (**2b**) (812 mg, 7.58 mmol, 1.00 equiv). The residue was purified by flash column chromatography (SiO₂, hexane/EtOAc, 7:1) and the title compound was obtained as brown solid in 33% yield (498 mg). Mp 58–62 °C; ¹H NMR (400 MHz, CDCl₃) δ 7.87 – 7.82 (m, 3H), 7.53 – 7.47 (m, 2H), 7.45 – 7.39 (m, 1H), 7.22 (ddd, *J* = 8.5, 7.1, 1.6 Hz, 1H), 6.83 (ddd, *J* = 8.2, 7.1, 1.3 Hz, 1H), 6.77 (dd, *J* = 8.2, 1.1 Hz, 1H), 5.90 (s, 2H). The analytical data correspond to literature.¹¹⁰

2-Amino-2'-nitro-*ortho*-azobenzene (3c). The title compound **3c** was prepared according to general procedure (condition B) from *o*-phenylenediamine (**1a**) (0.820 g, 7.58 mmol, 1.00 equiv) and 2-nitronitrosobenzene (**2c**) (1.15 g, 7.58 mmol, 1.00 equiv). The residue was purified by flash column chromatography (SiO₂, hexane/EtOAc, 2:1) followed by preparative TLC (SiO₂, hexane/CHCl₃, 1:1) and the title compound was obtained as brown solid in 4% yield (73.2 mg). Mp 95–97 °C; ¹H NMR (400 MHz, DMSO) δ 8.05 (dd, *J* = 8.1, 1.2 Hz, 1H), 7.92 (dd, *J* = 8.1, 1.2 Hz, 1H), 7.84 – 7.76 (m, 1H), 7.68 – 7.60 (m, 2H), 7.36 (s, 2H), 7.26 (ddd, *J* = 8.4, 6.9, 1.6 Hz, 1H), 6.88 (dd, *J* = 8.4, 1.0 Hz, 1H), 6.69 (ddd, *J* = 8.2, 6.9, 1.2 Hz, 1H); ¹³C NMR (101 MHz, DMSO) δ 146.7, 145.0, 144.2, 135.9, 134.1, 133.4, 130.0, 127.7, 124.1, 118.0, 117.4, 115.9; MS (EI, 70 eV): *m/z* (%) = 242 (57%) [M⁺], 92 (100%); C₁₂H₁₀N₄O₂ (242.24): calcd C 59.50, H 4.16, N 23.13; found C 59.35, H 4.14, N 22.88.

2-Nitro-*ortho*-azobenzene (3d). The title compound **3d** was prepared according to general procedure (condition B) from aniline (0.827 ml, 9.07 mmol, 1.00 equiv) and 2-nitronitrosobenzene (**2c**) (0.138 g, 0.907 mmol, 1.00 equiv). The residue was purified by flash column chromatography (SiO₂, hexane/EtOAc, 3:1) and the title compound was obtained as orange-brown solid in 24% yield (502 mg). Mp 66–70 °C (lit. 67–68 °C);¹¹¹ ¹H NMR (400 MHz, CDCl₃) δ 7.98 – 7.89 (m, 3H), 7.72 – 7.65 (m, 2H), 7.62 – 7.49 (m, 4H); ¹³C NMR (101 MHz, CDCl₃) δ 152.6, 147.6, 145.6, 133.2, 132.4, 130.6, 129.4 (2C), 124.2, 123.8 (2C), 118.6.

2,2'-Diacetamido-*ortho*-azobenzene (3g). The title compound **3g** was prepared according to general procedure (condition B) from *N*-(2-aminophenyl)acetamide (495 mg, 3.30 mmol, 1.00 equiv) and 2-nitrosoacetanilide (**2a**) (541 g, 3.30 mmol, 1.00 equiv). The residue was purified by flash column chromatography (SiO₂, DCM/EtOAc, 1:1) and 41.3 mg of orange product were obtained (4% yield). Mp 273–275 °C; ¹H NMR (400 MHz, CDCl₃) δ 9.38 (s, 2H), 8.68 (d, *J* = 8.4 Hz, 2H), 7.64 (d, *J* =

8.1 Hz, 2H), 7.52 (t, $J = 7.8$ Hz, 2H), 7.17 (t, $J = 7.7$ Hz, 2H), 2.30 (s, 6H). The analytical data correspond to literature.¹¹²

2-Acetamido-2'-nitro-*ortho*-azobenzene (3h). The title compound **3h** was prepared according to general procedure (condition B) from *N*-(2-aminophenyl)acetamide (500 mg, 3.31 mmol, 1.00 equiv) and 2-nitronitrosobenzene (**2c**) (506 mg, 3.33 mmol, 1.00 equiv). The residue was purified by flash column chromatography (SiO₂, hexane/EtOAc, 1:1). The solvent was evaporated and the orange product was obtained in 48% yield (449 mg). Mp 143–147 °C; ¹H NMR (400 MHz, CDCl₃) δ 10.27 (s, 1H), 8.74 (d, $J = 8.5$ Hz, 1H), 7.93 (dd, $J = 8.0, 1.4$ Hz, 2H), 7.81 (dd, $J = 8.0, 1.5$ Hz, 1H), 7.74 (td, $J = 7.7, 1.4$ Hz, 1H), 7.61 (ddd, $J = 8.0, 7.4, 1.5$ Hz, 1H), 7.57 – 7.47 (m, 1H), 7.22 (ddd, $J = 8.6, 7.3, 1.3$ Hz, 1H), 2.30 (s, 3H); ¹³C NMR (101 MHz, CDCl₃) δ 167.0, 146.2, 144.8, 138.9, 135.0, 134.6, 133.4, 130.9, 126.7, 124.5, 123.6, 120.9, 120.3, 25.4; MS (EI, 70 eV): m/z (%) = 284 (48%) [M⁺], 134 (100%); C₁₄H₁₂N₄O₃ (284.27): calcd C 59.15, H 4.25, N 19.71; found C 59.09, H 4.25, N 19.85.

2-Acetamido-*ortho*-azobenzene (3i). The title compound **3i** was prepared according to general procedure (condition B) from aniline (0.294 ml, 3.22 mmol, 1.00 equiv) and 2-nitrosoacetanilide (**2a**) (529 mg, 3.22 mmol, 1.00 equiv). The residue was purified by flash column chromatography (SiO₂, hexane/EtOAc, 1:1) and 555 mg of yellow product were obtained (72% yield). The same product was also prepared according to general procedure (condition B) from 2-acetamido-2'-amino-*ortho*-azobenzene (**3a**) (470 mg, 3.13 mmol, 1.00 equiv) and nitrosobenzene (**2b**) (357 mg, 3.33 mmol, 1.07 equiv). The residue was purified by flash column chromatography (SiO₂, hexane/EtOAc, 2:1) and 80.1 mg of yellow product were obtained (11 %). Mp 124–127 °C (lit. 127–129 °C);¹¹³ ¹H NMR (400 MHz, CDCl₃) δ 10.12 (s, 1H), 8.68 (d, $J = 8.4$ Hz, 1H), 7.91 – 7.81 (m, 3H), 7.58 – 7.50 (m, 3H), 7.50 – 7.45 (m, 1H), 7.21 – 7.14 (m, 1H), 2.28 (s, 3H); ¹³C NMR (101 MHz, CDCl₃) δ 168.7, 152.5, 138.9, 136.1, 133.1, 132.0, 129.5 (2C), 123.5, 122.8 (2C), 121.3, 120.4, 25.5.

2,2'-Diamino-*ortho*-azobenzene (3l). A solution of *o*-phenylenediamine (**1a**) (0.764 g, 7.07 mmol, 1.00 equiv) in toluene (50 ml) was degassed with a nitrogen stream for 15 min. Then, 2-nitrosoacetamide (1.16 g, 7.07 mmol, 1.00 equiv) and acetic acid (1.62 ml) were added. The mixture was stirred at 60 °C for 21 h and the solvent was removed under reduced pressure. The residue was purified by flash column chromatography (SiO₂, hexane/EtOAc, 2:1) and the compound **3a** was obtained as red solid (0.792 g, 44% yield). Then, a solution of 2-acetamido-2'-amino-*ortho*-azobenzene (**3a**) (740 mg, 2.91 mmol) in ethanol (138 ml) was treated with a solution of KOH (12.1 g) in ethanol (80 ml) and water (32 ml). The mixture was heated to 90 °C. After 1 h the mixture was poured onto ice (500 g), extracted with CH₂Cl₂ (3x100 ml). It was dried over Na₂SO₄ and concentrated to yield 0.583 g (94%). Mp 136-138 °C; ¹H NMR (400 MHz, CDCl₃) δ 7.68 (dd, $J = 8.0, 1.4$ Hz, 2H), 7.21 – 7.14 (m, 2H), 6.83 – 6.74 (m, 4H), 5.49 (s, 4H). The analytical data correspond to literature.⁸⁷

2-Acetamido-2''-amino-*ortho*-bisazobenzene (4a). The title compound **4a** was prepared according to general procedure (condition B) from 2,2'-diaminodiazobenzene (**3I**) (300 mg, 1.41 mmol, 1.00 equiv) and 2-nitrosoacetanilide (**2a**) (230 mg, 1.41 mmol, 1.00 equiv). After 2.5 days the solvent was removed under reduced pressure and the residue was purified by flash column chromatography (SiO₂, hexane/EtOAc, 2:1). The product was obtained as a red solid (80.3 mg, 16%). Mp 158–162 °C; ¹H NMR (400 MHz, CDCl₃) δ 10.12 (s, 1H), 8.69 (d, *J* = 8.3 Hz, 1H), 7.88 (dd, *J* = 8.1, 1.5 Hz, 1H), 7.85 (dd, *J* = 8.1, 1.5 Hz, 1H), 7.81 (dd, *J* = 7.9, 1.5 Hz, 1H), 7.72 (dd, *J* = 7.7, 1.6 Hz, 1H), 7.62 – 7.44 (m, 3H), 7.20 (ddd, *J* = 15.3, 8.4, 1.4 Hz, 2H), 6.87 – 6.81 (m, 1H), 6.74 (dd, *J* = 8.2, 1.0 Hz, 1H), 6.31 (s, 2H), 2.00 (s, 3H). The analytical data correspond to literature.⁸⁷

2-Amino-*ortho*-bisazobenzene (4b). The title compound **4b** was prepared according to general procedure (condition B) from 2,2'-diaminodiazobenzene (**3I**) (0.250 g, 1.19 mmol, 1.00 equiv) and nitrosobenzene (**2b**) (0.130 mg, 1.19 mmol, 1.00 equiv). The residue was purified by flash column chromatography (SiO₂, hexane/EtOAc, 7:1). The product was obtained as a brown solid (51.3 mg, 16%). Mp 97–100 °C; ¹H NMR (400 MHz, CDCl₃) δ 7.97 (dd, *J* = 8.0, 1.6 Hz, 1H), 7.95 – 7.88 (m, 3H), 7.76 (dd, *J* = 8.0, 1.4 Hz, 1H), 7.62 – 7.45 (m, 5H), 7.21 (ddd, *J* = 8.5, 7.1, 1.6 Hz, 1H), 6.86 (ddd, *J* = 8.2, 7.1, 1.3 Hz, 1H), 6.74 (dd, *J* = 8.3, 1.1 Hz, 1H), 6.69 (s, 2H); ¹³C NMR (101 MHz, CDCl₃) δ 153.3, 148.1, 147.9, 141.5, 138.0, 133.2, 132.3, 131.7, 131.4, 130.4, 129.3 (2C), 123.3 (2C), 117.3, 117.2, 117.1, 116.4; HRMS (ESI): *m/z* calcd for C₁₈H₁₅N₅⁺ [M+H⁺] 302.1406, found 302.1400.

2-Amino-2''-nitro-*ortho*-bisazobenzene (4c). To a round bottom flask was added the 2,2'-diaminoazobenzene (**3I**) (80.0 mg, 0.377 mmol, 1.00 equiv) and 2-nitronitrosobenzene (**2c**) (57.3 mg, 0.377 mmol, 1.00 equiv) followed by AcOH (11 ml). The mixture was stirred for 15 min. Then, water was added (50 ml/mmol) and the liquid was carefully turned basic with sodium carbonate (2 m Na₂CO₃ in H₂O, 5 ml/1ml AcOH). The mixture was then extracted with CH₂Cl₂ (3x20 ml/mmol), dried over MgSO₄ and the solvent was removed. The residual black solid was re-suspended in CH₂Cl₂ and purified by flash column chromatography (SiO₂, DCM/hexane 1:1). The product was obtained as a brown solid (106 mg, 81%). Mp 111–113 °C; ¹H NMR (400 MHz, CDCl₃) δ 7.97 (d, *J* = 7.0 Hz, 2H), 7.91 (d, *J* = 8.1 Hz, 1H), 7.77 (d, *J* = 8.1 Hz, 1H), 7.72 – 7.67 (m, 1H), 7.64 (t, *J* = 7.6 Hz, 1H), 7.62 – 7.56 (m, 2H), 7.51 (t, *J* = 7.6 Hz, 1H), 7.22 (d, *J* = 6.9 Hz, 1H), 6.87 (dd, *J* = 8.1, 7.0 Hz, 1H), 6.75 (d, *J* = 8.3 Hz, 1H), 6.62 (s, 2H); ¹³C NMR (101 MHz, CDCl₃) δ 149.0, 147.7, 147.4, 146.2, 141.7, 138.0, 133.3, 133.1, 133.0, 132.6, 130.6, 130.4, 124.3, 119.0, 117.31, 117.30, 117.26, 117.0; HRMS (ESI): *m/z* calcd for C₁₈H₁₅N₆O₂⁺ [M+H⁺] 347.1251, found 347.1260.

2-Nitro-*ortho*-bisazobenzene (4d). The title compound **4d** was prepared according to general procedure (condition A) from 2-amino-*ortho*-azobenzene (**3b**) (200 mg, 1.01 mmol, 1.00 equiv) and 2-nitronitrosobenzene (**2c**) (154 mg, 1.01 mmol, 1.00 equiv). The mixture was stirred for 21 h at 60 °C. The solvent was removed under reduced pressure and HCl (1 m aq. sol; 25 ml) was added. The

mixture was then extracted with CH₂Cl₂ (2x30 ml) and purified by flash column chromatography (SiO₂, hexane/EtOAc, 7:1). An oily orange solution was obtained (57.2 mg) in 17% yield. Mp 61–65 °C; ¹H NMR (400 MHz, CDCl₃) δ 8.01 – 7.97 (m, 2H), 7.97 – 7.93 (m, 1H), 7.83 – 7.78 (m, 1H), 7.76 (dd, *J* = 7.9, 1.4 Hz, 1H), 7.69 (dd, *J* = 5.2, 2.0 Hz, 2H), 7.67 – 7.61 (m, 1H), 7.61 – 7.50 (m, 5H); ¹³C NMR (101 MHz, CDCl₃) δ 153.1, 149.2, 147.6 (2C), 146.0, 133.3, 132.5, 131.7, 131.2, 130.7, 129.3 (2C), 124.3, 123.5 (2C), 119.11, 119.09, 117.9; HRMS (ESI): *m/z* calcd for C₁₈H₁₄N₅O₂⁺ [M+H⁺] 332.1142, found 332.1148.

2,2''-Diacetamido-*ortho*-bisazobenzene (4e). The title compound **4e** was prepared according to general procedure (condition A) from 2-acetamido-2'-amino-*ortho*-azobenzene (**3a**) (187 mg, 0.735 mmol, 1.00 equiv) and 2-nitrosoacetanilide (**2a**) (123 mg, 0.749 mmol, 1.02 equiv). The residue was purified by flash column chromatography (SiO₂, hexane/EtOAc, 1:2) and 130 mg of product were obtained (44%). Mp 182–184 °C; ¹H NMR (400 MHz, CDCl₃) δ 10.04 (s, 2H), 8.69 (d, *J* = 8.3 Hz, 2H), 7.86 (dd, *J* = 8.1, 1.4 Hz, 2H), 7.76 (dd, *J* = 6.0, 3.4 Hz, 2H), 7.65 (dd, *J* = 6.0, 3.4 Hz, 2H), 7.51 (t, *J* = 7.8 Hz, 2H), 7.18 (t, *J* = 7.7 Hz, 2H), 1.91 (s, 6H). The analytical data correspond to literature.⁸⁷

2-Acetamido-2''-nitro-*ortho*-bisazobenzene (4f). The title compound **4f** was prepared according to general procedure (condition A) from 2-acetamido-2'-amino-*ortho*-azobenzene (**3a**) (0.101 g, 0.393 mmol, 1.00 equiv) and 2-nitronitrosobenzene (**2c**) (59.8 mg, 393 μmol, 1.00 equiv). The residue was purified by flash column chromatography (SiO₂, hexane/EtOAc, 2:1) and 103 mg of orange product were obtained (66%). Mp 136–138 °C; ¹H NMR (400 MHz, DMSO) δ 10.19 (s, 1H), 8.32 – 8.27 (m, 1H), 8.15 (dd, *J* = 7.8, 1.5 Hz, 1H), 8.01 (dd, *J* = 8.0, 1.3 Hz, 1H), 7.88 – 7.71 (m, 5H), 7.66 (dd, *J* = 7.8, 1.5 Hz, 1H), 7.62 (dd, *J* = 8.0, 1.3 Hz, 1H), 7.59 – 7.53 (m, 1H), 7.27 – 7.20 (m, 1H), 1.97 (s, 3H); ¹³C NMR (101 MHz, CDCl₃) δ 169.4, 148.8, 147.3, 147.1, 146.1, 139.4, 134.8, 133.6, 133.4, 132.8, 131.5, 130.1, 126.2, 124.4, 123.5, 120.6, 119.1, 118.8, 117.8, 25.2; MS (EI, 70 eV): *m/z* (%) = 388 (51%) [M⁺], 106 (100%); C₂₀H₁₆N₆O₃ (388.39): calcd C 61.85, H 4.15, N 21.64; found C 61.46, H 4.17, N 21.50.

2-Acetamido-*ortho*-bisazobenzene (4g). The title compound **4g** was prepared according to general procedure (condition C) from 2-acetamido-2'-amino-*ortho*-azobenzene (**3a**) (195 mg, 767 μmol, 1.00 equiv) and nitrosobenzene (**2b**) (337 mg, 3.15 mmol, 4.00 equiv). After 3 h the reaction was finished and the solvent was removed under reduced pressure. The residue was purified by flash column chromatography (SiO₂, hexane/EtOAc, 1:1) and 116 mg (44%) of orange product were obtained. Mp 112–113 °C; ¹H NMR (400 MHz, CDCl₃) δ 10.49 (s, 1H), 8.70 (dd, *J* = 8.4, 1.1 Hz, 1H), 7.99 (dd, *J* = 8.1, 1.6 Hz, 1H), 7.92 – 7.87 (m, 2H), 7.85 (dd, *J* = 7.8, 1.6 Hz, 1H), 7.71 (dd, *J* = 7.7, 1.7 Hz, 1H), 7.61 (dq, *J* = 14.8, 7.3, 1.6 Hz, 2H), 7.55 – 7.45 (m, 4H), 7.25 – 7.19 (m, 1H), 1.72 (s, 3H); ¹³C NMR (101 MHz, CDCl₃) δ 169.4, 153.0, 149.7, 148.1, 147.1, 139.4, 135.2, 133.3, 131.8, 131.2, 129.4

(2C), 125.1, 123.4, 123.3 (2C), 120.6, 120.2, 118.0, 25.0; MS (EI, 70 eV): m/z (%) = 343 (83%) [M^+], 106 (100%). $C_{20}H_{17}N_5O$ (343.39): calcd C 69.96, H 4.99, N 20.40; found C 69.84, H 4.96, N 20.42.

2,2''-Diamino-bis-*ortho*-azobenzene (4i). A solution of 2,2''-diacetamido-*ortho*-bisazobenzene (**4e**) (3.76 g, 9.39 mmol, 1.00 equiv) in ethanol (341 ml) was treated with a solution of KOH (30.4 g, 542 mmol, 57.7 equiv) in ethanol (200 ml) and water (77 ml). The mixture was heated to 90 °C. After 1.5 h, the mixture was poured onto of ice (1.20 kg), extracted with CH_2Cl_2 (3x200 ml), dried over Na_2SO_4 and concentrated to yield a red oil (2.96 g), which crystallized in the refrigerator overnight (99 %). Mp: 95–98 °C. 1H NMR (400 MHz, $CDCl_3$) δ 7.88 (dd, J = 8.1, 1.5 Hz, 2H), 7.81 – 7.75 (m, 2H), 7.53 – 7.46 (m, 2H), 7.21 (ddd, J = 8.4, 7.1, 1.6 Hz, 2H), 6.87 – 6.81 (m, 2H), 6.75 (dt, J = 8.2, 3.9 Hz, 2H), 6.27 (s, 4H). The analytical data correspond to literature.⁸⁷

One-pot preparation of symmetric 2,2''-di-substitued bis-*ortho*-azobenzenes (4h). A solution of *ortho*-phenylenediamine (**1a**) (200 mg, 1.85 mmol, 1.00 equiv) in toluene (36 ml) was degassed with a nitrogen stream for 15 min. Then, nitrosobenzene (**2b**) (594 mg, 5.55 mmol, 3.00 equiv) and AcOH (215 μ l, 3.75 mmol, 2.00 equiv) were added. The mixture was stirred at 60 °C for 18 h and more AcOH (108 ml) was added. After 2 days the solvent was removed under reduced pressure. The residue was purified by flash column chromatography (SiO_2 , hexane/EtOAc, 7:1) and the solid that was obtained was recrystallized from EtOH to obtain 177 mg of a brown solid (33%). Mp: 106–109 °C; 1H NMR (400 MHz, $CDCl_3$) δ 8.01 – 7.94 (m, 4H), 7.79 – 7.73 (m, 2H), 7.61 – 7.46 (m, 8H). The analytical data correspond to literature.¹⁰²

General procedure for one-pot preparation of non-symmetric 2,2''-di-substitued bis-*ortho*-azobenzenes (condition D). A solution of *o*-phenylenediamine (**1a**) (1.00 equiv) in toluene (7 ml/mmol) was degassed under a nitrogen stream for 15 min. Then, the first nitroso compound (1.10 equiv) and AcOH (4.00 equiv) were added. The mixture was stirred at 60°C for 18h and the second nitroso compound (1.00 equiv) and more acetic acid (toluene/acetic acid, 1:3) were added. After 1 day the solvent was removed under reduced pressure. The residue was purified by flash column chromatography.

One-pot preparation of 2,2''-di-substitued bis-*ortho*-azobenzenes (4f). The title compound **4f** was prepared according to general procedure (condition D) from *o*-phenylenediamine (**1a**) (250 mg, 2.31 mmol, 1.00 equiv), 2-nitrosoacetanilide (**2a**) (417 mg, 2.54 mmol, 1.10 equiv) and 2-nitronitrosobenzene (**2c**) (352 mg, 2.31, 1.00 equiv). The residue was purified by flash column chromatography (SiO_2 , hexane/EtOAc, 2:1) and the product **4f** was obtained as an orange solid (450 mg, 50%).

One-pot preparation of 2,2''-di-substitued bis-*ortho*-azobenzenes (4g). The title compound **4g** was prepared according to general procedure (condition D) from *o*-phenylenediamine (**1a**) (1.80 g,

16.6 mmol, 1.00 equiv), 2-nitrosoacetanilide (**2a**) (2.73 g, 16.6 mmol, 1.00 equiv) and nitrosobenzene (**2b**) (7.13 g, 66.6, 4.00 equiv). The residue was purified by flash column chromatography (SiO₂, hexane/ EtOAc, 2:1) and the product was obtained in 23% yield (1.32 g).

2-Amino-2''acetamido-tris-ortho-azobenzene (5a). The title compound **5a** was prepared according to general procedure (condition B) from 2,2''-diamino-bis-*ortho*-azobenzene (**4i**) (250 mg, 0.790 mmol, 1.00 equiv) and 2-nitrosoacetanilide (**2a**) (131 mg, 0.869 mmol, 1.10 equiv). After 8 d the solvent was evaporated and the reaction mixture purified by flash column chromatography (SiO₂, hexane/EtOAc, 2:1 to 1:3) and the product was obtained in 17% yield (73.1 mg). Mp 177–180 °C; ¹H NMR (400 MHz, CDCl₃) δ 10.81 (s, 1H), 8.68 (d, *J* = 8.4 Hz, 1H), 7.99 (dd, *J* = 8.0, 1.6 Hz, 1H), 7.91 (dd, *J* = 3.5, 1.4 Hz, 1H), 7.89 (dd, *J* = 3.5, 1.4 Hz, 1H), 7.88 – 7.85 (m, 1H), 7.72 – 7.57 (m, 5H), 7.51 – 7.42 (m, 2H), 7.24 – 7.19 (m, 1H), 7.19 – 7.13 (m, 1H), 6.84 – 6.78 (m, 1H), 6.67 (dd, *J* = 8.2, 1.0 Hz, 1H), 6.53 (s, 2H), 1.74 (s, 3H); ¹³C NMR (101 MHz, CDCl₃) δ 169.7, 148.3, 148.1 (2C), 147.7, 141.71, 139.3, 137.9, 134.5, 133.3, 132.54, 132.50, 132.2, 131.6, 131.3, 130.2, 127.0, 123.4, 120.6, 119.5, 118.0, 117.8, 117.24, 117.22, 116.9, 25.2; HRMS (ESI): *m/z* calcd for C₂₆H₂₂N₈O⁺ [M+H⁺] 463.1989, found 463.1997.

2-Amino-tris-ortho-azobenzene 5b. The title compound **5b** was prepared according to general procedure (condition B) from 2,2''-diamine-bis-*ortho*-azobenzene (**4i**) (250 mg, 0.790 mmol, 1.00 equiv) and nitrosobenzene (**2b**) (84.6 mg, 0.790 mmol, 1.00 equiv). After 6 days the solvent was removed and the reaction mixture purified by flash column chromatography (SiO₂, hexane/EtOAc, 7:1) and the product was obtained in 50% yield (128 mg). Mp 156–159 °C; ¹H NMR (400 MHz, CDCl₃) δ 7.95 (dd, *J* = 8.0, 1.6 Hz, 3H), 7.92 – 7.88 (m, 1H), 7.82 (dd, *J* = 8.0, 1.3 Hz, 1H), 7.79 – 7.75 (m, 1H), 7.70 (dd, *J* = 7.3, 2.1 Hz, 1H), 7.64 – 7.54 (m, 3H), 7.54 – 7.43 (m, 4H), 7.22 – 7.15 (m, 1H), 6.84 (t, *J* = 7.0 Hz, 1H), 6.69 (d, *J* = 8.2 Hz, 1H), 6.64 (s, 2H); ¹³C NMR (101 MHz, CDCl₃) δ 153.1, 148.7, 148.5 (2C), 148.0, 141.5, 137.9, 133.3, 132.3, 132.1, 131.5, 131.2, 131.0, 130.3, 129.3 (2C), 123.4 (2C), 118.61, 118.57, 117.4, 117.3, 117.0, 116.5; HRMS (ESI): *m/z* calcd for C₂₄H₁₉N₇⁺ [M+H⁺] 406.1775, found 406.1779.

2-Nitro-tris-ortho-azobenzene 5c. The title compound **5c** was prepared according to general procedure (condition B) from 2-amino-*ortho*-bisazobenzene (**4b**) (300 mg, 0.996 mmol, 1.00 equiv) in toluene (10.0 ml) and 2-nitronitrosobenzene (**2c**) (167 mg, 1.10 mmol, 1.10 equiv) After 6 days the solvent was removed under reduced pressure and the product purified by flash column chromatography (SiO₂, hexane/EtOAc, 7:1 to 1:3) to give the product in 21% yield (91.1 mg). Mp 124–126 °C; ¹H NMR (400 MHz, CDCl₃) δ 7.95 – 7.81 (m, 5H), 7.80 – 7.70 (m, 2H), 7.69 – 7.55 (m, 5H), 7.54 – 7.38 (m, 5H); ¹³C NMR (101 MHz, CDCl₃) δ 152.9, 149.1, 148.5, 148.4, 147.6, 145.7, 135.0, 133.2, 132.3, 131.7, 131.6, 131.5, 131.0, 130.6, 129.2 (2C), 124.0, 123.3 (2C), 120.0, 118.9, 118.7, 118.3, 117.9; HRMS (ESI): *m/z* calcd for C₂₄H₁₇N₇O₂⁺ [M+H⁺] 436.1516, found 436.1522.

2-Acetamido-2'''-nitro-tris-*ortho*-azobenzene 5f. The title compound **5f** was prepared according to general procedure (condition B) from 2-acetamido-2''-amino-*ortho*-bisazobenzene (**4a**) (368 mg, 1.03 mmol, 1.00 equiv) in toluene (17 ml) and 2-nitronitrosobenzene (**2c**) (172 mg, 1.13 mmol, 1.10 equiv). After 6 d the solvent was removed under reduced pressure and the product purified by flash column chromatography (SiO₂, hexane/EtOAc, 2:1) to give the product in 58% yield (293 mg). mp 162–165 °C; ¹H NMR (400 MHz, CDCl₃) δ 10.83 (s, 1H), 8.62 (dd, *J* = 8.4, 1.1 Hz, 1H), 7.92 (dd, *J* = 8.0, 1.6 Hz, 1H), 7.87 – 7.80 (m, 3H), 7.76 (ddd, *J* = 13.4, 7.9, 1.8 Hz, 2H), 7.70 – 7.57 (m, 4H), 7.55 – 7.44 (m, 3H), 7.44 – 7.38 (m, 1H), 7.20 – 7.13 (m, 1H), 1.70 (s, 3H); ¹³C NMR (101 MHz, CDCl₃) δ 169.6, 149.2, 148.2, 147.7, 147.6, 147.0, 145.5, 139.2, 134.2, 133.3, 133.0, 132.3, 132.1, 131.6, 131.4, 130.8, 127.5, 124.1, 123.3, 120.6, 120.5, 118.7, 118.5, 118.4, 118.1, 25.0; MS (FAB): *m/z* (%) = 493 (81%) [M⁺], 345 (100%); C₂₆H₂₀N₈O₃ (492.49): calcd C 63.41, H 4.09, N 22.75; found C 63.42, H 4.14, N 22.60.

2,2''''-Dinitro-tetra-*ortho*-azobenzene 6. The title compound **6** was prepared according to general procedure (condition B) from diamine-bis-*ortho*-azobenzene (**4i**) (250 mg, 0.790 mmol, 1.00 equiv) and 2-nitronitrosobenzene (**2c**) (361 mg, 2.37 mmol, 3.00 equiv). After 4 days the solvent was removed and the reaction mixture purified by flash column chromatography (SiO₂, hexane/EtOAc, 2:1) and the product was obtained in 25% yield (114 mg). Mp 149–151 °C; ¹H NMR (400 MHz, CDCl₃) δ 7.90 – 7.83 (m, 4H), 7.80 – 7.74 (m, 2H), 7.64 (tt, *J* = 5.0, 2.5 Hz, 4H), 7.59 – 7.46 (m, 10H); ¹³C NMR (101 MHz, CDCl₃) δ 148.7, 148.4, 147.7 (2C), 145.6, 133.2, 132.3, 131.7, 131.6, 130.9, 124.0, 119.6, 119.0, 118.8, 117.8; HRMS (ESI): *m/z* calcd for C₃₀H₂₀N₁₀O₄⁺ [M+H⁺] 585.1742, found 585.1752.

Chapter 3 Phage selection of photoswitchable peptide ligands

This chapter is based on the following publication. Bellotto S., Chen S., Rentero Rebollo I., Wegner H.A., Heinis C. Phage selection of photoswitchable peptide ligands. *J. Am. Chem. Soc.* 2014, 136: 5880-5883. Reprinted with permission from the American Chemical Society. Copyright 2014.

3.1 Abstract

Photoswitchable ligands are powerful tools to control biological processes at high spatial and temporal resolution. Unfortunately, such ligands exist only for a limited number of proteins and their development by rational design is not trivial. We have developed an *in vitro* evolution strategy to generate light-activatable peptide ligands to targets of choice. In brief, random peptides were encoded by phage display, chemically cyclized with an azobenzene linker, exposed to UV light to switch the azobenzene into *cis* conformation, and panned against the model target streptavidin. Isolated peptides shared strong consensus sequences, indicating target-specific binding. Several peptides bound with high affinity when cyclized with the azobenzene linker and their affinity could be modulated by UV light. The presented method is robust and can be applied for the *in vitro* evolution of photoswitchable ligands to virtually any target.

3.2 Introduction

Photoswitchable ligands are used to control and study complex biological systems such as folding of proteins and peptides, enzymatic reactions or neuronal signaling.^{3,31,114-118} They are typically developed by conjugating photochromic compounds to known ligands so that exposure to light and a resulting conformational change of the photochrome changes the binding affinity of the ligand. Many light-responsive ligands are based on azobenzene, a molecule that undergoes a pronounced change in geometry upon photoisomerization from *trans* to *cis* in picoseconds.¹¹⁹ It has been linked to a wide range of small molecule ligands or peptides such as α -helices or β -hairpin

peptides.^{3,41,47,118,120,121} For many important protein targets, photoswitchable ligands do not exist or they suffer from limitations such as low affinity or a small difference in affinity between the two conformers. The transformation of existing ligands into light-responsive ones by rational design is not trivial. Combinatorial strategies based on the generation and screening of large molecule libraries for light-dependent binding could potentially revolutionize the development of photoswitchable ligands. *In vitro* display techniques such as phage display allow the genetic encoding of billions of random peptides and the identification of ligands within such pools. In recent years, strategies were developed to chemically modify or cyclize genetically encoded polypeptide libraries,^{122,123} or to incorporate unnatural amino acids.^{124,125} The availability of these novel techniques suggested that also photochromic compounds such as azobenzene could be incorporated into encoded peptides, and libraries screened.

Two first strategies for evolving light-responsive ligands *in vitro* have recently been proposed independently by the groups of Ito and Derda. Ito and co-workers incorporated an ϵ -(lysine)-azobenzene photoswitch into peptides encoded by mRNA using ribosome display and amber suppression.⁶⁰ The best binder isolated to the model target streptavidin was estimated to bind with a micromolar binding constant. Derda and co-workers cyclized phage-encoded peptides of the form ACX₇CG with azobenzene by connecting the two cysteines.⁵⁹ The best light-responsive ligand, identified also against streptavidin, had an affinity of 452 μ M in *trans* conformation and showed a more than 4.5-fold weaker apparent affinity in *cis* conformation.

Both of the two approaches generated peptide ligands that bind preferentially in *trans* conformation. This means that binders are inactivated by switching them into *cis* conformation by light. As only 70-80% of azobenzene can be switched to the *cis* conformation (for physical reasons), light cannot turn off these ligands completely. For example, if the photoswitchable peptide is an enzyme inhibitor, the concentration of active inhibitor is reduced maximally 5-fold, leaving most of the enzyme inhibited. Herein, we conceived a strategy to evolve peptide ligands that are activated by light rather than inactivated. Such peptide ligands bind the target when the azobenzene is switched to *cis*. A light-activatable ligand has the advantage that essentially all the peptide population (99.99%) is initially in the energetically favored *trans* conformation. In the example of the enzyme inhibitor, all peptide would initially be in the inactive *trans* conformation, leaving the enzyme fully active. Upon UV light exposure, all enzyme would be inhibited even if only a fraction of the ligand population is switched.

3.3 Results and discussion

Directed evolution of light-activatable peptide ligands requires that peptides are captured in their *cis* conformation, increasing the complexity of the selection process compared to the screening for *trans* binders. Combining the expertise of the Heinis laboratory in phage display and the knowhow of the Wegner group in azobenzene chemistry and UV spectrometry, we herein estab-

lished the photoswitching of peptides *in situ* on the surface of filamentous phage. We furthermore developed procedures to efficiently select light-responsive peptide ligands to targets of choice. While all *in vitro*-evolved ligands reported to date bind with K_d s in the high micromolar range, we aimed at developing binders with low micromolar or nanomolar K_d s. Affinities in this range are required for most applications.

We synthesized the photoswitchable compound 3,3'-bis (sulfonato)-4,4'-bis(bromoacetamido) azobenzene (BSBBA) in analogy to the prototype compound BSBCA developed by Woolley et al.^{32,126} and applied it to cyclize the phage-encoded peptides via the side chains of two flanking cysteines in a similar way as Derda et al.⁵⁹ (Figure 3.1a). BSBBA contains bromoacetamide that is slightly more reactive towards thiols than chloroacetamide in BSBCA.¹²⁶ We displayed peptides containing seven random amino acids flanked on each side by cysteines as fusion of pIII on filamentous phage (ACX₇CG-phage; complexity: 2.3×10^8 peptides). An engineered phage mutant deficient in three disulfide bridges in two domains of pIII was used.¹²⁷ This mutant allowed application of a broad range of reduction and alkylation conditions without affecting the functionality of the phage.^{53,128} We applied harsh reaction conditions to efficiently reduce the cysteines of displayed peptides (1 mM TCEP, 42 °C, 1 hr) and to alkylate the peptides quantitatively. 90 % of peptide was modified at 320 μ M BSBBA in 20% ACN, 80% NH₄HCO₃, pH 8, 30 °C (Figure 3.1b and 3.1c).

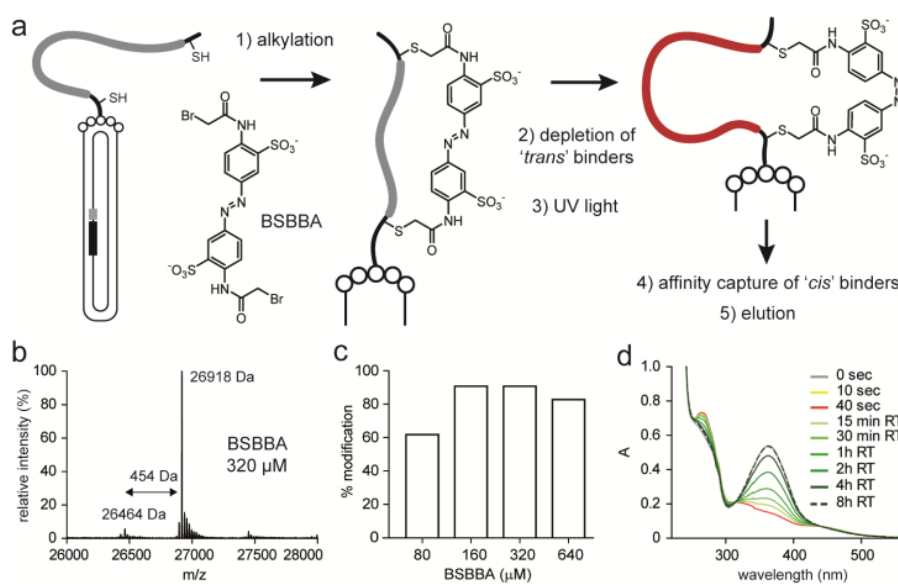


Figure 3.1. Phage selection of light-activated peptide ligands. (a) Schematic depiction of the selection strategy. (b) Mass spectrum of peptide genetically fused to phage coat protein pIII (domains D1 and D2) after incubation with 320 μ M BSBBA for 1 hr (expected Δ mass = 454 Da). (c) Fraction of azobenzene-cyclized peptide-D1-D2 at different BSBBA concentrations estimated by mass spectrometry. (d) Absorption spectra of peptide cyclized with BSBBA in the presence of phage particles.

Towards the photoswitching on phage, we found that filamentous phage exposed 20 min to a 100 W light source ($\lambda = 365/66$; distance of the cuvette = 21 cm) remained fully functional. To assess if the peptides switch under these conditions, we spiked the same phage preparation with a

BSBBA-cyclized model peptide ($\text{H}_2\text{N-AGSCHSASVCWG-CONH}_2$; 22 μM) and followed the switching by absorption spectrometry (Figure 3.1d). Maximal switching to *cis* (around 70 %) was achieved in 40 s. We performed selections against the model target streptavidin that was applied by the groups of Ito and Derda and allowed comparison of the isolated peptides.^{59,60} The CX₇C phage library cyclized with BSBBA was subjected to two consecutive selection rounds against streptavidin as follows. The population was first depleted of *trans* binders by adding and discarding 7 times 10 μL magnetic streptavidin beads. The remaining phage were exposed 5 min to the UV light and incubated with 20 μL magnetic streptavidin beads to capture *cis* binders. Binders were eluted by addition of biotin and buffer with a low pH (2.2). A control experiment was performed in parallel with phage-peptides that were not cyclized with BSBBA and exposed to UV light. Sequencing of 62 clones after two rounds of selection showed strong consensus sequences. Most peptides contained a 'HPQ' motif,^{69,129} that is characteristic for peptides binding to the biotin-binding site of streptavidin (Figure 3.2a, left). In the control selection without BSBBA-cyclization and UV light exposure, a similar but different consensus sequence was observed than in the actual selection, indicating that the peptides were efficiently cyclized with the azobenzene compound (Figure 3.2a, right). We were pleased to find consensus sequences among the isolated peptides as this is a clear indication for target-specific binders. It was the first time that a consensus sequence was found in directed evolution of azobenzene-modified peptides.

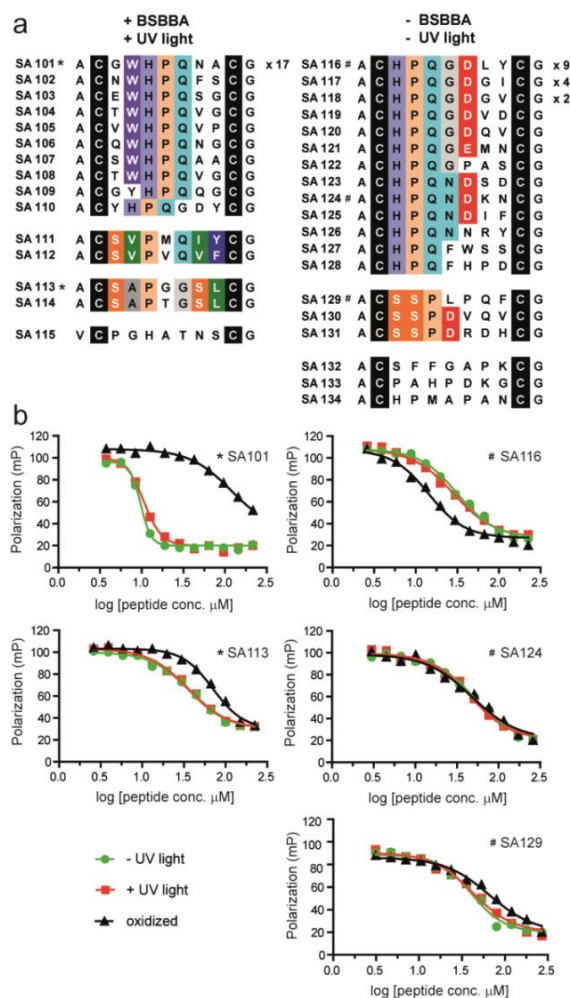


Figure 3.2. Phage selection of light-switchable streptavidin ligands from the CX₇C peptide library. (a) Peptides isolated after cyclization of the peptide phage library with BSBBA and exposure to UV light (left column) or without alkylation and UV light exposure (right column). Sequence similarities are highlighted in color. (b) Binding of peptides to streptavidin measured in a fluorescence polarization competition assay. Peptides are labeled with an asterisk (*) if they were selected with BSBBA and UV light, and with a hash symbol (#) if they were isolated as disulfide-cyclized (oxidized) peptides.

Five peptides of the selection against streptavidin were synthesized, cyclized with BSBBA or oxidized to form disulfide-cyclized peptides, and the binding affinities measured in a fluorescence polarization competition assay. Light in the fluorescence polarization measurement did not interfere with the photoswitching of the peptide (Supplementary Figure S4). All peptides competed with the disulfide-cyclized fluorescent peptide fluorescein-AEHPQGPCIEG (F1) which binds with a K_d of $3.1 \pm 0.4 \mu\text{M}$ to the biotin-binding site of streptavidin (Figure 3.2b, Appendix, Supporting table S1). The peptides isolated in phage selections after BSBBA-cyclization (SA101 and SA113) bound much better when modified with BSBBA than when oxidized. Conversely, peptides isolated in the control selection omitting BSBBA (SA116, SA124, SA129) bound worse or equal when BSBBA-cyclized. These results implied that the alkylation reaction on phage was successful and that peptides were isolated as BSBBA conjugates in the phage panning. All characterized BSBBA-cyclized peptides could be switched efficiently into the *cis*-conformation (50-80%) but the binding affinities of the *cis* and *trans* conformers were essentially the same (Appendix, Supporting table S1). We speculated that light-responsive

ligands were not selected due to the long peptide loops: the amino acids next to the cysteines might be too flexible so that a conformational change of the linker is not transformed into a conformational change of the contact-forming amino acids. In fact, an X-ray structure of a peptide with HPQ motif in complex with streptavidin shows that the central 3-4 amino acids including HPQ are sufficient for binding.^{62,70}

We subsequently turned to peptides with shorter loops. A library of the format AXC₅CXG-phage was cloned (complexity: 1.05 x 10⁷ peptides) and subjected to affinity selections against streptavidin. Isolated peptides showed four different consensus sequences (Figure 3.3a and 3.3b). Three out of the four consensus sequences were not found in the control selection in which BSBBA was omitted. This suggested that the binding of peptides of these consensus groups could potentially be modulated by light.

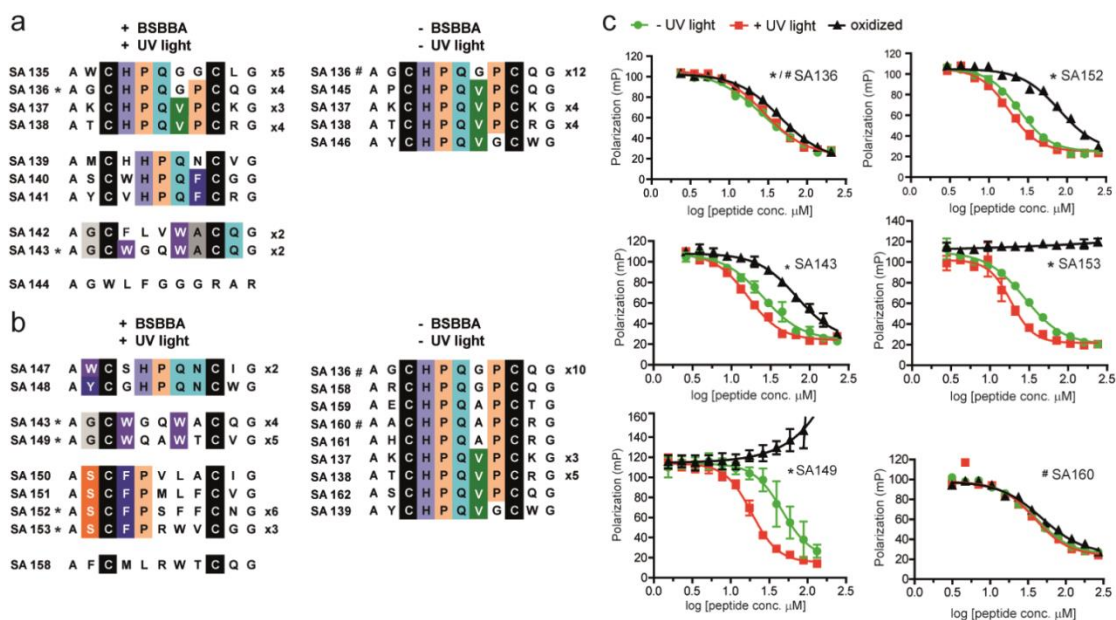


Figure 3.3. Phage selection of light-switchable streptavidin ligands from the CX₅C library. (a and b) Peptides isolated after cyclization of the peptide phage library with BSBBA and exposure to UV light (left columns) or without alkylation and UV light exposure (right columns). The library was either depleted from *trans* binders prior to UV light exposure (a) or no negative selections were performed (b) prior to capture of *cis* binders. (c) Binding of peptides to streptavidin measured by fluorescence polarization. Peptides are labeled with an asterisk (*) if they were selected with BSBBA and UV light and with a hash symbol (#) if they were isolated as disulfide-cyclized (oxidized) peptides. The binding of light-responsive ligands was measured in independent assays and error bars are indicated.

The peptides of the XCX₅CX library bound streptavidin with K_ds between 1.8 ± 0.1 and 6.7 ± 2 μM when cyclized with BSBBA (Figure 3.3c, Table 3.1). Some peptides isolated with BSBBA did not bind streptavidin at all when cyclized by a disulfide bridge, confirming that the peptides were selected as BSBBA conjugates. Upon UV light exposure, the peptides of two consensus groups changed their binding affinity; the *cis* conformers bound up to 3-fold more tightly than the peptides in *trans* conformation (Figure 3.3c and Table 3.1).

Name	Consensus sequence	$K_d^{\text{dark a}}$ (μM)	$K_d^{\text{light a}}$ (μM)	$K_d^{\text{S-S b}}$ (μM)
SA143	G_W__W	3.4 \pm 0.6	1.8 \pm 0.1	9.5 \pm 1
SA149	G_W__W	6.7 \pm 2	2.2 \pm 0	> 250
SA152	S_FP	3.1 \pm 0.1	2.1 \pm 0.2	11 \pm 0
SA153	S_FP	3.6 \pm 0.3	2.0 \pm 0.5	> 250

[a] Peptides cyclized with BSBBA, [b] Disulfide-cyclized peptides

Table 3.1. Photo-responsive peptides.

In contrast, peptides identified in the control selections without BSBBA and synthesized as BSBBA conjugates did not change their affinity upon light exposure (Supplementary Table S1). The change in affinity was quantitatively reverted by incubation in dark as shown in Figure 3.4a and 3.4b. The peptides could be switched between the *cis* and *trans* conformation for several cycles without losing any activity, as shown for SA153 in Figure 3.4c.

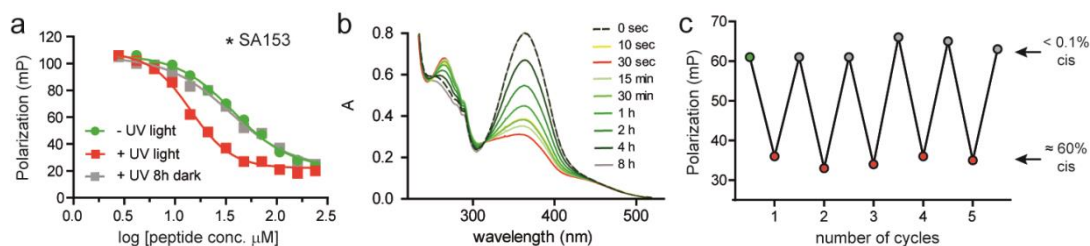


Figure 3.4. Switching ‘on’ and ‘off’ streptavidin-binding peptides. (a) Binding of BSBBA-cyclized peptide SA153 was measured i) before exposure to UV light, ii) immediately after UV light exposure, and iii) after UV light exposure and 8 hrs incubation in the dark. (b) Absorption spectra of SA153 after exposure to UV light for 10 or 30 seconds and incubation in the dark for the indicated times. (c) Binding of SA153 to streptavidin after repetitive exposure to UV light (red dots) and incubation at 40 °C in dark for 1 hr (grey dots) measured in a competition fluorescence polarization assay.

3.4 Conclusions

In conclusion, we were able to isolate light-responsive peptide ligands that bind with K_d s in the single-digit micromolar range and thus > 300-fold better than those developed previously with other *in vitro* evolution procedures to the same model protein target. Use of a disulfide-free phage mutant and custom-made libraries allowed application of robust peptide modification procedures. An important aspect of our approach is the switching of peptides *in situ* on the phage surface to the *cis* conformation, enabling the isolation of ‘activatable ligands’. The affinity difference between *cis* and *trans* conformation likely depends much on the target and binding site, and significantly larger changes may be obtained in selections with other proteins. The robust and general approach should be applicable for the directed evolution of light-responsive peptide ligands to virtually any target and promises to additionally fuel the fast growing field of optogenetics.

3.5 Materials and methods

Synthesis of 3,3'-bis(sulfonato)-4,4'-bis(bromoacetamido)azobenzene (BSBBA)

Sodium 3,3'-bis(sulfonato)-4,4'-bis(amino)azobenzene was prepared following procedures developed by Woolley and co-workers.³² To 291 mg (0.802 mmol, 1.00 equiv.) of this compound, bromoacetic acid (2.67 g, 19.2 mmol, 24.0 equiv.) and bromoacetic anhydride (5.00 g, 19.2 mmol, 24.0 equiv.) were added in a Pyrex Culture Tube Screw Cap, the tube put under nitrogen atmosphere and stirred at 87 °C overnight. The reaction mixture was cooled to RT, diluted to 50 mL with milliQ water and purified by reversed-phase chromatography on a Vydac C18 (218TP) column (22 x 250 mm) (Grace & Vydac, Hesperia, USA) using a solvent system of H₂O/0.1 % trifluoroacetic acid (TFA) and ACN/0.1 % TFA. After lyophilization the product was obtained in 23% yield (111 mg, 0.181 mmol).

¹H NMR (400 MHz, D₂O) δ 8.24 (d, J = 2.2 Hz, 2H), 8.14 (d, J = 8.8 Hz, 2H), 7.90 (dd, J = 8.8, 2.1 Hz, 2H), 4.20 (s, 4H) ¹³C NMR (101 MHz, DMSO) δ 164.73, 146.89, 137.02, 136.47, 126.16, 120.16, 119.39, 30.56. HRMS (ESI) m/z calcd for C₁₆H₁₂Br₂N₄O₈S₂²⁻ [M/2]⁻ 305.9227, found 305.9204.

Peptide synthesis

Peptides were synthesized on an Advanced ChemTech 348Ω peptide synthesizer (Aapptec, Louisville, USA) by standard Fmoc (9-fluorenylmethyloxycarbonyl) solid phase chemistry using Rink Amide AM resin (0.03 mmol scale). The coupling step was carried out twice for all amino-acids using 0.12 mmol Fmoc-protected amino acid, 0.12 mmol HBTU, 0.12 mmol HOBt and 0.18 mmol DIEA in 1.3 mL DMF. Fmoc groups were removed using a 20% (v/v) solution of piperidine in DMF (2 x 2.5 mL). The peptides were deprotected and cleaved from the resin by treatment with 5 mL of cleavage solution (90% TFA, 2.5% phenol, 2.5% thioanisole, 2.5% 1,2-ethanedithiol (EDT) and 2.5% water), for 3 hrs at RT under shaking. The resin was removed by centrifugation 1 min at 1000 rpm and filtration under vacuum. The peptides were precipitated with ice-cold diethyl ether (50 mL), incubated 30 min at - 20 °C and centrifuged 5 min at 4000 rpm. The precipitated peptides were washed and centrifuged 5 min at 4,000 rpm twice with ice-cold ether (35 and 20 mL, respectively). Samples were re-suspended in water/ACN (ratio 5:2) containing 0.1% TFA and lyophilized.

Peptide cyclization with BSBBA

Crude peptide (1.00 equivalent; typically 10 mg) was reacted with BSBBA (1.1 equivalent) in 90-50% aqueous buffer (20 mM NH₄HCO₃, pH 8.0) and 10-50% ACN for 1 hr at 30 °C. The product was purified by reversed-phase chromatography on a C18 column (Vydac C18, 218TP column, 22 x 250 mm) using a solvent system of 99.9% H₂O/0.1% TFA and 99.9%ACN/0.1 % TFA. The peptide was lyophilized and the mass was confirmed by electrospray ionization (ESI) mass spectrometry.

Peptide cyclization by oxidation

Crude peptide (typically 10 mg) was dissolved in 9 mL aqueous buffer (20 mM NH_4HCO_3 , pH 8.0) and 1 mL DMSO, and incubated for 1-2 days at RT. The product was purified by reversed-phase chromatography on a C18 column (Vydac C18, 218TP column, 22 x 250 mm) using a solvent system of 99.9% H_2O /0.1% TFA and 99.9% ACN/0.1% TFA. The peptide was lyophilized and the mass was confirmed by ESI mass spectrometry.

Buffers

Reaction buffer: 20 mM NH_4HCO_3 , 5 mM EDTA, pH 8.0

Washing buffer: 10 mM Tris-HCl, pH 7.4, 150 mM NaCl, 10 mM MgCl_2 , 1 mM CaCl_2

Modification of the peptide-D1-D2 fusion protein

Peptide-D1-D2 fusion protein (ACGSGSGSGCG-D1-D2) was expressed and purified as described by Angelini, A. et al.⁵⁷ 680 μg of the fusion protein in 1 mL aqueous buffer was incubated with 1 mM tris(2-carboxyethyl) phosphine (TCEP) for 1 hr at 42 °C to reduce the cysteine residues. The concentration of TCEP was reduced by size exclusion chromatography on a PD-10 column (GE Healthcare, Uppsala, Sweden) using 20 mM NH_4HCO_3 buffer, pH 8. The protein (30 μM) was incubated with increasing concentrations of BSBBA (80, 160, 320, 640 μM) in 25% acetonitrile and 75% 20 mM NH_4HCO_3 for 1h at 30 °C in a final volume of 200 μL . The protein was purified by reversed-phase chromatography on a C4 column (Vydac C4 column, 5 μm , 4.6 x 250 mm) using a solvent system of 99.9% H_2O /0.1% TFA and 99.9%ACN/0.1% TFA. The mass was determined by ESI mass spectrometry.

Testing photoswitching of peptide in presence of phage

A solution of filamentous phage (10^{11} phage/mL) was spiked with the peptide H_2N -AGSCHSASVCWG-CONH₂ cyclized with BSBBA in washing buffer at a concentration of 22 μM and placed into a 1 cm quartz cuvette. The sample was irradiated with light at the 365/66 nm peak generated by a HBO 100 mercury illuminating system (100-watt high-pressure mercury plasma lamp) at a distance of 21 cm using appropriate filters and the absorption spectra were measured at different time points.

Testing phage infectivity after BSBBA modification and UV irradiation

Phage of the CX₇C library was produced in four 0.5 L cultures as described by Rentero-Rebollo, I. et al.¹²⁸ Aliquots of phage (10^{11} t.u.) in 1 mL 80% 20 mM NH_4CO_3 , pH 8.0, 5 mM EDTA and 20% ACN were incubated with increasing concentrations of BSBBA (final concentration: 0, 40, 80,160, 320, 640 μM) for 1 hr at 30 °C. The reactions were quenched by addition of cysteine at concentrations 20-fold higher than those of BSBBA. The number of infective phage was measured as described by Rentero-Rebollo, I.¹²⁸ et al. 2 mL of phage from the same preparation were transferred

to a quartz cuvette and irradiated with the HBO 100 mercury illuminating system as described above. At each time point (0, 30 sec, 1, 2, 4, 8, 16 min) the solution was mixed and 20 µL were taken for phage titration.

Cloning of the phage peptide libraries

The phage peptide libraries CX₇C and XCX₅CX were cloned using a protocol described by Rentero-Rebollo, I. et al.¹²⁸ The following DNA primers were used:

Primer name:	Sequence (5'-3'):
Sfi1cx7cba	TATGCGGCCAGCCGGCCATGGCAGCATGCNNKNNKNNKNNKNNKNNKNNKTGTG GCGGTTCTGGCGCTG
L3_1C5C1	TATGCGGCCAGCCGGCCATGGCAGCANNKTGCNNKNNKNNKNNKNNKTGCNNKG GCGGTTCTGGCGCTG

Phage of these libraries display peptides with the following formats. The indicated sequence 'AETV...' represents the N-terminus of pIII. The complexities of the libraries are also indicated.

Library name:	Format:	Diversity:
CX ₇ C	ACXXXXXXXXCGGSG-AETV...	2.3 x 10 ⁸
XCX ₅ CX	AXXXXXXXXXCXGGSG-AETV...	1.05 x 10 ⁷

Production of phage peptide libraries cyclized with BSBBA

Two 2 L flasks each containing 0.5 L 2YT media and 30 µg/mL chloramphenicol were inoculated with TG1 E. coli cells harbouring the CX₇C or the XCX₅CX phage library to reach an OD₆₀₀ of 0.1. The flasks were shaken (220 rpm) for 16 hrs at 30 °C. The cells were pelleted by centrifugation at 8,000 rpm for 30 min at 4 °C. The supernatant was transferred to an ice-cold solution of 20% PEG, 2.5 M NaCl (20% of culture volume) and incubated on ice for 45 minutes. Precipitated phage were pelleted by centrifugation at 8,000 rpm for 30 min at 4 °C. The phage pellet was resuspended in 20 mL of reaction buffer and centrifuged at 4,000 rpm for 15 min at 4 °C. The supernatant was split into two fractions of 10 mL to either cyclize the peptides by BSBBA or to allow peptides to oxidize and form disulfide bridges. Phage in the first tube were complemented with 10 mL reaction buffer and TCEP (final concentration 1 mM), and incubated at 42 °C for 1 hr to reduce the cysteines. Phage were cooled on ice and concentrated by centrifugation at 4,000 rpm in a Vivaspin-20 filter (molecular weight cut off of 100,000; GE Healthcare) to 1 mL, diluted with 9 mL ice-cold reaction buffer. This procedure was repeated to reduce the TCEP concentration to 1 µM in 1 mL. Traces of phage stuck to the filter were detached by pipetting. The solution was adjusted to 4 mL with the same buffer. 1 mL of BSBBA in milliQ water was added to the phage to reach a final concentration of 0.32 mM and the

reaction was incubated at 30 °C for 1 hr. Phage were separated from non-reacted BSBBA by precipitation with 1 mL 20% (w/v) PEG, 2.5 M NaCl on ice and centrifugation at 4,000 rpm for 30 min. The phage pellet was resuspended in 1 mL washing buffer and stored at 4°C. Phage in the second tube were incubated with 2.5 mL ice-cold 20% PEG, 2.5 M NaCl solution for 30 min and centrifuged at 4,000 rpm for 30 min at 4 °C. The phage pellet was resuspended in 1 mL washing buffer.

Phage selection of photoswitchable streptavidin ligands

The affinity selection was performed with streptavidin Dynabeads® M-280 (Life Technologies, Carlsbad, USA). Beads were blocked by exchanging the storage solution to washing buffer containing 1% w/v BSA and 0.1% v/v Tween 20 and inverting on a rotating wheel (10 rpm) for 30 min at RT.

For the phage selection with the CX₇C library (results shown in Figure 3.2a), the following procedures were applied. Both, the BSBBA-modified phage (1 mL) and the oxidized phage (1 mL) were blocked in parallel by addition of 0.5 mL washing buffer containing 3% w/v BSA and 0.3% v/v Tween 20 and inversion on a rotating wheel (10 rpm) for 30 min at RT. The blocked phage were subjected to seven rounds of negative selection as follows: each phage solution was incubated with 10 µL of blocked streptavidin beads and inverted on a rotating wheel (10 rpm) for 10 min. The supernatant was collected and incubated with 10 µL of new blocked streptavidin beads. The procedure was repeated six times. Modified phage were split into two tubes (0.75 mL for each tube) and one of the two fractions was irradiated for 5 min with UV light (365/66 nm) using the HBO 100 mercury lamp as described above. Immediately after UV light exposure, each one of the three phage populations (BSBBA-modified phage irradiated, 0.75 mL; BSBBA-modified phage not irradiated, 0.75 mL; oxidized phage with disulfide cyclized peptides, 1.5 mL) were incubated in parallel with 20 µL of blocked streptavidin beads and rotated on a wheel (10 rpm) for 30 min. The beads were washed four times with 1 mL washing buffer containing 1% BSA and 0.1% v/v Tween 20, three times with washing buffer containing 0.1% v/v Tween 20 and three times with 1 mL washing buffer. The bound phage were eluted by incubation for 5 min with 1 mL of biotin solution (30 µg/ml in milliQ water). Additionally, remaining phage were eluted by incubation of the beads in 50 µL 50 mM glycine, pH 2.2 for 5 min. The eluate was neutralized with 100 µL 1 M Tris-HCl, pH 8.0. Eluted phage was added to exponentially growing TG1 cells (OD₆₀₀ = 0.4; 30 mL), incubated for 90 min at 37 °C, pelleted by centrifugation at 4,000 rpm for 5 min, plated on large 2YT/chloramphenicol (30 µg/mL) agar plates and incubated over night at 37 °C. From the selection with BSBBA-treated and UV light-irradiated phage and the selection with oxidized phage, new phage was produced in 0.5 mL 2YT media as described above. Two additional rounds of phage selection were performed applying identical procedures.

For the phage selection with the XCX₅CX library, two different procedures were applied (results of the first procedure are shown in Figure 3.3a and those of the second procedure in Figure

3.3b). The first procedure is exactly the same as described above for the panning with the CX₇C library. In the second procedure, the negative selection for depletion of *trans* binders was omitted.

Labeling of peptides with fluorescein

Peptides were labelled with fluorescein by incubating 1 mM peptide (typically 0.3 mg, 1.0 equiv.) with 2.5 mM 5(6)-carboxyfluorescein N-hydroxysuccinimide ester (NHS-fluorescein; 2.5 equiv. 21878 Sigma-Aldrich, St. Louis, USA) in 200 μ L 99,75% v/v dry DMSO and 0.25% v/v N,N-Diisopropylethylamine (DIPEA) for 3 hrs at RT. 0.8 mL H₂O containing 0.1% TFA (v/v) was added to the reaction mixture and the peptide purified by HPLC on an analytical C18 column (Vydac C18, 218TP column, 4.6 x 250 mm) using a solvent system of 99.9% H₂O/0.1% TFA and 99.9% ACN/0.1% TFA. The fluorescein-modified peptide was lyophilized and the mass confirmed by ESI-MS.

Measuring K_d by fluorescence polarization

Streptavidin (S4762; Sigma-Aldrich; 66 μ M in washing buffer) was serially diluted in washing buffer (final concentration range 33 μ M - 0.01 μ M). Fluorescein-labeled peptide at a concentration of 100 nM was prepared in washing buffer. 20 μ L of streptavidin and fluorescein-peptide were transferred into a well of a black 96-well half area microplate (675076 Greiner Bio-One international AG) and incubated at room temperature for at least 15 min. The fluorescence polarization of each solution was measured in a multiwell plate reader (Infinite[®] 200 PRO, TECAN, Maennedorf, Switzerland) using a 485 nm excitation filter and a 535 nm emission filter.

The dissociation constants (K_d) were determined by non-linear regression analyses of fluorescence polarization (F_p) versus total concentration of streptavidin [P]_T using the following equation.¹³⁰

$$F_p = F_{pmin} + (F_{pmax} - F_{pmin}) \times \left\{ \frac{([L]_T + K_d + [P]_T - \sqrt{([L]_T + K_d + [P]_T)^2 - 4[L]_T[P]_T})}{2[L]_T} \right\}$$

F_{pmin} and F_{pmax} are the fluorescence polarization for the free peptide and the fully bound peptide, respectively and [L]_T is the total concentration of fluorescent ligand. GraphPad Prism 5 software (GraphPad software) was used for the analysis.

Competitive fluorescence polarization

20 μ L of 6 μ M streptavidin in washing buffer was mixed with 20 μ L of 150 nM fluorescent peptide F1 (in washing buffer) and incubated for 15 minutes. 20 μ L of serial dilutions of sample peptide were added. The sample peptide was either cyclized with BSBBA or a disulfide bridge. BSBBA-cyclized peptide was optionally exposed to UV light for 7 min as described above. I50 (total concentration of competing ligand I causing 50 % displacement of bound fluorescent peptide) was calculated with GraphPad Prism 5 software using the log(inhibitor) vs. response variable slope model. The K_d was determined as reported by Rossi and Taylor.¹³¹

Repetitive switching of light-responsive peptides

450 μL of 90 μM BSBBA-cyclized SA153 in washing buffer were subjected to four iterative cycles of *i*) irradiation for 2 minutes at 365/366 nm (as described above) and *ii*) incubation in a water bath for 1 hr at 40 °C. Before the first exposure to UV light and after each cycle, two aliquots of 30 μL were taken and their complete back-isomerization to *trans* was confirmed by measuring the absorbance at 363 nm on a NanoDrop device (NanoDrop ND-1000 UV-Vis Spectrophotometer, NanoDrop Technologies, Inc. Wilmington, DE, USA). One of the two aliquots was subjected to an additional irradiation at 365/366 nm for 2 min. 20 μL of each sample was added to 20 μL of 6 μM streptavidin in washing buffer previously incubated with 20 μL of 150 nM fluorescent peptide F1. Fluorescence polarization was measured for all samples in parallel.

Chapter 4 Phage selection of photoswitchable peptides inhibitors of uPA

4.1 Abstract

Photoswitchable ligands are powerful tools for the study of biological processes at high spatial and temporal resolution. Recently, methods were developed to evolve photoswitchable peptide ligands by directed evolution techniques such as phage display. All methods employed peptides modified with azobenzene photoswitches and were tested with streptavidin as a model target.^{59,60,132} A limitation of the isolated peptide ligands was the relatively small difference in binding affinity before and after photoswitching. In this work, we aimed at developing light-switchable peptides binding to a second target to see if this is a general limitation of the method. We subjected a phage display peptide library of the format XCX₅CX cyclized with an azobenzene linker to affinity selections against the serine protease urokinase-type plasminogen activator. By high-throughput sequencing, we were able to identify several families of peptides that have different consensus sequences and inhibit uPA through different binding modes. Interestingly, peptides within the same consensus family had similar binding properties. Overall, the change in affinity upon light exposure was again rather small.

4.2 Introduction

Recently, random strategies based on the generation and screening of large molecule libraries for light-dependent binding were developed using directed evolution approaches.^{59,60} Ito and co-workers incorporated a ϵ -(lysine)-azobenzene photoswitch into the peptide ribosome display libraries with the formats X₃YX₇ and X₇YX₃ (Y = ϵ -(lysine)-azobenzene, X = any amino acid) using amber suppression and screened them for binding in *trans* conformation to streptavidin. The best binder was estimated to bind with a micromolar binding constant. As anticipated, it bound more tightly in the *trans* conformation. The difference in affinity between *cis* and *trans* form was not quantified.⁶⁰ Derda and co-workers cyclized phage-encoded peptides of the form ACX₇CG with 3,3'-bis(sulfonato)-

4,4'-bis(chloroacetamido)azobenzene (BSBCA) and screened them also for binding in *trans* conformation to streptavidin. The best light-sensitive ligand identified had an affinity of 452 μM and showed at least a 4.5-fold apparent weaker affinity in *cis* conformation.⁵⁹ Our laboratory has recently developed a strategy to evolve peptide ligands that bind protein targets with higher affinity after light exposure.¹³² We displayed peptides flanked by two cysteines residues on phage and cyclized them with an azobenzene compound similar as Derda and co-workers. In contrast to this latter work, we isolated peptides after UV light exposure in order to capture 'light-activatable' binders. We succeeded in isolating a range of peptide ligands that displayed high affinity for the model target streptavidin. The largest change in affinity upon UV light exposure was 3-fold.

A limitation of all photoswitchable peptide ligands developed with the three new *in vitro* evolution strategies is the small difference in affinity between the peptides in *cis* and *trans* conformation. In phage selections with our strategy, we found that peptides with similar sequences show similar binding properties. For example peptides isolated against streptavidin, containing the 'HPQ' sequence motif in different positions between the flanking cysteines, changed not at all their affinity upon switching their conformation from *trans* to *cis*. In contrast, peptides isolated against the same target, containing the consensus motif 'GCWXXW', change their binding affinity when they were switched into the *cis* conformation. Similarly, all peptides with the peptide motif 'SCFP' changed also their affinity after switching them into the *cis* conformation. It appeared that the extent of affinity change between *cis* and *trans* conformation depends much on the binding site and the manner that peptides bind. Peptides that mainly interact through a central motif but not the peptide termini may be less sensitive on a small change in the relative position of the two ends. In contrast, peptides that interact via the cysteines or close by residues may be much affected by a conformational change.

In this work, we aimed at investigating the switching properties of a wider range of peptides that bind to different surface regions of a protein, or to the same region but by forming different interactions. Towards this end, we selected photoswitchable peptides against the target urokinase-type plasminogen activator (uPA). Selections of (bi)cyclic peptides against the protease target previously yielded several groups of peptides that each shared a different consensus sequence.^{57,58,82,83} Peptides containing different consensus sequences typically bind to the target through different interactions. To capture as many peptides with different binding modes as possible, we applied high-throughput DNA sequencing to analyze many phage-selected peptides. The target uPA was primarily chosen as a model target to further assess the potential of phage display approach in delivering photoswitchable peptide ligands. However, as the function of the extracellular serine protease in tumor growth and invasion is not fully understood, a light-activatable inhibitor of uPA could potentially be used to study the function of the protease in extracellular proteolysis and signaling in normal and tumor cells.

4.3 Results and discussion

In the selections against uPA, the XCX_5CX phage library was cyclized with BSBBA as described in our previous work and two different panning procedures were applied.

In the first one, biotinylated uPA immobilized on magnetic streptavidin beads was first added to the phage and the beads discarded to remove peptides binding in *trans* conformation. This depletion step was repeated six times. The phage were then exposed to UV light and binders captured on uPA beads to enrich *cis* binders. The phage were eluted, incubated in the dark to allow relaxation of the photoswitch and followed by another seven negative selections to remove *trans* binders that were possibly still present in solution. In parallel, a control experiment was performed in which the same library, not cyclized with BSBBA and not exposed to UV light, was panned against uPA. Several clones isolated in the selection experiment and in the control experiment were sequenced (Figure 4.1a). In the selection with BSBBA-cyclized peptides exposed to UV light, five different consensus sequences were found. Most peptides were sharing the consensus sequence $D^K/R^Y/F^T/S$ (Figure 4.1a, left). In the control experiment, the major consensus sequence $D^K/R^Y/F^T/S$ was found too. Additionally, two different consensus sequences were identified (Figure 4.1a, right).

In the second panning procedure the negative selections were omitted and the phage captured after UV light exposure. To apply more stringent conditions the irradiation and the elution were repeated once and twice in selection rounds two and three. Control experiments with phage peptide library not cyclized with BSBBA were performed in parallel in the same way. In the selection with peptides cyclized with BSBBA and irradiated with UV light, four consensus sequences were found, including the major consensus sequence $D^K/R^Y/F^T/S$ (Figure 4.1b, left). In the control selection omitting BSBBA-cyclization and UV light exposure, three consensus sequences were found. Again, most peptides were sharing the major consensus motif $D^K/R^Y/F^T/S$ (Figure 4.1b, right).

From the sequencing result, we concluded that the peptides from the major consensus sequence $D^K/R^Y/F^T/S$, found in all the four selection procedures, are binding uPA independent of the cyclization linker, being BSBBA or a disulfide bridge. Several of the minor consensus sequences were different in the BSBBA selections and the controls, suggesting that binding of some of the peptides depends on the linker or even linker conformation. A limitation of our analysis was that only few peptides were found for the minor consensus groups.

In the last years, the development of next generation sequencing (NGS) technologies allowed the analysis of massive volumes of sequences increasing exponentially the potential of *in vitro* selection methods. Our laboratory had recently applied Ion Torrent sequencing to analyze phage-selected peptides. Further MatLab scripts were developed to evaluate vast sequence data and to identify consensus sequences. With these new methods, consensus sequences could be found even after one round of selection.¹³³

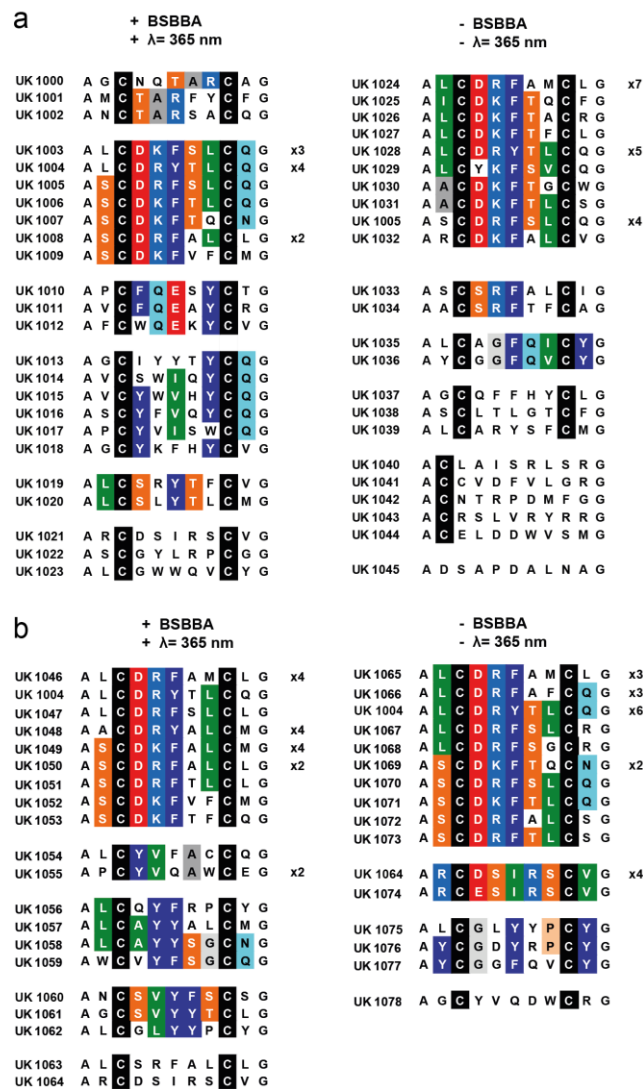


Figure 4.1. Phage selection of light-switchable uPA ligands from the CXCx library. (a and b) Peptides isolated after cyclization of the peptide phage library with BSBBA and exposure to UV light (left columns) or without alkylation and UV exposure (right columns). Two protocols were applied to isolate *cis* binders: the library was either depleted from *trans* binders before and after the capture of *cis* binders (a) or no negative selections were performed prior to capture of *cis* binders (b). In the latter protocol, the procedure of phage capture after UV light exposure and elution was repeated once and twice in selection rounds 2 and 3.

We decided to apply high-throughput sequencing to analyze a substantially higher number of clones to have a more detailed picture of the selected peptides and to identify even more consensus sequences. The DNA of the phage isolated with the first panning strategy was PCR amplified and run on an Ion 316™ Chip. More than 10^4 clones from the BSBBA-modified (Figure 4.2) and oxidized population (Figure 4.3) were identified, analyzed and grouped according to consensus sequence using the specific MatLab script. The abundance of every clone in each one of the two conditions is also indicated. Eleven consensus sequences were found and several sub-families could be identified for each one of them. Four of these consensus sequences (A, B, C, D) were found almost exclusively in the azobenzene modified phage population (Figure 4.2a) suggesting that the peptides were effi-

ciently cyclized with BSBBA and that the selection could have led to the identification of target-specific photo-modulated binders. The peptides belonging to consensus families E, F, G, H, I, J, K were mostly found also in the control. The high-throughput sequencing of the control selection clones (disulfide-bridge phage) revealed the presence of only one additional consensus sequence (Figure 4.3a, consensus L). The majority of the sequences were found also in the BSBBA modified population (Figure 4.3b).

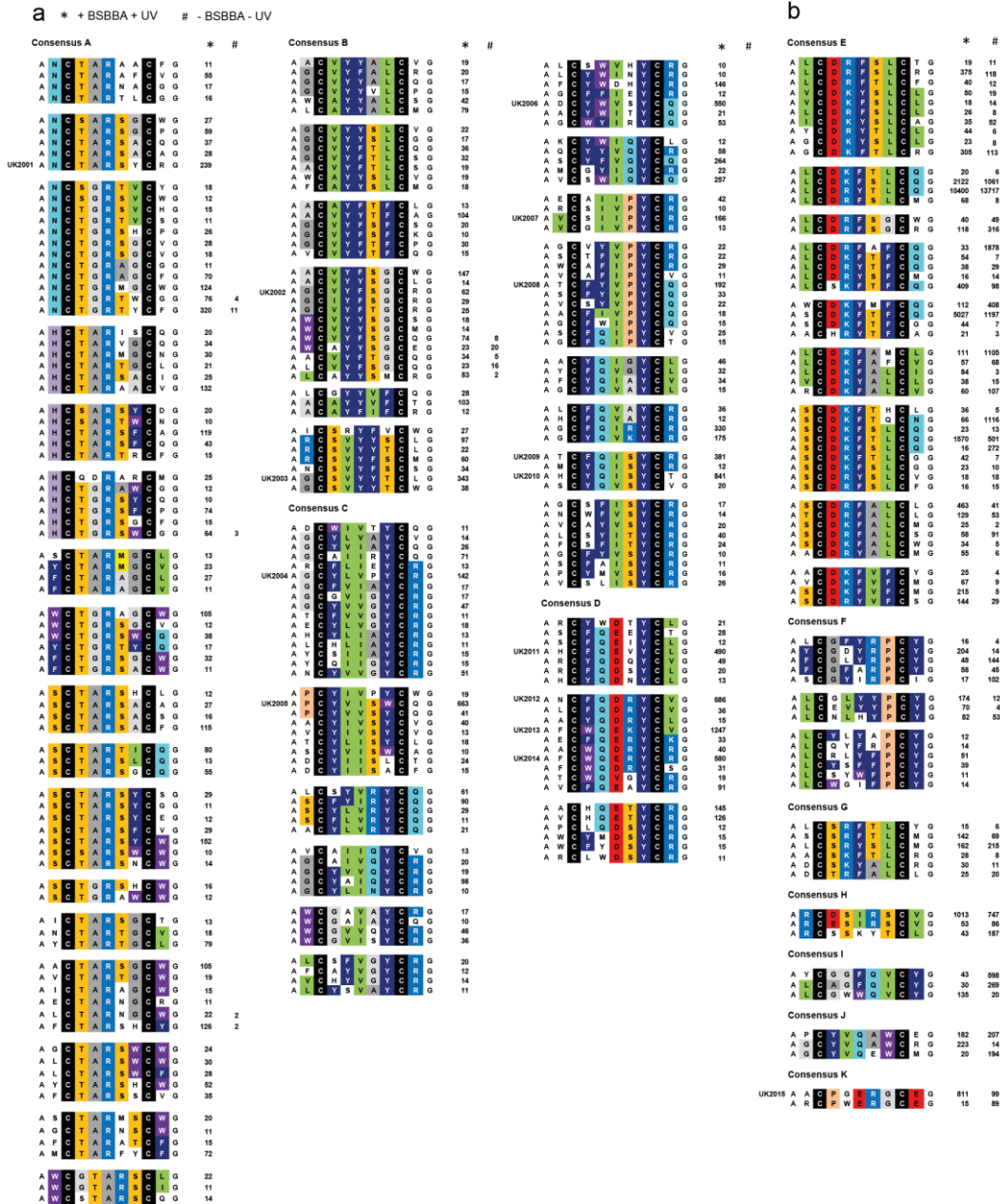


Figure 4.2. Identification of clones by Ion Torrent PGM platform. All the peptides were isolated after cyclization of the phage library with BSBBA, depletion from *trans* binders before and after the capture of *cis* binders. a) Consensus sequences found mostly or exclusively in the actual selection with modified and irradiated phage (+BSBBA + UV); b) Consensus sequences found also in the control selection without alkylation and UV exposure (-BSBBA - UV). (*) Abundance of each clone in the +BSBBA + UV condition. (#) Abundance of each clone in the -BSBBA - UV condition.

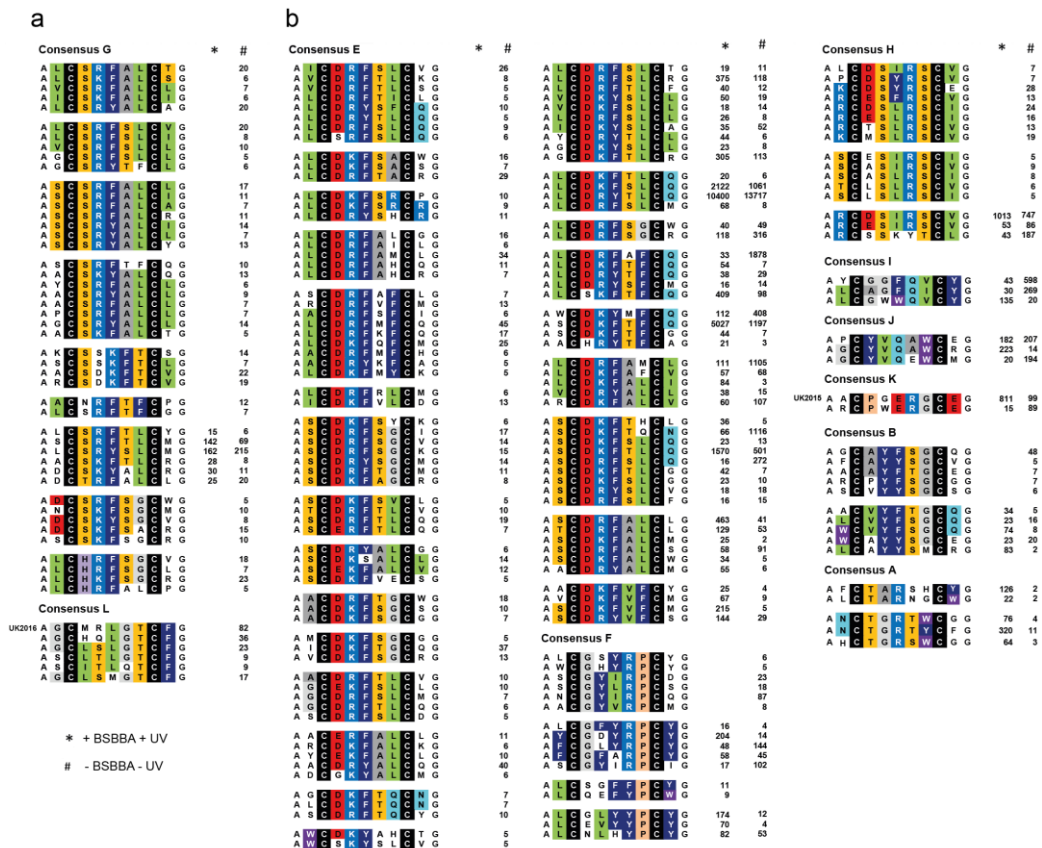


Figure 4.3. Identification of clones by Ion Torrent PGM platform. All the peptides were isolated after cyclization of the phage library by oxidation. a) Consensus sequences found mostly or exclusively in the control selection without alkylation and UV exposure (-BSBBA - UV). b) Consensus sequences found also in the actual selection with modified and irradiated phage (-BSBBA - UV). The abundance of each clone is labeled with an asterisk (*) if they were selected with BSBBA and UV light irradiation and with a hash symbol (#) if they were isolated as disulfide-cyclized peptides.

To confirm the specificity of the selected clones and verify whether the inhibition of uPA could be modulated by UV light, several peptides found with high frequency in the consensus sequences A, B, C, D were synthesized and either cyclized with BSBBA or by oxidation. Their inhibitory activity was tested using a fluorogenic substrate. Peptides UK2015 and UK2016 (consensus sequence K and L respectively) isolated from the disulfide-bridge phage selection were also tested as control (Figure 4.4). Light in the activity assay measurement did not interfere with the photoswitching of the peptide and the absorbance of BSBBA did not prevent the excitation of the fluorophore (Appendix, Supplementary Figure S5). UK2001 (consensus motif N_TARS) did not exhibit any change in inhibitory activity whether cyclized by a disulfide bridge or as BSBBA conjugates. The TAR motif is known to bind the target independently on the conformation as it was isolated in selections performed against uPA using different loop length libraries and linkers.⁸³ UK2002 and UK2003 (consensus motif G_VYFSG and G_SVYYT respectively) showed a higher inhibition when oxidized and their activity seemed to do not be modulated by UV light. Peptides selected from consensus C and D did not inhibit the target at all when cyclized by a disulfide bridge indicating that they were selected as BSBBA conjugates. Furthermore they all showed (except UK2005 and UK2008) a decrease, even if modest,

of their inhibitory activity when irradiated by UV light (Table 4.1). Peptides with the consensus motif V_IIPY_R and WQERY_R presented a 2-fold change of inhibition. The results obtained with control peptides UK2015 and UK2016 were not clear as the inhibition assay should be repeated using higher peptide concentrations. All characterized BSBBA-cyclized peptides could be switched efficiently into the *cis* conformation (50-70%) and showed a half-life between 30 and 155 minutes. It was also shown that the peptides backisomerized when incubated in the dark and could be switched between the *cis* and *trans* conformation for several times without losing any inhibitory activity, as shown in Figure 4.5. Supporting table S2 (Appendix) summarizes the IC₅₀ values as well as the half-life and the percentage of *cis* at the photostationary state of all the analyzed peptides.

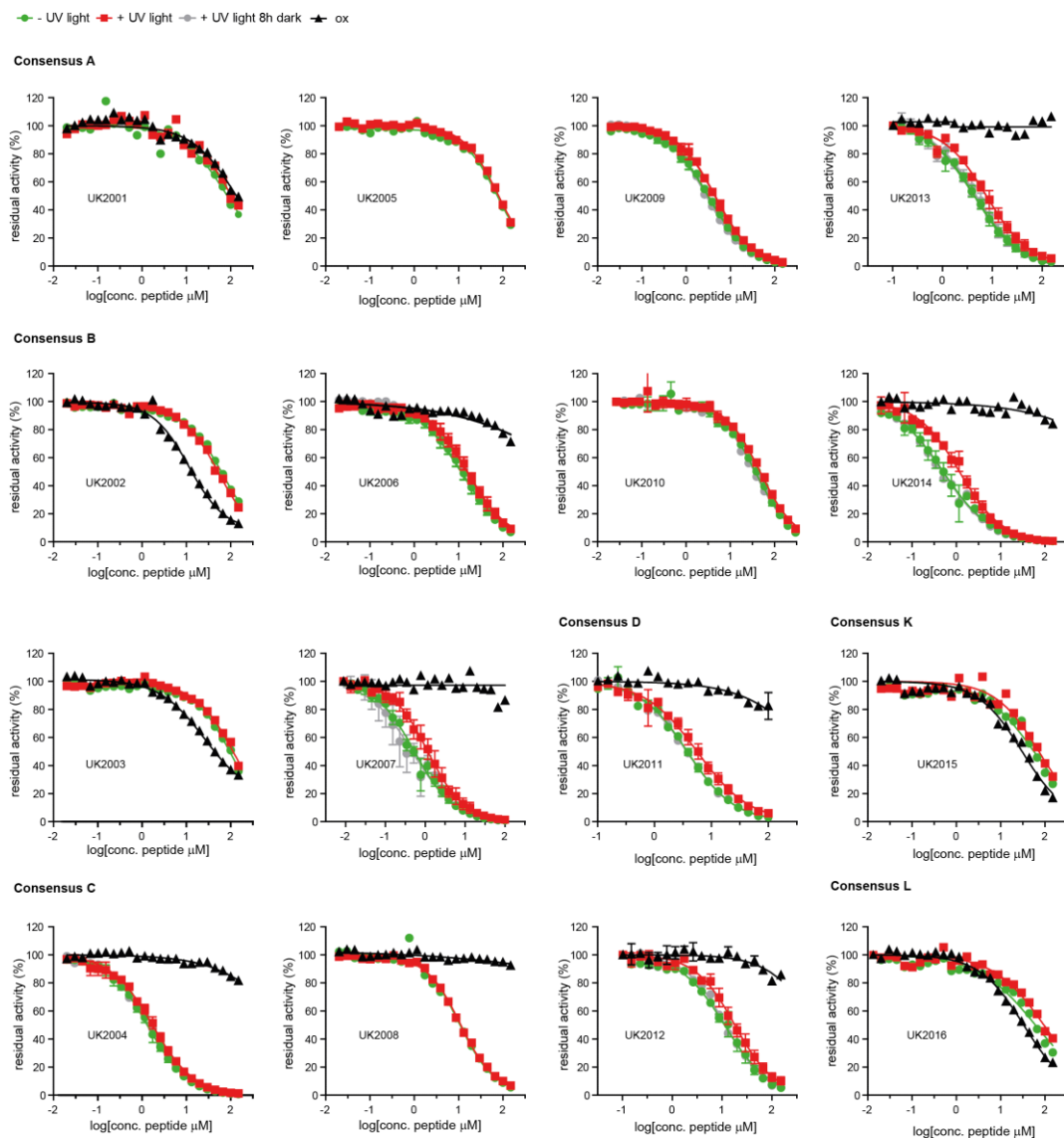


Figure 4.4. Inhibitory activity of peptides binding uPA *i)* BSBBA modified prior UV irradiation (green), *ii)* BSBBA modified after irradiation at 365 nm (red), *iii)* BSBBA modified after UV irradiation and incubation over night in the dark, *iv)* cyclized by oxidation (black).

Name	Consensus sequence	Selection	IC ₅₀ (μM) + UV light	IC ₅₀ (μM) - UV light	% <i>cis</i>	t _{1/2} (min)	IC ₅₀ S-S (μM)
UK2004	G_YLV_Y_R	+ BSBBA	1.9±0.2	1.4±0.2	68	103	*
UK2006	YWV_Y_Q	+ BSBBA	16.5±3.7	12.9±3.3	55	112	>200
UK2007	V_IIPY_R	+ BSBBA	1.9±0.65	0.99±0.21	66	120	>200
UK2009	FQISY_R	+ BSBBA	4.5±0.5	3.4±0.3	64	74	*
UK2010	YQISY	+ BSBBA	24.0±3.1	19±1.2	65	27	*
UK2011	FQE_Y_L	+ BSBBA	6.9±0.6	4.7±0.65	70	116	>200
UK2012	FQDRY_V	+ BSBBA	15±0.1	9.2±0.4	58	124	>200
UK2013	WQEKY_V	+ BSBBA	6.3±0.25	3.8±0.45	58	102	>200
UK2014	WQERY_R	+ BSBBA	0.97±0.04	0.54±0.02	59	99	>200

Table 4.1. IC₅₀ values, half-life and percentage of *cis* isomer at the photostationary state of the peptides that changed inhibitory activity after irradiation. The asterisk (*) indicates the values which could not be calculated due to insolubility of the peptides tested.

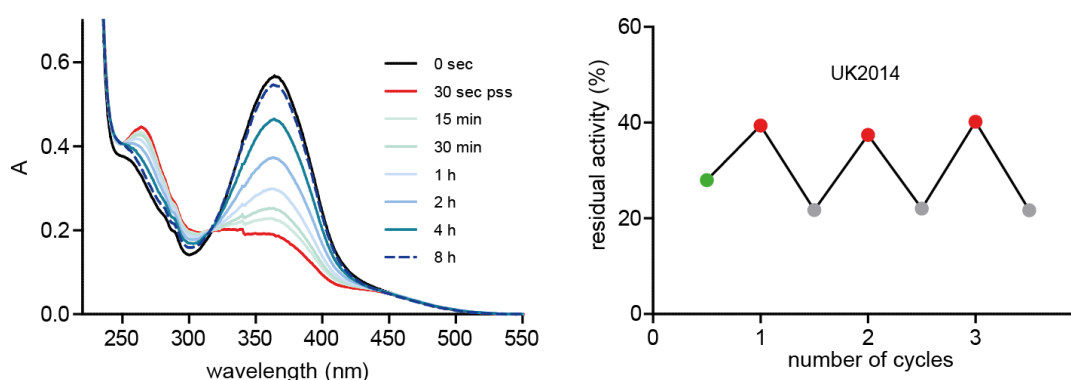


Figure 4.5. Absorption spectra of UK2007 after exposure to UV light for 30 seconds and incubation in the dark for the indicated times (left). (c) Residual uPA activity after incubation with UK2014 and repetitive exposure to UV light (red dots) and incubation at 42 °C in dark for 1 hr (grey dots).

In conclusion, we have successfully applied the recently developed phage display technique for evolving *in vitro* peptide ligands containing an azobenzene linker to a second target, the serine protease uPA. We found again peptides that show large differences in affinity when they are cyclized via the azobenzene linker and a disulfide bridge. Unfortunately, the affinity change of the peptides upon UV exposure was again rather small. We have successfully employed high-throughput sequencing to identify a range of peptides with different consensus sequences and thus different interaction modes. Despite testing several peptides of different consensus families, we could not find peptides that show large affinity changes upon photoswitching. Our findings suggested that the conforma-

tional change induced by the azobenzene photoswitch might be too small to achieve a sufficient difference in affinity and therefore lead to the amplification of phage that bind selectively in only one of the two conformations. Photoswitchable linkers allowing induction of a larger conformational change should be therefore considered in future work.

4.4 Materials and methods

Synthesis of 3,3'-bis(sulfonato)-4,4'-bis(bromoacetamido)azobenzene (BSBBA), solid phase peptide synthesis, peptide cyclization with BSBBA or by oxidation.

See chapter 3.

Phage selection of photoswitchable uPA ligands

The phage production has been performed as described in chapter 3, materials and methods section. The affinity selection was performed with biotinylated uPA immobilized on Dynabeads[®] M-280 streptavidin. The catalytic domain of uPA was expressed, activated, purified and biotinylated as described by Chen *et al.*⁸³ 12 µg of biotinylated uPA was immobilized per 100 µL streptavidin beads. The protein was added to the beads and the beads were washed three times with washing buffer. The beads were blocked by exchanging the storage solution to washing buffer containing 1% w/v BSA and 0.1% v/v Tween 20 and inverting on a rotating wheel (10 rpm) for 30 min at RT.

For the phage selection using the XCX₅CX library, the following procedures were applied. In the first procedure, the BSBBA-modified phage (1 mL) and the oxidized phage (1 mL) were blocked in parallel by addition of 0.5 mL of washing buffer containing 3% w/v BSA and 0.3% v/v Tween 20 and inversion on a rotating wheel (10 rpm) for 30 min at RT. The blocked phage were subjected to seven rounds of negative selection as follows: each phage solution was incubated with 10 µL of blocked uPA/streptavidin beads and inverted on a rotating wheel (10 rpm) for 10 min. The supernatant was collected and incubated with 10 µL of new blocked streptavidin beads. The procedure was repeated six times. BSBBA-modified phage were split into two tubes (0.75 mL for each tube) and one of the two fractions was irradiated for 5 min with UV light (365/66 nm) using the HBO 100 mercury lamp as described above. Immediately after UV light exposure, each one of the three phage populations (BSBBA-modified and UV light-irradiated phage, 0.75 mL; BSBBA-modified phage not irradiated, 0.75 mL; oxidized phage with disulfide cyclized peptides, 1.5 mL) were incubated in parallel with 50 µL of blocked uPA/streptavidin beads and rotated on a wheel (10rpm) for 10 min. The beads were washed four times with 1 mL washing buffer containing 1% BSA and 0.1% v/v Tween 20, three times with washing buffer containing 0.1% v/v Tween 20 and three times with 1 mL washing buffer. The bound phage were eluted by incubation of the beads with 50 µL of 50 mM glycine, pH 2.2 for 5 min. The pH was adjusted to 7.4 by adding 10 µL of 1 M Tris-HCl, pH 8.0 and 3 mL of washing buffer containing

1% BSA and 0.1% v/v Tween 20. After overnight incubation at RT to allow the linker backisomerization the three populations were subjected to other seven rounds of negative selection to further deplete the *trans* binders.

In the second procedure, the negative selection for depletion of *trans* binders was omitted. The panning (UV irradiation, capture on immobilized uPA and elution) was repeated twice and three times, in the second and third round of selection, respectively. After the elution in these selection rounds, the pH was adjusted to 7.4 by adding 10 μ L of 1 M Tris-HCl, pH 8.0 and 3 mL of washing buffer containing 1% BSA and 0.1% v/v Tween 20.

The phage from the three different selection procedures were added to exponentially growing TG1 cells ($OD_{600} = 0.4$; 30 mL), incubated for 90 min at 37 °C, pelleted by centrifugation at 4000 rpm for 5 min, plated on large 2YT/chloramphenicol (30 μ g/mL) agar plates and incubated overnight at 37 °C. From the selection with BSBBA-treated and UV-irradiated phage and the selection with oxidized phage, new phage were produced in volumes of 0.5 mL 2YT media as described above. Two additional rounds of phage selection were performed applying identical procedures.

Activity assay measurements

Inhibition of human uPA was measured by incubating 33 μ L of 4.5 nM human uPA, 33 μ L of serial dilutions of sample peptide (either cyclized with BSBBA or a disulfide bridge. BSBBA-cyclized peptide was optionally irradiated with UV light for 5 min as described above) in washing buffer containing 1% BSA and 0.1% v/v Tween 20 and 33 μ L of fluorogenic substrate Z-Gly-Gly-Arg-AMC (50 μ M final concentration in washing buffer; Bachem, Bubendorf, Switzerland). The fluorescence was measured over 30 min on a Tecan infinite M200 PRO® fluorescence plate reader (Switzerland; excitation at 368 nm, emission recording at 467 nm). The IC_{50} were calculated with GraphPad Prism 5 software using the log(inhibitor) vs. response variable slope model.

Effect of fluorescence measurement on peptide back-isomerization

A 1 mL solution of UK2001 (25 μ M in washing buffer) was prepared and divided in two aliquots. One was irradiated and two samples of 100 μ L each were pipetted in a 96 well plate. One of the two samples per condition was subjected to 10 min of fluorescence measurement with the same program used for activity assay (see paragraph 4.3.3). The absorbance spectrum was recorded before and after UV irradiation and fluorescence measurement.

Interaction between BSBBA peptide and AMC

A solution of i) 50 μ M 7-amino-4-methylcoumarin, ii) 50 μ M 7-amino-4-methylcoumarin and 25 μ M BSBBA modified peptide ACQNSKFSGCG iii) 25 μ M BSBBA modified peptide ACQNSKFSGCG in washing buffer were excited at 335 nm and the emission spectra were recorded from 370 to 750 nm using a Tecan infinite M1000 PRO® plate reader (Switzerland).

Repetitive switching of light-responsive peptides

1 mL of 1 μ M BSBBA-cyclized UK2007 in washing buffer were subjected to three iterative cycles of i) irradiation for 2 minutes at 365/366 nm (as described above) and ii) incubation in a water bath for 1 hr at 42 °C. Before the first exposure to UV light and after each cycle, two aliquots of 50 μ L were collected and their complete back-isomerization to *trans* was confirmed by measuring the absorbance at 363 nm on a NanoDrop device (NanoDrop ND-1000 UV-Vis Spectrophotometer, NanoDrop Technologies, Inc. Wilmington, DE, USA). One of the two aliquots was subjected to an additional irradiation at 365/366 nm for 2 min. 33 μ L of each sample were used to perform activity assay as described above.

Preparation of samples and analysis by high-throughput DNA sequencing

For detailed protocols see Rentero Rebollo et al. *Nucleic Acids Research*, 2014.¹³³

Chapter 5 Conclusions

5.1 Synthesis and characterization of *ortho*-substituted azobenzenes

The aim of the first project was the synthesis of oligo-*ortho* azobenzenes and the study of their photoisomerization properties, which have not been explored systematically so far. Additionally, the work with this class of molecules allowed me to gain experience in organic synthesis. Since only few examples of *ortho*-substituted multiple azobenzenes have been studied, I have prepared mono-, bis-, tris and tetra *ortho*-nitrogen-substituted azobenzenes using a procedure previously developed in the lab. For the synthesis of the mono *ortho*-nitrogen-substituted the optimized conditions were used (toluene as solvent and AcOH in stoichiometric amounts) and the efficiency was shown to depend on the substituents. It was found that when the aniline was substituted with electron withdrawing groups its reactivity was reduced. Interestingly, the classical Mills conditions (AcOH as solvent) were preferred for the preparation of the bis-*ortho*-nitrogen-substituted and the same substituent effect was observed. Different asymmetric and symmetric tris- and tetra- substituted azobenzenes were also isolated. As expected a correlation between the number of the azobonds formed and the reaction time was noticed. The absorption spectra of all compounds were measured in chloroform and were defined by the substituents. Furthermore, only the mono-substituted azobenzenes could be isomerized upon UV irradiation and the presence of electron withdrawing groups reduced the photoisomerization properties as previously reported in literature. Several of the described procedures are still used by other lab members for the synthesis of azobenzene derivatives. The reason for the inhibition of isomerization in bis-*ortho*-azobenzene is currently under investigation in collaboration with the group of Prof. Wachtveitl, Goethe-university, Frankfurt.

5.2 Phage selection of photoswitchable peptides

The main goal of my PhD thesis was the development of a phage display-based method for the *in vitro* evolution of photoswitchable peptide ligands. Recent access of phage display peptide libraries to chemical modification suggested that it would be possible to modify phage-encoded peptide libraries with photoswitchable compounds such as azobenzene. However, the method that looked simple and intriguing on paper had to be established experimentally. There were several open questions such as the following ones: i) Can peptides displayed on phage be chemically modi-

fied with the relatively hydrophobic azobenzene compound in an aqueous buffer? ii) Does exposure of phage to UV light switch the peptide-linker azobenzene compound without destroying the phage coat or the phage DNA? iii) Can peptide ligands containing azobenzene linkers be isolated by affinity selection? iv) Do affinity selected azobenzene-peptides in *cis* and *trans* conformation bind with different affinities to the protein target? v) Is the method generally applicable to a wide range of protein targets?

In experiments described in chapter 3, I had established the procedures to isolate peptides cyclized with azobenzene by phage display, using streptavidin as a model target. I was able to answer several of the above described questions. Peptides on phage were efficiently modified with an azobenzene linker via cysteines. Isolated peptide ligands were clearly dependent on the azobenzene linker. Peptides cyclized by disulfide bridges did not bind at all to streptavidin, or much weaker. Testing of several peptides binding streptavidin revealed that some of them changed their affinity slightly when they were exposed to UV light and thus switched from *trans* into the *cis* conformation. We were highly satisfied that cyclic peptides ligands containing the azobenzene linker could be evolved by phage display, and that some of the peptides changed the affinity upon UV exposure. The publication of this work had raised a great deal of interest in the fields of photoswitchable ligands and protein, as well as beyond these fields. While it has been challenging to develop photoswitchable ligands by rational design, this method promised to offer a general strategy to evolve photoswitchable peptides to virtually any target. One concern was the relatively small change in affinity when the azobenzene group was switched from *trans* to the *cis* conformation. It was not clear if peptides with larger changes in affinity could be engineered with the phage display approach. Furthermore, streptavidin was a relatively easy target and it was not clear if peptide ligands cyclized by azobenzene could be isolated in phage selections against other protein targets.

In order to address the open questions above, I applied the phage display approach for the selection of ligands to a second target, the serine protease uPA. These results are described in chapter 4. An important goal was to isolate peptides that have different binding modes and bind through different interactions to uPA. Towards this end, I applied a high-throughput sequencing method for analyzing hundred-thousands of phage-selected peptides. In this way, I found peptide families with many different consensus sequences. A study of several of these peptides showed that they bind with good affinity to uPA. The binding of most peptides was again dependent on the azobenzene group. This finding indicated that the peptides were truly isolated as azobenzene-cyclized structures in the phage panning experiment. Unfortunately, several peptides did not change their affinity upon switching the conformation of the azobenzene moiety from *trans* to *cis*. Some peptides changed the affinity but the difference between *cis* and *trans* conformation was again rather small. The finding of relatively small affinity differences between *cis* and *trans* conformers for also the second target, uPA, suggested that this could be a general limitation of the approach.

Towards the improvement of the technology, we propose the following potential solutions:

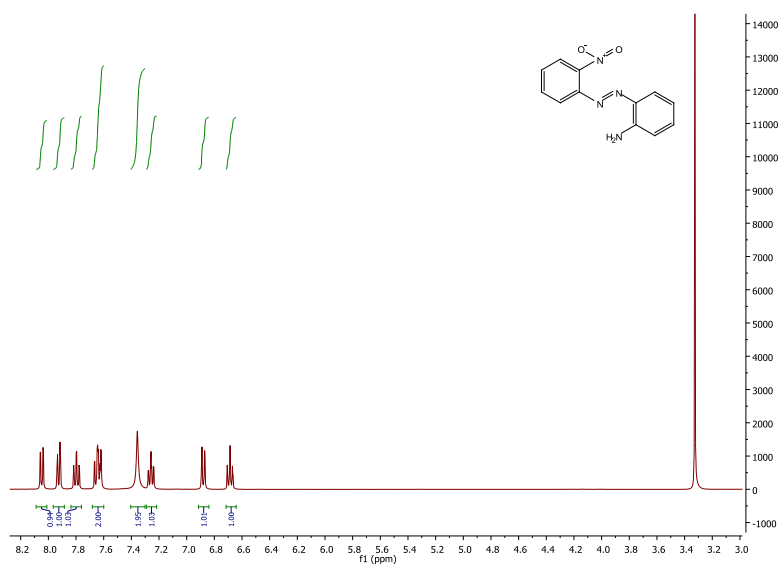
- i) The chemical linkers used should induce a larger conformational change in the peptide. Different light-responsive linkers may be tested. Ideally, the distance of the thiol-reactive groups of the linker should change dramatically upon light exposure.
- ii) Different peptide libraries need to be developed and applied. It will be key that the amino acids close to the cysteine residues form the contacts with the target protein. In this way, a conformational change of the photoswitch will have a maximal effect on the conformation of the peptide ligands.
- iii) New screening protocols may need to be developed to more efficiently deplete ligands in one of the two conformations. The methods established in this PhD thesis will offer an ideal basis to further develop the phage display-based approach. There is a high chance that the method will be applied for the directed evolution of a range of photoswitchable peptide ligands.

Appendix

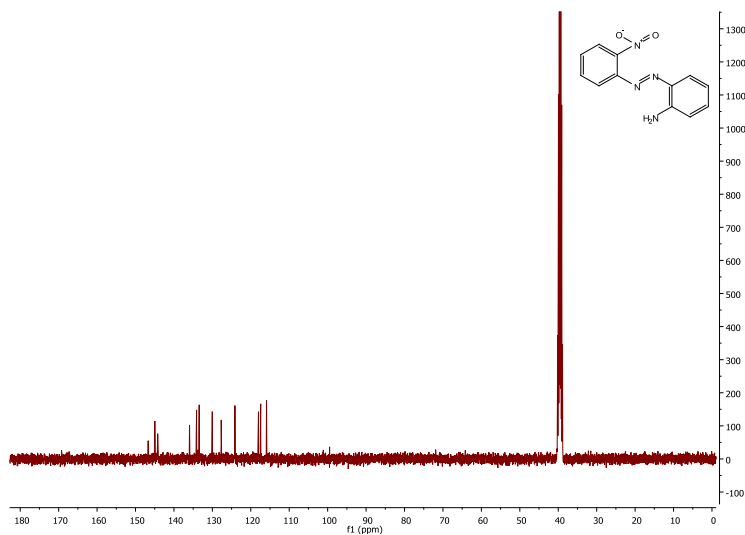
1. Supplementary information chapter 2

2-Amino-2'-nitro-*ortho*-azobenzene (3c)

^1H NMR (400 MHz, DMSO)



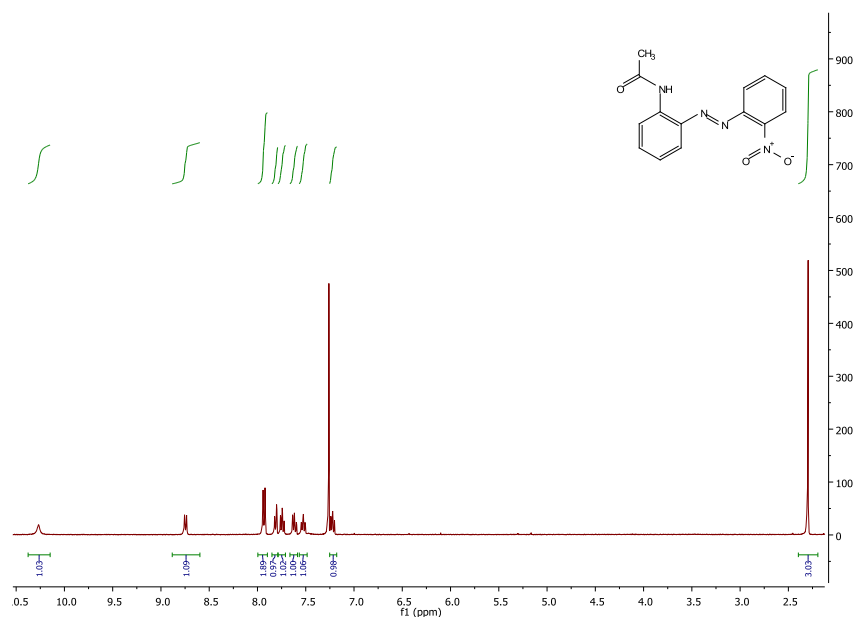
^{13}C NMR (101 MHz, DMSO)



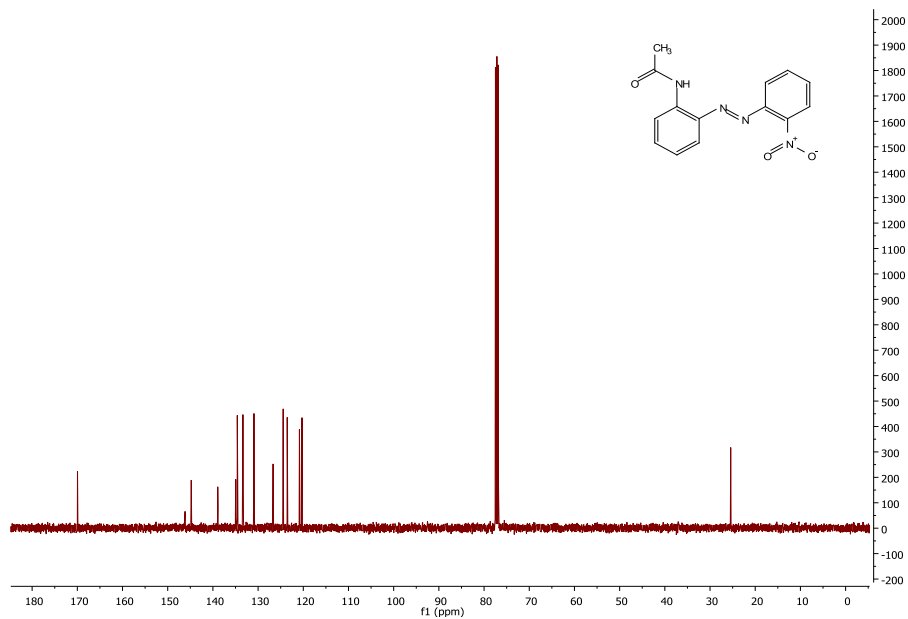
Appendix

2-Acetamido-2'-nitro-*ortho*-azobenzene (3h)

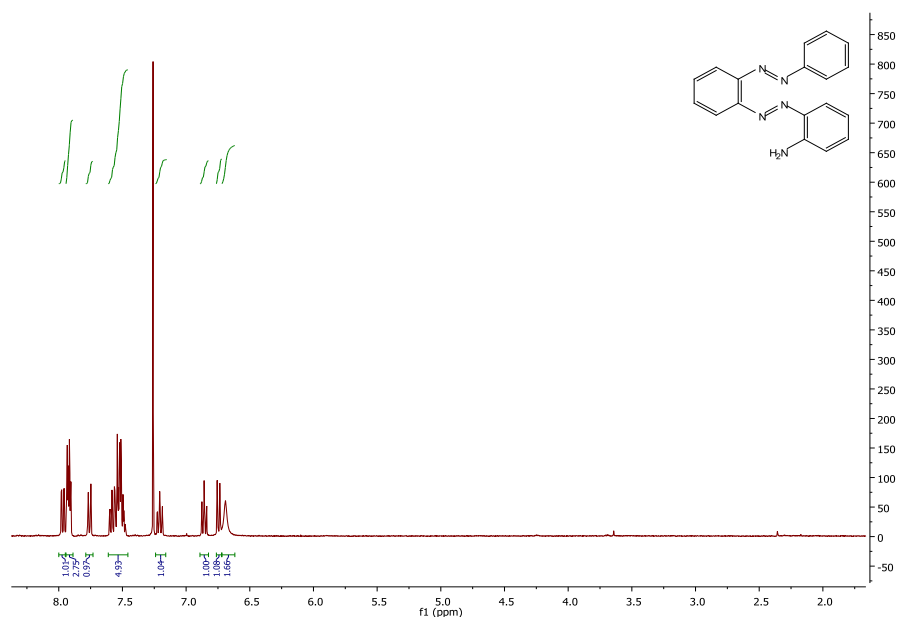
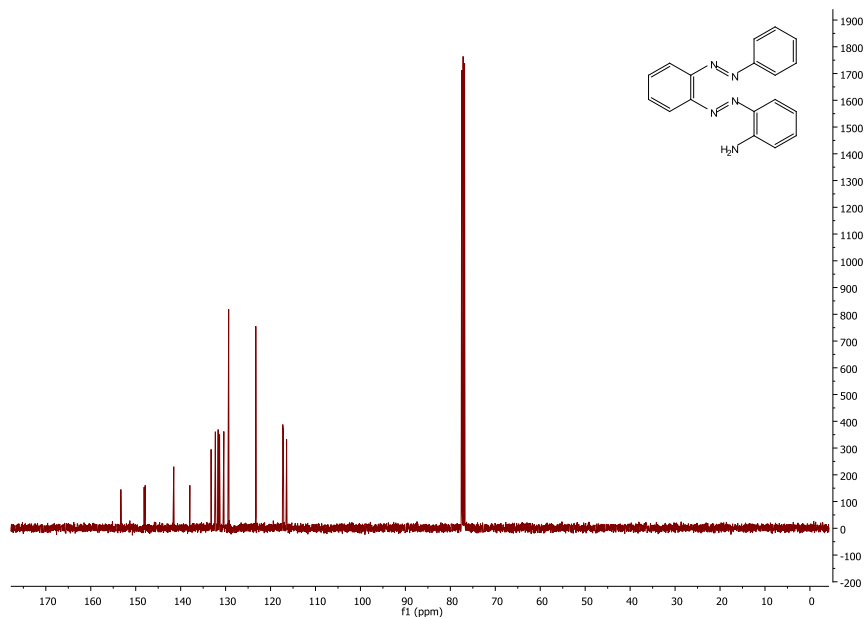
^1H NMR (400 MHz, CDCl_3)



^{13}C NMR (101 MHz, CDCl_3)



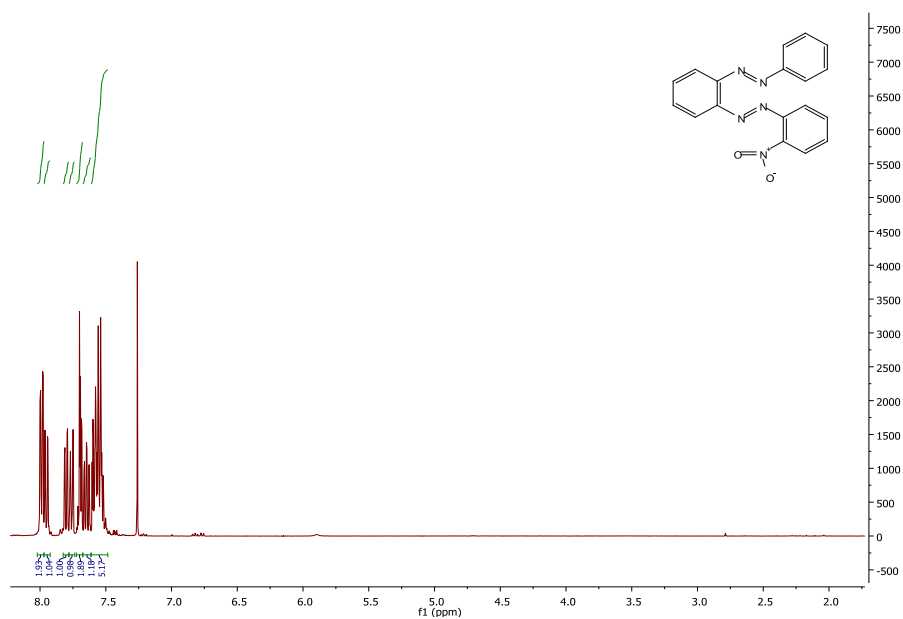
2-Amino-ortho-bisazobenzene (4b)

 ^1H NMR (400 MHz, CDCl_3) ^{13}C NMR (101 MHz, CDCl_3)

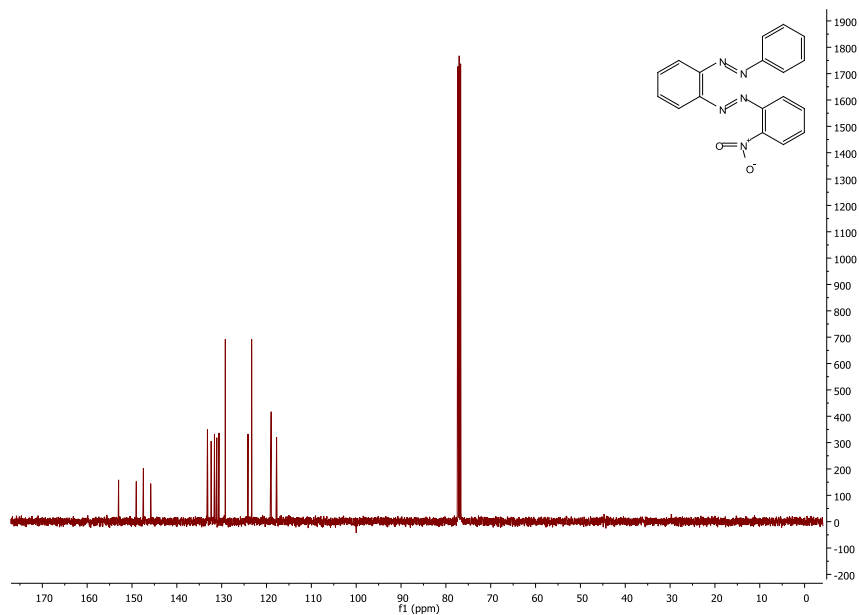
Appendix

2-Nitro-*ortho*-bisazobenzene (4d)

^1H NMR (400 MHz, CDCl_3)



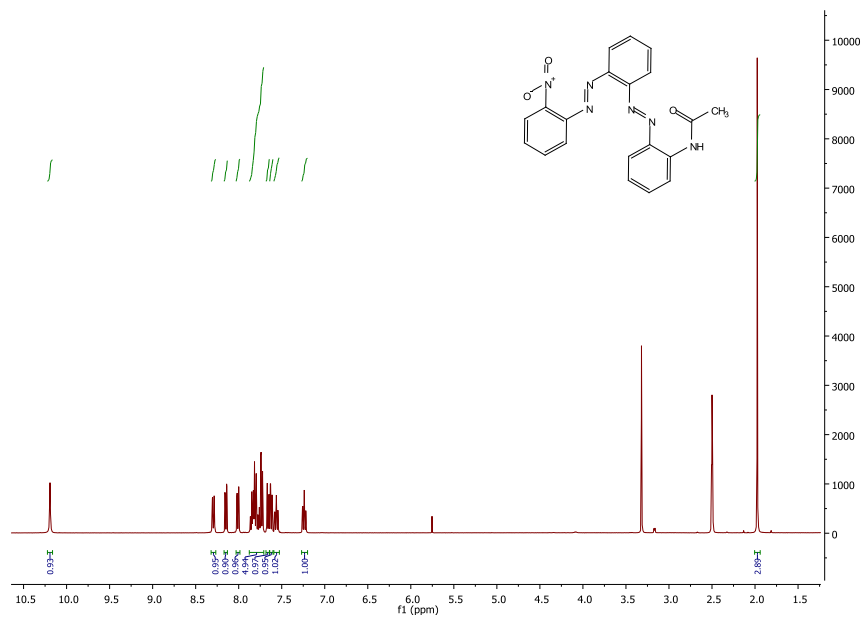
^{13}C NMR (101 MHz, CDCl_3)



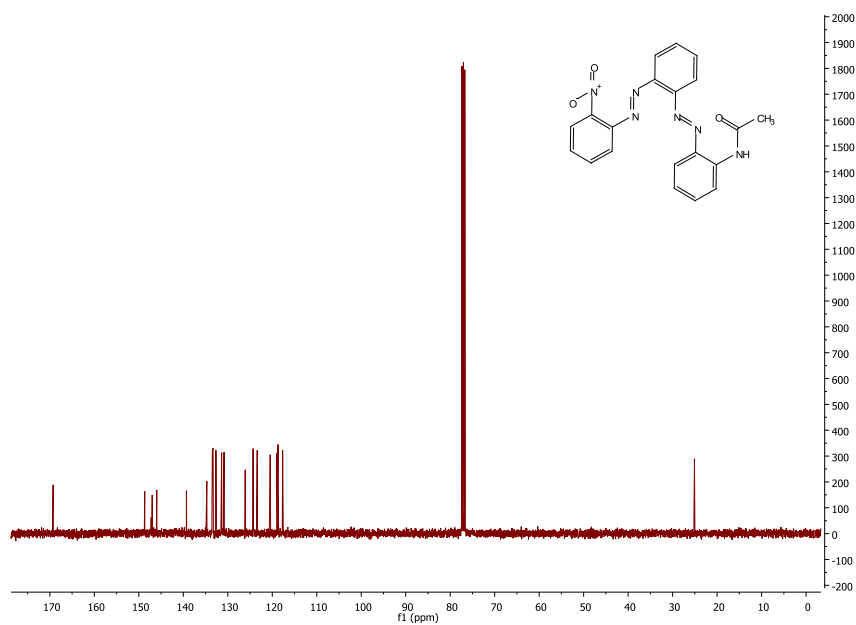
Appendix

2-Acetamido-2''-nitro-*ortho*-bisazobenzene (4f)

^1H NMR (400 MHz, DMSO)



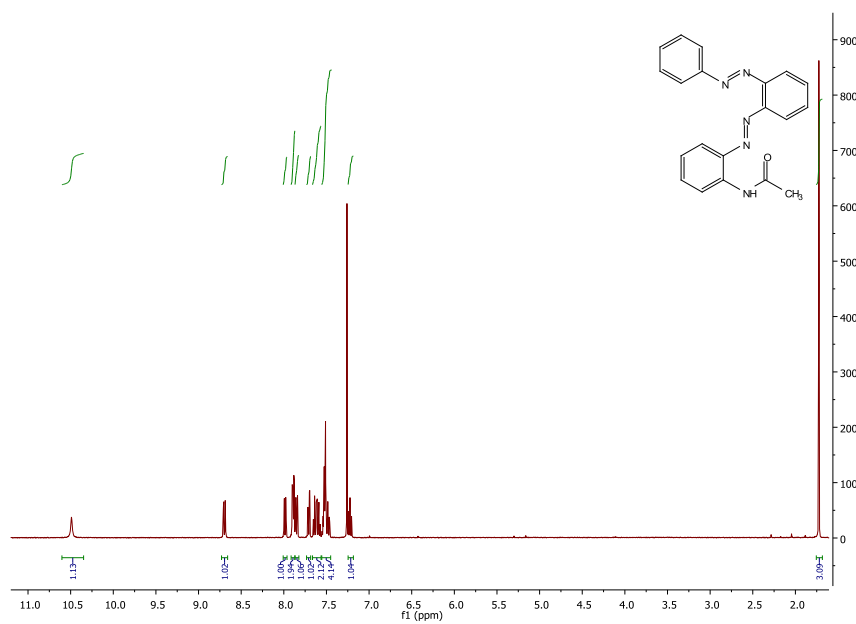
^{13}C NMR (101 MHz, CDCl_3 , δ/ppm)



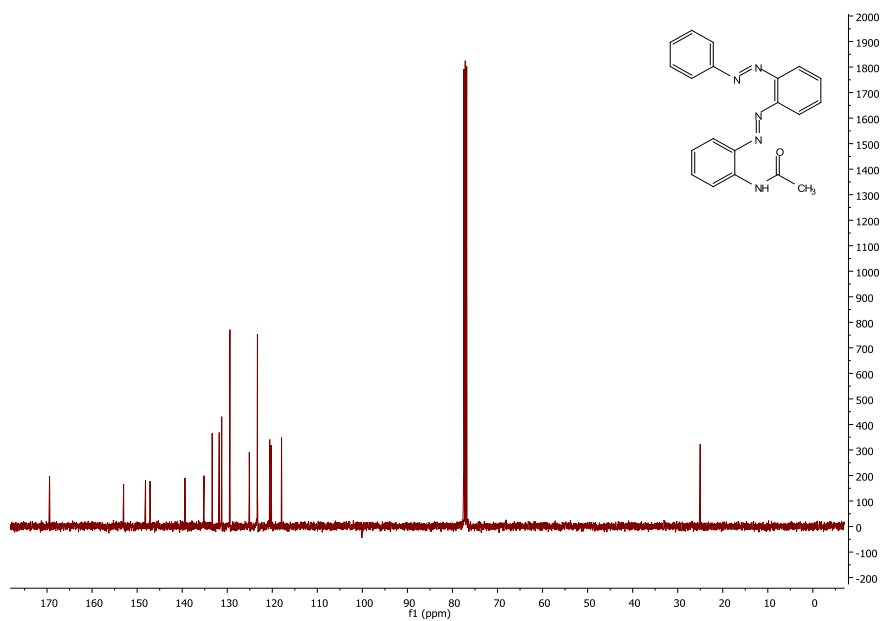
Appendix

2-Acetamido-ortho-bisazobenzene (4g)

^1H NMR (400 MHz, CDCl_3)



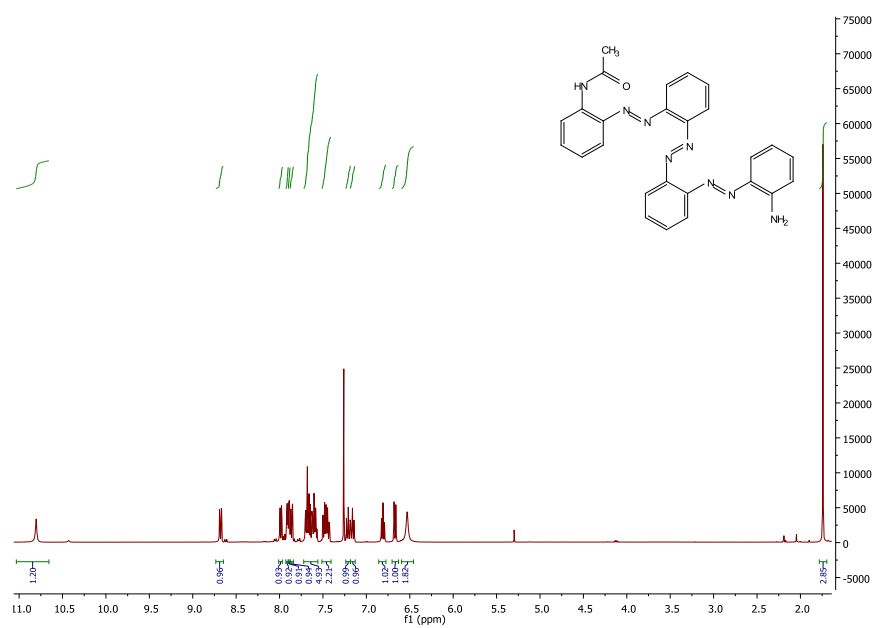
^{13}C NMR (101 MHz, CDCl_3)



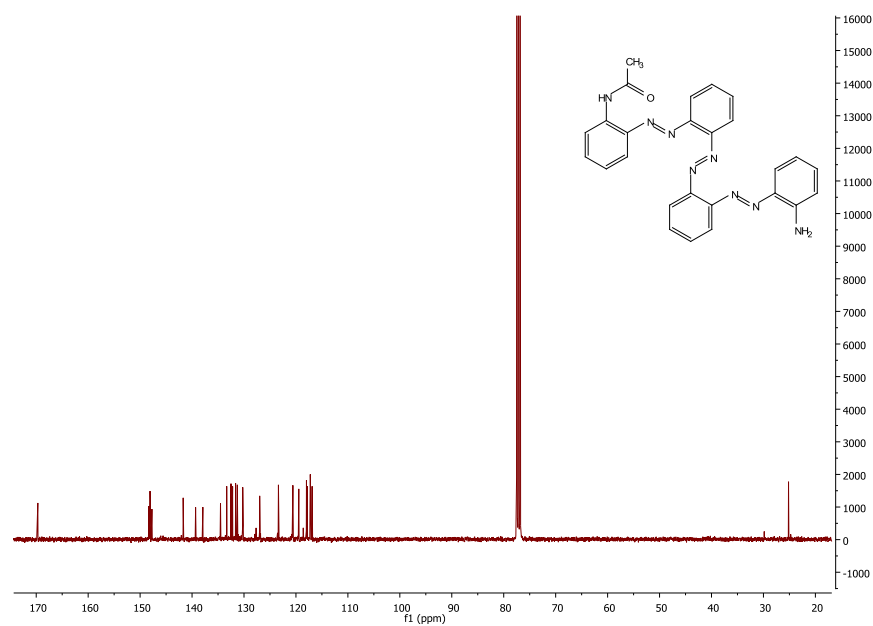
Appendix

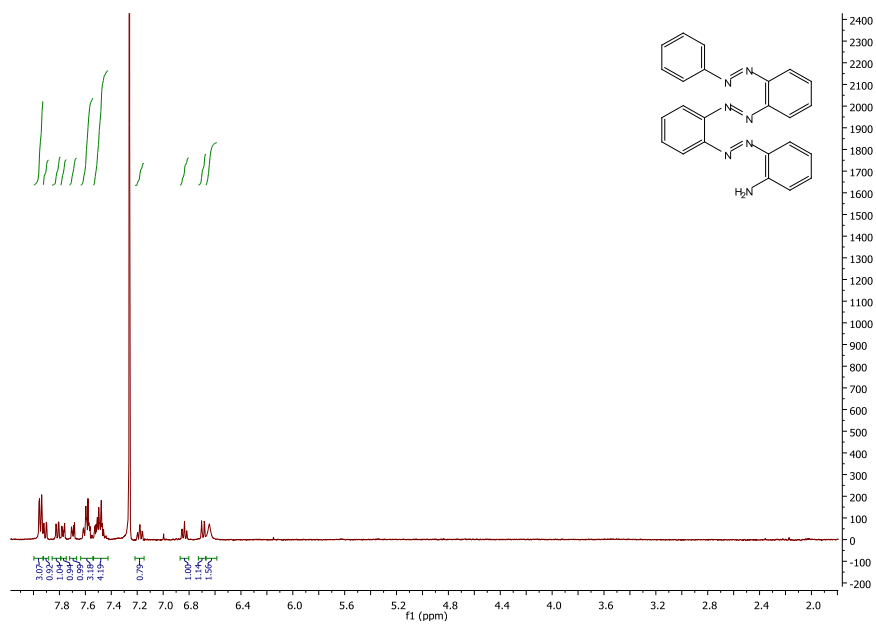
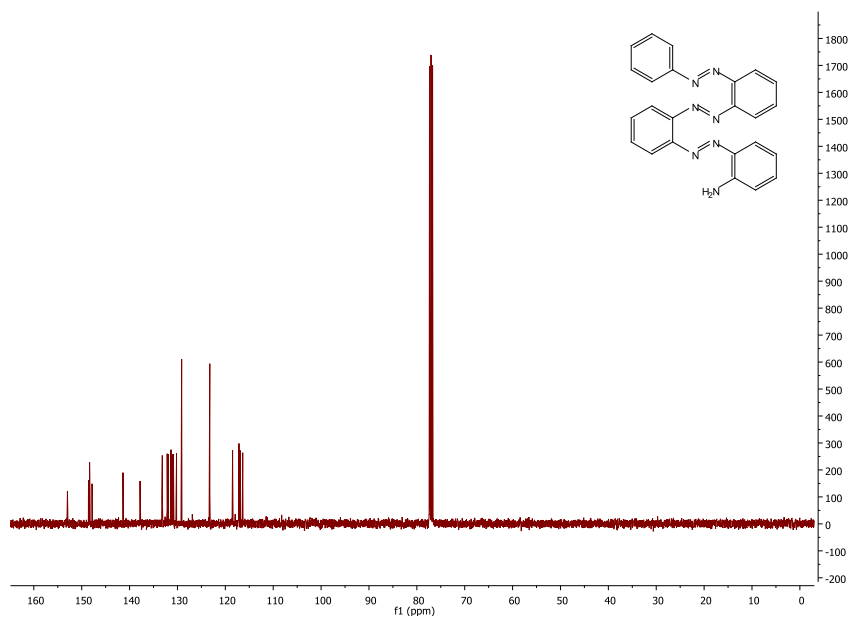
2-Amino-2'''acetamido-tris-ortho-azobenzene (5a)

^1H NMR (400 MHz, CDCl_3)



^{13}C NMR (101 MHz, CDCl_3)

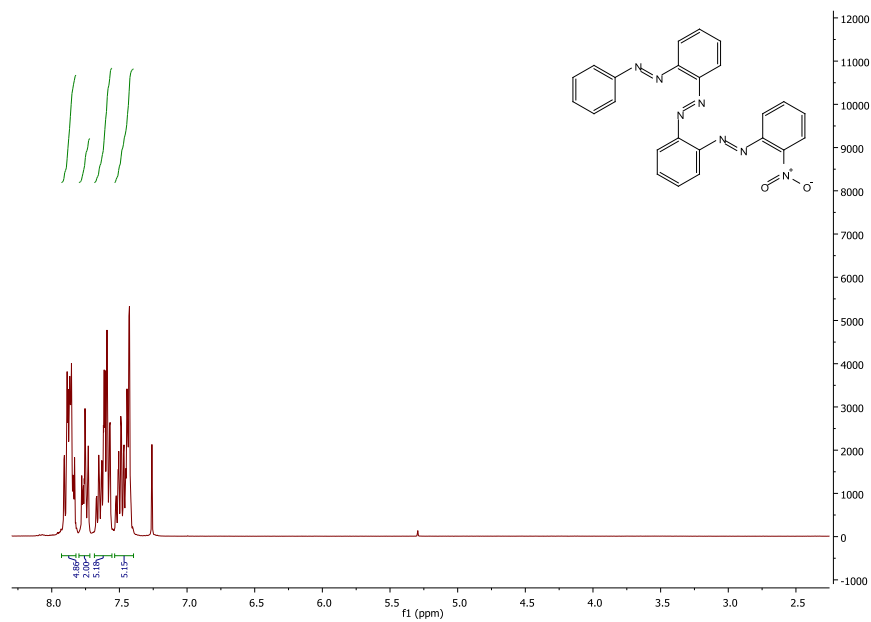


2-Amino-tris-ortho-azobenzene (5b)¹H NMR (400 MHz, CDCl₃)¹³C NMR (101 MHz, CDCl₃)

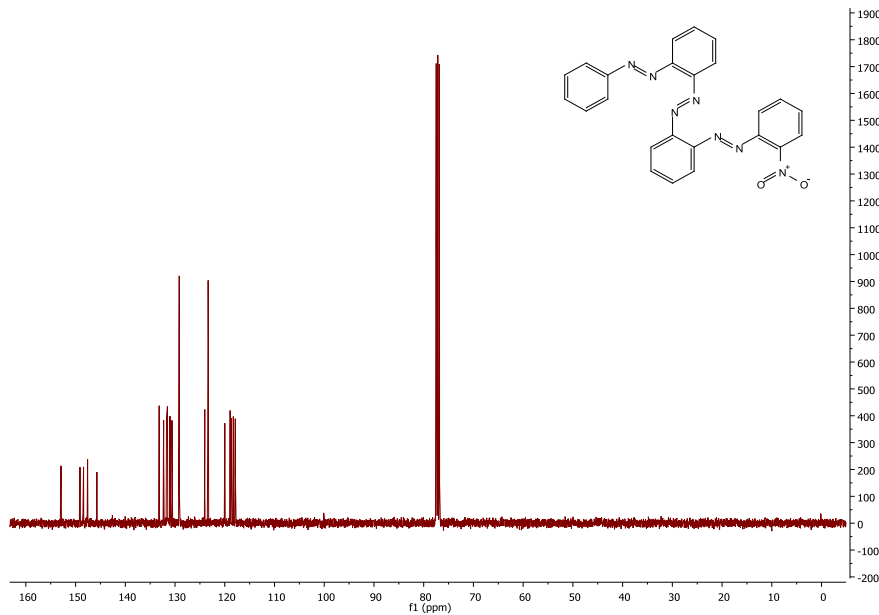
Appendix

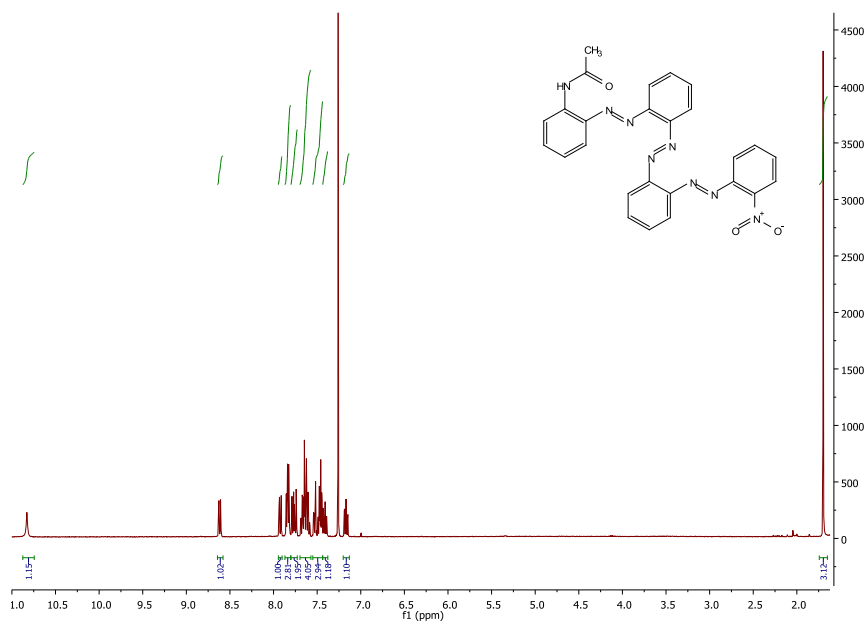
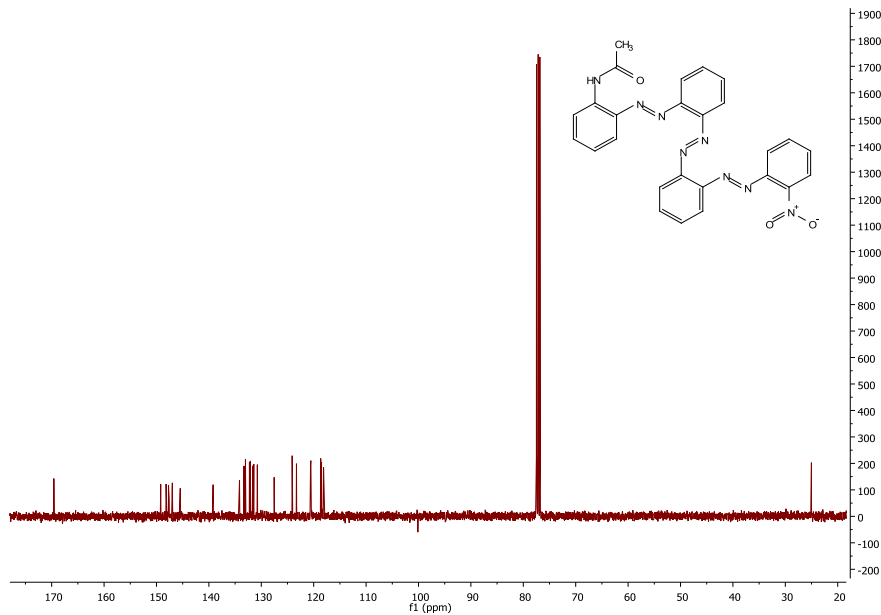
2-Nitro-tris-ortho-azobenzene (5c)

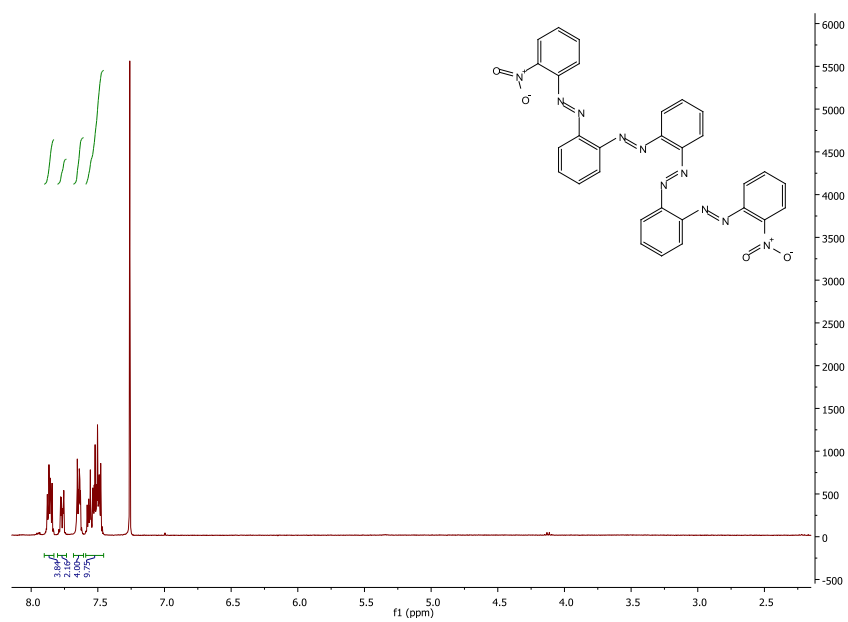
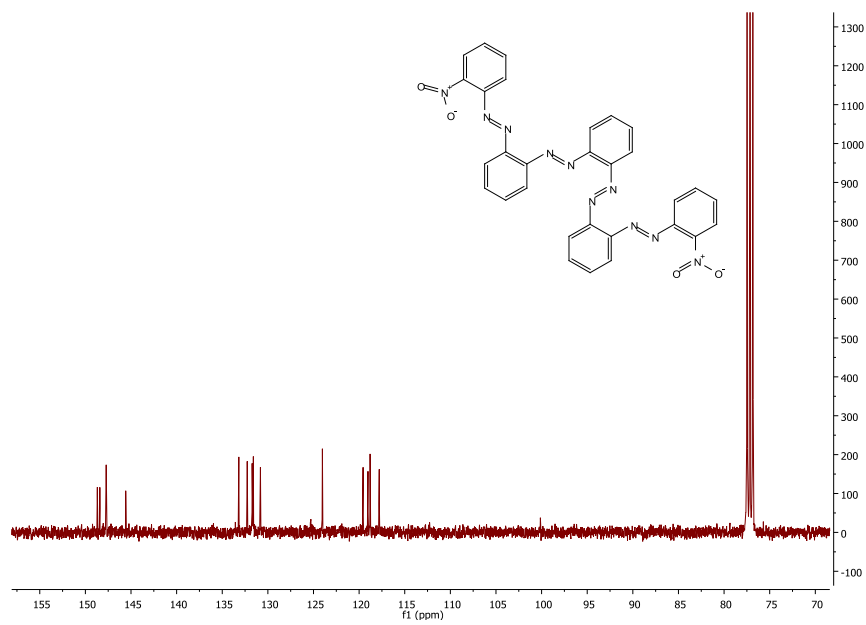
^1H NMR (400 MHz, CDCl_3)



^{13}C NMR (101 MHz, CDCl_3)



2-Acetamido-2'''-nitro-tris-ortho-azobenzene (5f) ^1H NMR (400 MHz, CDCl_3) ^{13}C NMR (101 MHz, CDCl_3)

2,2''''-Dinitro-tetra-ortho-azobenzene (6)¹H NMR (400 MHz, CDCl₃)¹³C NMR (101 MHz, CDCl₃)

Appendix

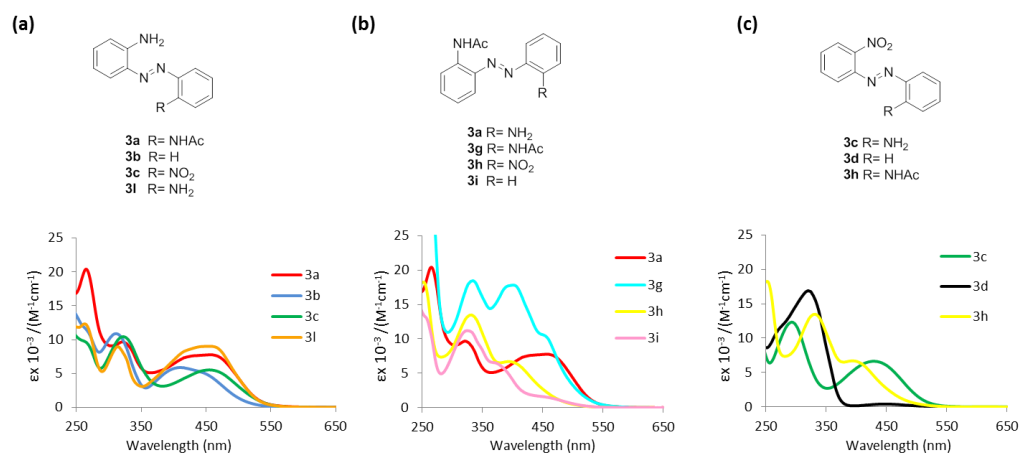


Figure S1. Absorption spectra of the *ortho*-amino (Figure S1a), acetamido (Figure S1b) and nitro (Figure S1c) substituted mono-azobenzenes in chloroform.

Appendix

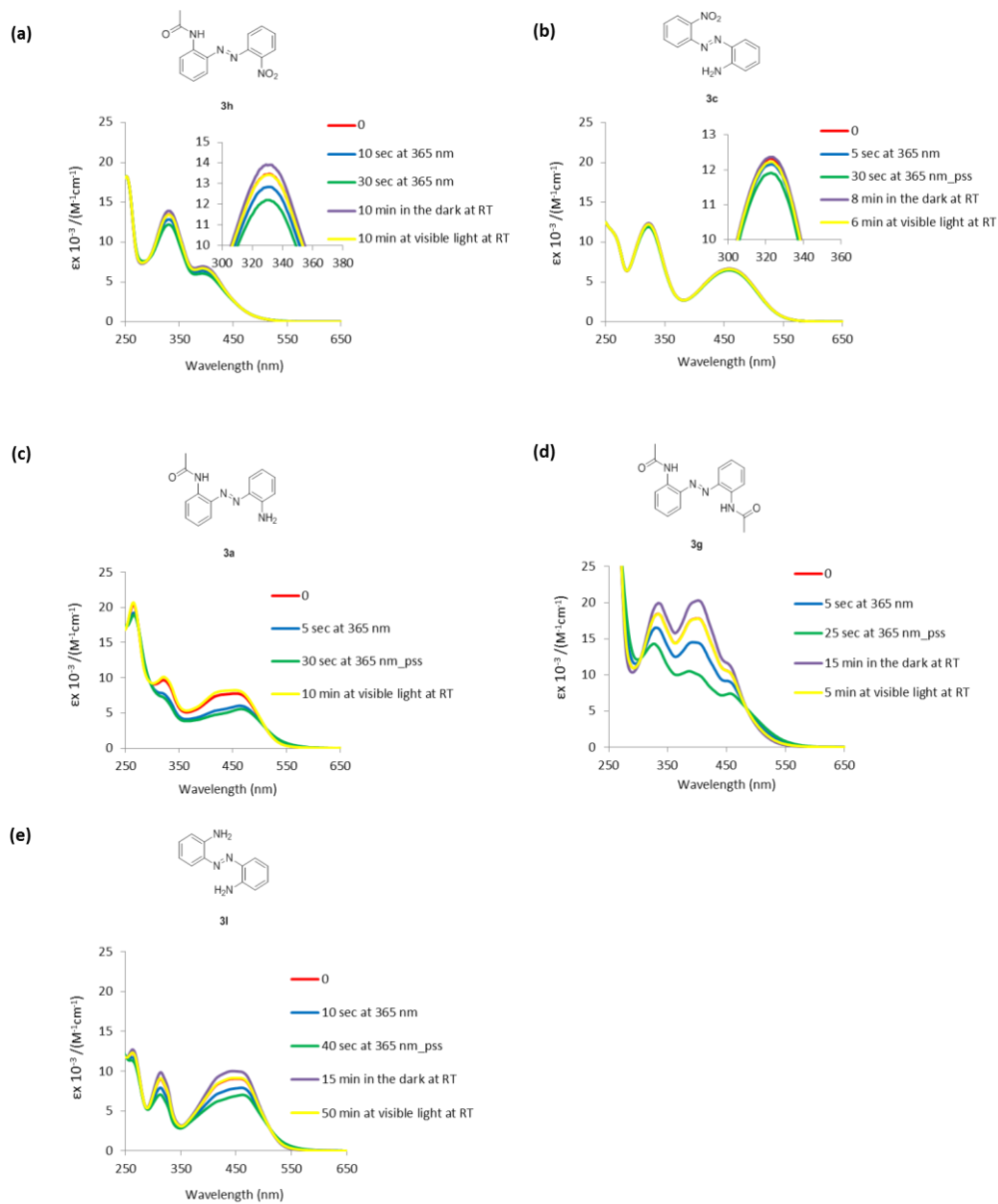


Figure S2. Photoisomerization of the *ortho*-nitrogen substituted mono-azo-benzenes in chloroform.

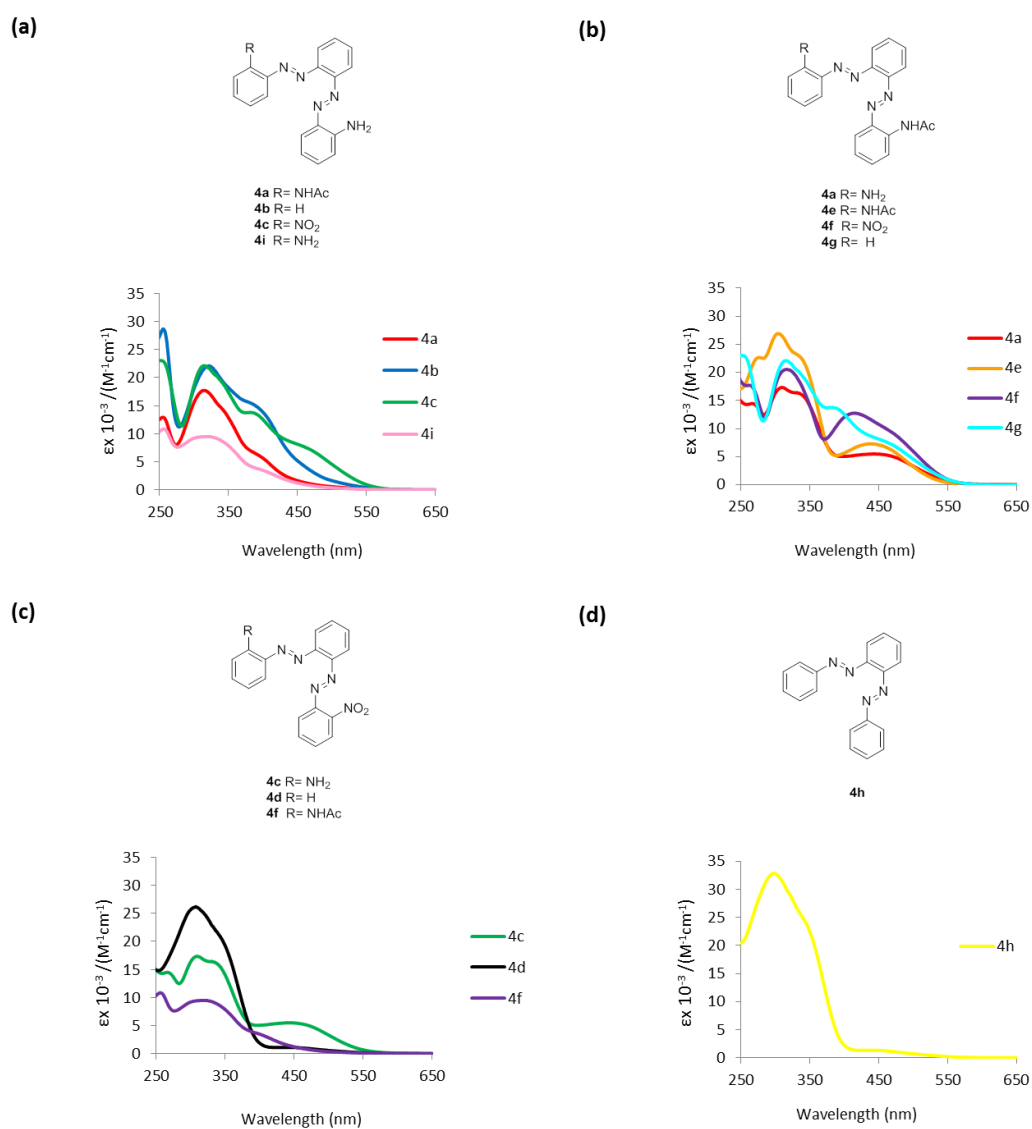


Figure S3. Absorption spectra of the *ortho*-amino (Figure S3a), acetamido (Figure S3b), nitro (Figure S3c) and hydrogen (Figure S3d) substituted bis-azobenzenes **4** in chloroform.

2. Supplementary information chapter 3

Name	Library	Consensus sequence	Selection	$K_d^{\text{dark a}}$ (μM)	$K_d^{\text{light a}}$ (μM)	% <i>cis</i>	$t_{1/2}$ (min) ^a	$K_d \text{ S-S}^b$ (μM)
SA101	CX ₇ C	WHPQ	+ BSBBA	< 1 ^c	< 1 ^c	67	66	> 20
SA113	CX ₇ C	SAP_GSL	+ BSBBA	4.8	4.7	71	50	9.9
SA116	CX ₇ C	HPQ_D	- BSBBA	3.6	4.1	73	62	1.5
SA124	CX ₇ C	HPQ_D	- BSBBA	6.9	6.2	72	60	6.5
SA129	CX ₇ C	SSP	- BSBBA	5.6	5.4	72	80	9.2
SA136	XCX ₅ CX	HPQ_P	+/- BSBBA	3.3	3.6	75	64	6.1
SA143	XCX ₅ CX	G_W__W	+ BSBBA	3.4±0.6	1.8±0.1	58	103	9.5±1
SA149	XCX ₅ CX	G_W__W	+ BSBBA	6.7±2	2.2±0	63	130	> 250
SA152	XCX ₅ CX	S_FP	+ BSBBA	3.1±0.1	2.1±0.2	74	112	11±0
SA153	XCX ₅ CX	S_FP	+ BSBBA	3.6±0.3	2.0±0.5	70	103	> 250
SA160	XCX ₅ CX	HPQ_P	- BSBBA	5.4	5.2	74	59	6.5

[a] Peptides cyclized with BSBBA, [b] Disulfide-cyclized peptides, [c] K_d s below 1 μM could not be determined accurately in the competition assay as the concentration of streptavidin monomer was 8 μM .

Supporting table S1. Photo-responsive peptides. The binding affinity was measured multiple times and standard deviations are indicated.

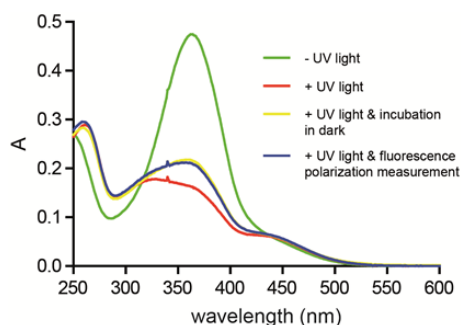


Figure S4. Effect of fluorescence polarization measurement on peptide back-isomerization. Absorption spectra of BSBBA-modified peptide (20 μM in PBS, peptide sequence ACVWHPQVPCG) before irradiation (- UV light), at the photostationary state after irradiation at 365 nm (+ UV light), after irradiation and incubation in the darkness for 10 min (+ UV light & incubation in dark), and after irradiation and fluorescence polarization measurement in a plate reader for 10 min (+ UV light & fluorescence polarization measurement).

3. Supplementary information chapter 4

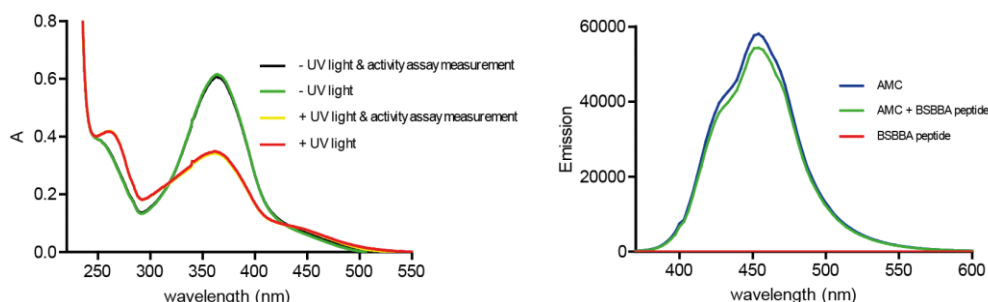


Figure S5. Effect of activity assay measurement on peptide back-isomerization. a) Absorption spectra of BSBBA-modified peptide (peptide UK2001, 25 μM in washing buffer) before irradiation (- UV light), at the photostationary state after irradiation at 365 nm (+ UV light), after irradiation and incubation in the darkness for 10 min (+ UV light), and after irradiation and activity assay measurement in a plate reader for 10 min (+ UV light & activity assay measurement).

b) Emission spectra of i) 50 μM 7-amino-4-methylcoumarin (AMC), ii) 50 μM 7-amino-4-methylcoumarin and 25 μM BSBBA modified peptide ACQNSKFSGCG iii) 25 μM BSBBA modified peptide ACQNSKFSGCG in washing buffer excited at 335 nm. The inhibitory activity of one representative peptide should be tested with a chromogenic substrate (ex. H-Glu-Gly-Arg-pNA) in order to exclude the possibility that AMC emission induces the backisomerization of the azobenzene moiety.

Name	Consensus sequence	Selection	IC ₅₀ (μM) + UV light	IC ₅₀ (μM) - UV light	% <i>cis</i>	t _{1/2} (min)	IC ₅₀ S-S (μM)
UK2001	N_TARS	+ BSBBA	n.d.	n.d.	63	64	n.d.
UK2002	G_VYFSG_R	+ BSBBA	n.d.	n.d.	64	97	11
UK2003	G_SVYYT	+ BSBBA	n.d.	n.d.	63	102	n.d.
UK2004	G_YLV_Y_R	+ BSBBA	1.9±0.2	1.4±0.2	68	103	*
UK2005	P_YVISW	+ BSBBA	80	78	57	97	*
UK2006	YWV_Y_Q	+ BSBBA	16.5±3.7	12.9±3.3	55	112	>200
UK2007	V_IIPY_R	+ BSBBA	1.9±0.65	0.99±0.21	66	120	>200
UK2008	FYVPY_Q	+ BSBBA	10.8	10.4	64	155	>200
UK2009	FQISY_R	+ BSBBA	4.5±0.5	3.4±0.3	64	74	*
UK2010	YQISY	+ BSBBA	24.0±3.1	19±1.2	65	27	*
UK2011	FQE_Y_L	+ BSBBA	6.9±0.6	4.7±0.65	70	116	>200
UK2012	FQDRY_V	+ BSBBA	15±0.1	9.2±0.4	58	124	>200
UK2013	WQEKY_V	+ BSBBA	6.3±0.25	3.8±0.45	58	102	>200
UK2014	WQERY_R	+ BSBBA	0.97±0.04	0.54±0.02	59	99	>200
UK2015	P_ERG_E	+/- BSBBA	n.d.	n.d.	64	57	n.d.
UK2016	G_LGT_F	- BSBBA	n.d.	n.d.	64	63	n.d.

Supporting table S2. IC₅₀ values, half-life and percentage of *cis* isomer at the photostationary state of all the analyzed peptides. The asterisk (*) indicates the values which could not be calculated due to insolubility of the peptides tested. (n.d.) indicates the values that could not be determined precisely because the plateau of the residual activity could not be reached.

References

- (1) Griffiths, J. *Chemical Society Reviews* **1972**, *1*, 481.
- (2) Bellotto, S.; Reuter, R.; Heinis, C.; Wegner, H. A. *The Journal of Organic Chemistry* **2011**, *76*, 9826.
- (3) Beharry, A. A.; Woolley, G. A. *Chemical Society Reviews* **2011**, *40*, 4422.
- (4) Merino, E.; Ribagorda, M. *Beilstein Journal of Organic Chemistry* **2012**, *8*, 1071.
- (5) Crecca, C. R.; Roitberg, A. E. *The Journal of Physical Chemistry A* **2006**, *110*, 8188.
- (6) Mancheva, I.; Nacheva, E.; Petrova, T.; Tomova, N.; Dragostinova, V.; Todorov, T.; Nikolova, L. 2003; Vol. 5226, p 199.
- (7) Wen, Y.; Yi, W.; Meng, L.; Feng, M.; Jiang, G.; Yuan, W.; Zhang, Y.; Gao, H.; Jiang, L.; Song, Y. *The Journal of Physical Chemistry B* **2005**, *109*, 14465.
- (8) Dohno, C.; Uno, S. N.; Nakatani, K. *Journal of the American Chemical Society* **2007**, *129*, 11898.
- (9) Matsunaga, D.; Asanuma, H.; Komiyama, M. *Journal of the American Chemical Society* **2004**, *126*, 11452.
- (10) Biswas, M.; Burghardt, I. *Biophysical journal* **2014**, *107*, 932.
- (11) Backus, E. H.; Kuiper, J. M.; Engberts, J. B.; Poolman, B.; Bonn, M. *The journal of physical chemistry. B* **2011**, *115*, 2294.
- (12) Kuiper, J. M.; Engberts, J. B. *Langmuir : the ACS journal of surfaces and colloids* **2004**, *20*, 1152.
- (13) Kuiper, J. M.; Stuart, M. C.; Engberts, J. B. *Langmuir : the ACS journal of surfaces and colloids* **2008**, *24*, 426.
- (14) Hamada, T.; Sato, Y. T.; Yoshikawa, K.; Nagasaki, T. *Langmuir : the ACS journal of surfaces and colloids* **2005**, *21*, 7626.
- (15) Srinivas, O.; Mitra, N.; Surolia, A.; Jayaraman, N. *Journal of the American Chemical Society* **2002**, *124*, 2124.
- (16) Srinivas, O.; Mitra, N.; Surolia, A.; Jayaraman, N. *Glycobiology* **2005**, *15*, 861.
- (17) Kaufman, H.; Vratsanos, S. M.; Erlanger, B. F. *Science* **1968**, *162*, 1487.
- (18) Bartels, E.; Wassermann, N. H.; Erlanger, B. F. *Proceedings of the National Academy of Sciences of the United States of America* **1971**, *68*, 1820.
- (19) Volgraf, M.; Gorostiza, P.; Numano, R.; Kramer, R. H.; Isacoff, E. Y.; Trauner, D. *Nature chemical biology* **2006**, *2*, 47.
- (20) Kienzler, M. A.; Reiner, A.; Trautman, E.; Yoo, S.; Trauner, D.; Isacoff, E. Y. *Journal of the American Chemical Society* **2013**, *135*, 17683.
- (21) Lien, L.; Jaikaran, D. C. J.; Zhang, Z.; Woolley, G. A. *Journal of the American Chemical Society* **1996**, *118*, 12222.
- (22) Velema, W. A.; van der Berg, J. P.; Hansen, M. J.; Szymanski, W.; Driessen, A. J.; Feringa, B. L. *Nature chemistry* **2013**, *5*, 924.
- (23) Velema, W. A.; Szymanski, W.; Feringa, B. L. *Journal of the American Chemical Society* **2014**, *136*, 2178.
- (24) Bose, M.; Groff, D.; Xie, J.; Brustad, E.; Schultz, P. G. *Journal of the American Chemical Society* **2006**, *128*, 388.
- (25) Liu, D.; Karanicolas, J.; Yu, C.; Zhang, Z.; Woolley, G. A. *Bioorganic & Medicinal Chemistry Letters* **1997**, *7*, 2677.
- (26) James, D. A.; Burns, D. C.; Woolley, G. A. *Protein engineering* **2001**, *14*, 983.
- (27) Muranaka, N.; Hohsaka, T.; Sisido, M. *FEBS letters* **2002**, *510*, 10.
- (28) Parisot, J.; Kurz, K.; Hilbrig, F.; Freitag, R. *Journal of separation science* **2009**, *32*, 1613.
- (29) Behrendt, R.; Schenk, M.; Musiol, H. J.; Moroder, L. *Journal of peptide science : an official publication of the European Peptide Society* **1999**, *5*, 519.
- (30) Wachtveitl, J.; Sporlein, S.; Satzger, H.; Fonrobert, B.; Renner, C.; Behrendt, R.; Oesterhelt, D.; Moroder, L.; Zinth, W. *Biophysical journal* **2004**, *86*, 2350.
- (31) Renner, C.; Moroder, L. *Chembiochem* **2006**, *7*, 868.
- (32) Zhang, Z.; Burns, D. C.; Kumita, J. R.; Smart, O. S.; Woolley, G. A. *Bioconjugate chemistry* **2003**, *14*, 824.
- (33) Zhang, F.; Sadovski, O.; Woolley, G. A. *Chembiochem* **2008**, *9*, 2147.
- (34) Samanta, S.; Woolley, G. A. *Chembiochem* **2011**, *12*, 1712.
- (35) Woolley, G. A. *Accounts of chemical research* **2005**, *38*, 486.
- (36) Kumita, J. R.; Flint, D. G.; Smart, O. S.; Woolley, G. A. *Protein engineering* **2002**, *15*, 561.
- (37) Beharry, A. A.; Sadovski, O.; Woolley, G. A. *Journal of the American Chemical Society* **2011**, *133*, 19684.
- (38) Samanta, S.; Beharry, A. A.; Sadovski, O.; McCormick, T. M.; Babalhavaeji, A.; Tropepe, V.; Woolley, G. A. *Journal of the American Chemical Society* **2013**, *135*, 9777.
- (39) Dong, S. L.; Loweneck, M.; Schrader, T. E.; Schreier, W. J.; Zinth, W.; Moroder, L.; Renner, C. *Chemistry* **2006**, *12*, 1114.
- (40) Hoppmann, C.; Seedorff, S.; Richter, A.; Fabian, H.; Schmieder, P.; Ruck-Braun, K.; Beyermann, M. *Angewandte Chemie* **2009**, *48*, 6636.
- (41) Hoppmann, C.; Schmieder, P.; Domaing, P.; Vogelreiter, G.; Eichhorst, J.; Wiesner, B.; Morano, I.; Ruck-Braun, K.; Beyermann, M. *Angewandte Chemie* **2011**, *50*, 7699.
- (42) Ulysse, L. G., Jr.; Chmielewski, J. *Chemical biology & drug design* **2006**, *67*, 127.
- (43) Flint, D. G.; Kumita, J. R.; Smart, O. S.; Woolley, G. A. *Chemistry & biology* **2002**, *9*, 391.
- (44) Beharry, A. A.; Wong, L.; Tropepe, V.; Woolley, G. A. *Angewandte Chemie* **2011**, *50*, 1325.

- (45) Kneissl, S.; Loveridge, E. J.; Williams, C.; Crump, M. P.; Allemann, R. K. *Chembiochem* **2008**, *9*, 3046.
- (46) Schutt, M.; Krupka, S. S.; Milbradt, A. G.; Deindl, S.; Sinner, E. K.; Oesterheld, D.; Renner, C.; Moroder, L. *Chemistry & biology* **2003**, *10*, 487.
- (47) Auernheimer, J.; Dahmen, C.; Hersel, U.; Bausch, A.; Kessler, H. *Journal of the American Chemical Society* **2005**, *127*, 16107.
- (48) Kuil, J.; van Wandelen, L. T.; de Mol, N. J.; Liskamp, R. M. *Journal of peptide science : an official publication of the European Peptide Society* **2009**, *15*, 685.
- (49) Nevola, L.; Martin-Quiros, A.; Eckelt, K.; Camarero, N.; Tosi, S.; Llobet, A.; Giral, E.; Gorostiza, P. *Angewandte Chemie* **2013**, *52*, 7704.
- (50) Brustad, E. M.; Arnold, F. H. *Current opinion in chemical biology* **2011**, *15*, 201.
- (51) Parrill, A. L.; Rami Reddy, M.; American Chemical Society. Division of Computers in Chemistry.; American Chemical Society. Meeting *Rational drug design : novel methodology and practical applications*; American Chemical Society: Washington, DC, 1999.
- (52) Marks, C.; Marks, J. D. *The New England journal of medicine* **1996**, *335*, 730.
- (53) Heinis, C.; Rutherford, T.; Freund, S.; Winter, G. *Nature chemical biology* **2009**, *5*, 502.
- (54) Ullman, C. G.; Frigotto, L.; Cooley, R. N. *Briefings in functional genomics* **2011**, *10*, 125.
- (55) Rakonjac, J.; Bennett, N. J.; Spagnuolo, J.; Gagic, D.; Russel, M. *Curr Issues Mol Biol* **2011**, *13*, 51.
- (56) Bonnycastle, L. L.; Mehroke, J. S.; Rashed, M.; Gong, X.; Scott, J. K. *Journal of molecular biology* **1996**, *258*, 747.
- (57) Angelini, A.; Cendron, L.; Chen, S.; Touati, J.; Winter, G.; Zanotti, G.; Heinis, C. *ACS Chemical Biology* **2012**, *7*, 817.
- (58) Chen, S.; Bertoldo, D.; Angelini, A.; Pojer, F.; Heinis, C. *Angewandte Chemie International Edition* **2014**, *53*, 1602.
- (59) Jafari, M. R.; Deng, L.; Kitov, P. I.; Ng, S.; Matochko, W. L.; Tjhung, K. F.; Zeberoff, A.; Elias, A.; Klassen, J. S.; Derda, R. *ACS Chemical Biology* **2013**.
- (60) Liu, M.; Tada, S.; Ito, M.; Abe, H.; Ito, Y. *Chemical communications* **2012**, *48*, 11871.
- (61) Tausig, F.; Wolf, F. J. *Biochemical and Biophysical Research Communications* **1964**, *14*, 205.
- (62) Katz, B. A.; Cass, R. T. *The Journal of biological chemistry* **1997**, *272*, 13220.
- (63) Schmidt, T. G. M.; Skerra, A. *Nat. Protocols* **2007**, *2*, 1528.
- (64) Dundas, C.; Demonte, D.; Park, S. *Appl Microbiol Biotechnol* **2013**, *97*, 9343.
- (65) Le Trong, I.; Wang, Z.; Hyre, D. E.; Lybrand, T. P.; Stayton, P. S.; Stenkamp, R. E. *Acta crystallographica. Section D, Biological crystallography* **2011**, *67*, 813.
- (66) Freitag, S.; Le Trong, I.; Klumb, L.; Stayton, P. S.; Stenkamp, R. E. *Protein science : a publication of the Protein Society* **1997**, *6*, 1157.
- (67) Weber, P. C.; Ohlendorf, D. H.; Wendoloski, J. J.; Salemme, F. R. *Science* **1989**, *243*, 85.
- (68) Weber, P. C.; Pantoliano, M. W.; Thompson, L. D. *Biochemistry* **1992**, *31*, 9350.
- (69) Giebel, L. B.; Cass, R. T.; Milligan, D. L.; Young, D. C.; Arze, R.; Johnson, C. R. *Biochemistry* **1995**, *34*, 15430.
- (70) Katz, B. A. *Biochemistry* **1995**, *34*, 15421.
- (71) Caparon, M. H.; De Ciechi, P. A.; Devine, C. S.; Olins, P. O.; Lee, S. C. *Molecular diversity* **1996**, *1*, 241.
- (72) Roberts, D.; Guegler, K.; Winter, J. *Gene* **1993**, *128*, 67.
- (73) Winter, J. *Drug Development Research* **1994**, *33*, 71.
- (74) Schmidt, T. G.; Skerra, A. *Protein engineering* **1993**, *6*, 109.
- (75) Korndorfer, I. P.; Skerra, A. *Protein science : a publication of the Protein Society* **2002**, *11*, 883.
- (76) Spraggon, G.; Phillips, C.; Nowak, U. K.; Ponting, C. P.; Saunders, D.; Dobson, C. M.; Stuart, D. I.; Jones, E. Y. *Structure* **1995**, *3*, 681.
- (77) Smith, H. W.; Marshall, C. J. *Nature reviews. Molecular cell biology* **2010**, *11*, 23.
- (78) Baran, M.; Mollers, L. N.; Andersson, S.; Jonsson, I. M.; Ekwall, A. K.; Bjersing, J.; Tarkowski, A.; Bokarewa, M. *Journal of cellular and molecular medicine* **2009**, *13*, 3797.
- (79) Andreassen, P. A.; Kjoller, L.; Christensen, L.; Duffy, M. J. *International journal of cancer. Journal international du cancer* **1997**, *72*, 1.
- (80) Sgier, D.; Zuberbuehler, K.; Pfaffen, S.; Neri, D. *Protein engineering, design & selection : PEDS* **2010**, *23*, 261.
- (81) Zhao, G.; Yuan, C.; Wind, T.; Huang, Z.; Andreassen, P. A.; Huang, M. *Journal of Structural Biology* **2007**, *160*, 1.
- (82) Chen, S.; Gfeller, D.; Buth, S. A.; Michielin, O.; Leiman, P. G.; Heinis, C. *Chembiochem* **2013**, *14*, 1316.
- (83) Chen, S.; Rentero Rebollo, I.; Buth, S. A.; Morales-Sanfrutos, J.; Touati, J.; Leiman, P. G.; Heinis, C. *Journal of the American Chemical Society* **2013**, *135*, 6562.
- (84) Mills, C. *Journal of the Chemical Society, Transactions* **1895**, *67*, 925.
- (85) Hamon, F.; Djedaini-Pilard, F.; Barbot, F.; Len, C. *Tetrahedron* **2009**, *65*, 10105.
- (86) Lim, Y.-K.; Lee, K.-S.; Cho, C.-G. *Organic Letters* **2003**, *5*, 979.
- (87) Reuter, R.; Hostettler, N.; Neuburger, M.; Wegner, H. A. *European Journal of Organic Chemistry* **2009**, *2009*, 5647.
- (88) Kumar, G. S.; Neckers, D. C. *Chemical Reviews* **1989**, *89*, 1915.
- (89) Yim, K. S.; Fuller, G. G. *Physical Review E* **2003**, *67*, 041601.
- (90) Petrova, T. S.; Mancheva, I.; Nacheva, E.; Tomova, N.; Dragostinova, V.; Todorov, T.; Nikolova, L. *Journal of Materials Science: Materials in Electronics* **2003**, *14*, 823.
- (91) Pan, X.; Wang, C.; Xu, H.; Zhang, X. *Appl. Phys. B* **2007**, *86*, 693.
- (92) El Halabieh, R. H.; Mermut, O.; Barrett, C. J. In *Pure and Applied Chemistry* 2004; Vol. 76, p 1445.

- (93) Stoll, R. S.; Hecht, S. *Angewandte Chemie International Edition* **2010**, *49*, 5054.
- (94) Birnbaum, P. P.; Linford, J. H.; Style, D. W. G. *Transactions of the Faraday Society* **1953**, *49*, 735.
- (95) Albini, A.; Fasani, E.; Pietra, S. *Journal of the Chemical Society, Perkin Transactions 2* **1983**, 1021.
- (96) Bléger, D.; Dokić, J.; Peters, M. V.; Grubert, L.; Saalfrank, P.; Hecht, S. *The Journal of Physical Chemistry B* **2011**, *115*, 9930.
- (97) Cisnetti, F.; Ballardini, R.; Credi, A.; Gandolfi, M. T.; Masiero, S.; Negri, F.; Pieraccini, S.; Spada, G. P. *Chemistry – A European Journal* **2004**, *10*, 2011.
- (98) Meldola, R. *Journal of the Chemical Society, Transactions* **1884**, *45*, 106.
- (99) Ruggli, P.; Rohner, J. *Helvetica Chimica Acta* **1942**, *25*, 1533.
- (100) Ruggli, P.; Wüst, W. *Helvetica Chimica Acta* **1945**, *28*, 781.
- (101) Ruggli, P.; Iselin, E. *Helvetica Chimica Acta* **1947**, *30*, 733.
- (102) Hilpert, H.; Hoesch, L.; Dreiding, A. S. *Helvetica Chimica Acta* **1985**, *68*, 325.
- (103) Sebe, I.; Cornel, T. M. *Rev. Roum. Chim.* **1995**, *40*, 275.
- (104) Bandara, H. M. D.; Cawley, S.; Gascón, J. A.; Burdette, S. C. *European Journal of Organic Chemistry* **2011**, *2011*, 2916.
- (105) Shirin, Z.; Thompson, J.; Liable-Sands, L.; Yap, G. P. A.; Rheingold, A. L.; Borovik, A. S. *Journal of the Chemical Society, Dalton Transactions* **2002**, 1714.
- (106) Tie, C.; Gallucci, J. C.; Parquette, J. R. *Journal of the American Chemical Society* **2006**, *128*, 1162.
- (107) Tibiletti, F.; Simonetti, M.; Nicholas, K. M.; Palmisano, G.; Parravicini, M.; Imbesi, F.; Tollari, S.; Penoni, A. *Tetrahedron* **2010**, *66*, 1280.
- (108) Apasov, E. T.; Churakov, A. M.; Strelenko, Y. A.; Ioffe, S. L.; Djetigenov, B. A.; Tartakovsky, V. A. *Tetrahedron* **1995**, *51*, 6775.
- (109) de Mendoza, J.; Millan, C.; Rull, P. *Journal of the Chemical Society, Perkin Transactions 1* **1981**, 403.
- (110) Kaiya, T.; Fujiwara, T.; Kohda, K. *Chemical Research in Toxicology* **2000**, *13*, 993.
- (111) Roling, P. V.; Kirt, D. D.; Dill, J. L.; Hall, S.; Hollstrom, C. *Journal of Organometallic Chemistry* **1976**, *116*, 39.
- (112) Jirman, J. *Collect. Czech. Chem. Commun.* **1991**, *56*, 2160.
- (113) Skulski, L.; Waclawek, W. *Bull. Acad. Pol. Sci., Ser. Sci. Chim.* **1971**, *19*, 277.
- (114) Fehrentz, T.; Schonberger, M.; Trauner, D. *Angewandte Chemie* **2011**, *50*, 12156.
- (115) Gorostiza, P.; Isacoff, E. Y. *Science* **2008**, *322*, 395.
- (116) Kramer, R. H.; Mourot, A.; Adesnik, H. *Nat Neurosci* **2013**, *16*, 816.
- (117) Kramer, R. H.; Chambers, J. J.; Trauner, D. *Nature chemical biology* **2005**, *1*, 360.
- (118) Russew, M. M.; Hecht, S. *Adv Mater* **2010**, *22*, 3348.
- (119) Bandara, H. M.; Burdette, S. C. *Chemical Society Reviews* **2012**, *41*, 1809.
- (120) Aemissegger, A.; Hilvert, D. *Nat Protoc* **2007**, *2*, 161.
- (121) Mart, R. J.; Wysoczanski, P.; Kneissl, S.; Ricci, A.; Brancale, A.; Allemann, R. K. *Chembiochem* **2012**, *13*, 515.
- (122) Angelini, A.; Heinis, C. *Current opinion in chemical biology* **2011**, *15*, 355.
- (123) Ng, S.; Jafari, M. R.; Derda, R. *ACS Chemical Biology* **2012**, *7*, 123.
- (124) Hipolito, C. J.; Suga, H. *Current opinion in chemical biology* **2012**, *16*, 196.
- (125) Tian, F.; Tsao, M. L.; Schultz, P. G. *Journal of the American Chemical Society* **2004**, *126*, 15962.
- (126) Burns, D. C.; Zhang, F.; Woolley, G. A. *Nat Protoc* **2007**, *2*, 251.
- (127) Kather, I.; Bippes, C. A.; Schmid, F. X. *Journal of molecular biology* **2005**, *354*, 666.
- (128) Rentero Rebollo, I.; Heinis, C. *Methods* **2013**, *60*, 46.
- (129) McLafferty, M. A.; Kent, R. B.; Ladner, R. C.; Markland, W. *Gene* **1993**, *128*, 29.
- (130) Kolodziej, A. F.; Nair, S. A.; Graham, P.; McMurry, T. J.; Ladner, R. C.; Wescott, C.; Sexton, D. J.; Caravan, P. *Bioconjugate chemistry* **2012**, *23*, 548.
- (131) Rossi, A. M.; Taylor, C. W. *Nat Protoc* **2011**, *6*, 365.
- (132) Bellotto, S.; Chen, S.; Rentero Rebollo, I.; Wegner, H. A.; Heinis, C. *Journal of the American Chemical Society* **2014**, *136*, 5880.
- (133) Rentero Rebollo, I.; Sabisz, M.; Baeriswyl, V.; Heinis, C. *Nucleic Acids Res* **2014**.

Curriculum Vitae

Silvia BELLOTTO

Born in Italy, Pordenone, on 28th May 1986

Address: BCH 5201, Bâtochime, EPFL
1015 Lausanne, VD, Switzerland

E-mail: silvia.bellotto@epfl.ch

Professional experience & projects

- Dec. 2010-now **Ph.D candidate in the Laboratory of Therapeutic Proteins and Peptides (LPPT).
Doctoral program in Chemistry and Chemical Engineering at École Polytechnique
Fédérale de Lausanne (EPFL). PhD advisor Prof. C. Heinis
Visiting Ph.D student at Universität Basel and Justus Liebig Universität
Gießen. PhD co-advisor Prof. H.A. Wegner**
The interdisciplinary project lead to the development of an innovative method for
the selection of highly specific and light-activatable peptide inhibitors using phage
display technology.
- 2010 **Master thesis – Biochemistry department of University of Lausanne – Erasmus
scholarship**
The aim of the project was to test a new approach for differentiation therapy of
squamous cell carcinoma. It was shown that Notch activation via inducible system
in one cancer cell line is sufficient to induce differentiation in the neighbouring
cancer cells.
- 2008 **Bachelor thesis – Biomedical department of University of Padua**
In six months of internship I have tested the therapeutic potential of several new
proteasome inhibitors for the treatment of Limb-girdle muscular dystrophy.

Education

- 2010 – now **Ph.D candidate at EPFL**
Doctoral school in Chemistry and Chemical Engineering
- 2010 **University of Padua, Master degree**
Pharmaceutical biotechnology (*summa cum laude*)
- 2008 **University of Padua, Bachelor degree**
Medical biotechnology (*summa cum laude*)

Publication list:

1. Bellotto S., Chen S., Rentero Rebollo I., Wegner A.H. and Heinis C. Phage selection of photoswitchable peptide ligands. *J. Am. Chem. Soc.* **136**, 5880–5883 (2014).
2. Pollaro L., Diderich P., Angelini A., Bellotto S., Wegner A.H. and Heinis C. Measuring net protease activities in biological samples using selective peptidic inhibitors. *Anal. Biochem.* **427**, 18-20, (2012).
3. Bellotto S., Reuter R., Heinis C. and Wegner A.H. Synthesis and photochemical properties of oligo-*ortho*-azobenzenes. *J. Org. Chem.* **76**, 9826-9834, (2011).